General Disclaimer

One or more of the Following Statements may affect this Document

- This document has been reproduced from the best copy furnished by the organizational source. It is being released in the interest of making available as much information as possible.

- This document may contain data, which exceeds the sheet parameters. It was furnished in this condition by the organizational source and is the best copy available.

- This document may contain tone-on-tone or color graphs, charts and/or pictures, which have been reproduced in black and white.

- This document is paginated as submitted by the original source.

- Portions of this document are not fully legible due to the historical nature of some of the material. However, it is the best reproduction available from the original submission.

Produced by the NASA Center for Aerospace Information (CASI)

NASA TECHNICAL MEMORANDUM

NASA TM-73741

NASA TM-73741

(NASA-TM-73741) MINIMUM TIME ACCELERATION OF AIRCRAFT TURBOFAN ENGINES BY USING AN ALGORITHM BASED ON NONLINEAR PROGRAMMING (NASA) 182 p HC A09/MF A01 CSCL 21E

N77-33167

Unclas
G3/07 50728

MINIMUM TIME ACCELERATION OF AIRCRAFT TURBOFAN ENGINES BY USING AN ALGORITHM BASED ON NONLINEAR PROGRAMMING

by Fred Teren
Lewis Research Center
Cleveland, Ohio 44135
September 1977

NOV 1977
RECEIVED
NASA STI FACILITY

MINIMUM TIME ACCELERATION OF AIRCRAFT TURBOFAN ENGINES BY USING AN ALGORITHM BASED ON NONLINEAR PROGRAMMING

Fred Teren, Ph.D.
Stanford University, 1977

Minimum time accelerations of aircraft turbofan engines are presented. The calculation of these accelerations is made by using a piecewise-linear engine model, and a new algorithm based on nonlinear programming. Use of this model and algorithm allows such trajectories to be readily calculated on a digital computer with a minimal expenditure of computer time.

The new algorithm may be used for solution of optimal control problems which are nonlinear in the state variables, and linear in the control variables. Specifically, the most general problem considered is to minimize a performance index subject to satisfaction of the system dynamic equations, a set of terminal constraints, and path inequality constraints. The performance index, system equations, and path constraints are all linear in the control variables.

It is shown that the optimal control for such problems is bang-bang, except for possible singular arcs, which are not considered. The algorithm requires that a nominal bang-bang solution be found which satisfies the system dynamic equations and terminal constraints. Once such a feasible solution has been found, influence functions are generated which determine if the necessary conditions for optimality have been satisfied. If not, additional control switches are needed. Nonlinear optimization (gradient search) techniques are then used to vary the control switching times in order to improve the solution.

The algorithm is used to find minimum time acceleration histories for the F100 engine, a two-spool turbofan engine which powers the F15 and F16

aircraft. A piecewise-linear engine model is used. The linearized model used at a given time in the trajectory is determined by calculating a normalized "distance" from the current state to the state at each of several equilibrium points; the model linearized about the "closest" equilibrium point is then used. Minimum time solutions are obtained, and the resulting control histories are used as inputs to a nonlinear simulation of the F100 engine to verify the accuracy of the piecewise linear solution.

In addition to the transient results, the linear models are also used to find the control settings which minimize steady-state specific fuel consumption.

Approved for publication:

By _____

By _____
Dean of Graduate Studies

MINIMUM TIME ACCELERATION OF AIRCRAFT TURBOFAN ENGINES BY USING AN ALGORITHM BASED ON NONLINEAR PROGRAMMING

A DISSERTATION

SUBMITTED TO THE DEPARTMENT OF AERONAUTICS AND ASTRONAUTICS

AND THE COMMITTEE ON GRADUATE STUDIES

OF STANFORD UNIVERSITY

IN PARTIAL FULFILLMENT OF THE REQUIREMENTS

FOR THE DEGREE OF

DOCTOR OF PHILOSOPHY

By

Fred Teren

September 1977

I certify that I have read this thesis and that in my opinion it is fully adequate, in scope and quality, as a dissertation for the degree of Doctor of Philosophy.

I certify that I have read this thesis and that in my opinion it is fully adequate, in scope and quality, as a dissertation for the degree of Doctor of Philosophy.

I certify that I have read this thesis and that in my opinion it is fully adequate, in scope and quality, as a dissertation for the degree of Doctor of Philosophy.

Approved for the University Committee
on Graduate Studies:

Dean of Graduate Studies

ACKNOWLEDGMENTS

This research has been supported by the NASA Lewis Research Center graduate study program. I would like to thank Lewis management and the Lewis training office for their support of this effort. In particular, I would like to thank Miss Gertrude Collins of the training section for her support, advice, and encouragement. The members of the Lewis Dynamics and Controls Branch also deserve thanks for their assistance and technical discussions. Sue Krosel and Ron Blaha deserve special mention for having provided some of the computer results presented herein.

I also would like to thank my coadvisors Dr. Arthur E. Bryson and Dr. J. David Powell for their time, encouragement, and excellent technical advice. Last, but not least, I want to thank my wife, Sandra, for her constant encouragement and understanding, and my wife and children, Lisa and Robby, for their sacrifices, without which this dessertation could never have been completed.

ABSTRACT

Minimum time accelerations of aircraft turbofan engines are presented. The calculation of these accelerations is made by using a piecewise-linear engine model, and a new algorithm based on nonlinear programming. Use of this model and algorithm allows such trajectories to be readily calculated on a digital computer with a minimal expenditure of computer time.

The new algorithm may be used for solution of optimal control problems which are nonlinear in the state variables, and linear in the control variables. Specifically, the most general problem considered is to minimize a performance index subject to satisfaction of the system dynamic equations, a set of terminal constraints, and path inequality constraints. The performance index, system equations, and path constraints are all linear in the control variables.

It is shown that the optimal control for such problems is bang-bang, except for possible singular arcs, which are not considered. The algorithm requires that a nominal bang-bang solution be found which satisfies the system dynamic equations and terminal constraints. Once such a feasible solution has been found, influence functions are generated which determine if the necessary conditions for optimality have been satisfied. If not, additional control switches are needed. Nonlinear optimization (gradient search) techniques are then used to vary the control switching times in order to improve the solution.

The algorithm is used to find minimum time acceleration histories for the F100 engine, a two-spool turbofan engine which powers the F15 and F16 aircraft. A piecewise-linear engine model is used. The linearized model used at a given time in the trajectory is determined by calculating a normalized "distance" from the current state to the state at each of several equilibrium points; the model linearized about the "closest" equilibrium point is then used. Minimum time solutions are obtained, and the resulting control histories are used as inputs to a nonlinear simulation of the F100 engine to verify the accuracy of the piecewise linear solution.

In addition to the transient results, the linear models are also used to find the control settings which minimize steady-state specific fuel consumption.

TABLE OF CONTENTS

	Page
LIST OF TABLES	viii
LIST OF ILLUSTRATIONS	ix
LIST OF SYMBOLS	xi
I. INTRODUCTION	1
A. Motivation	1
B. Related Work	2
C. Contributions	4
D. Organization of the Report	7
II. A NONLINEAR OPTIMAL CONTROL PROBLEM, LINEAR IN CONTROL	8
A. Problem Statement	8
B. Necessary Conditions for a Local Minimum	10
C. Singular Arcs	12
D. Determination of Optimal Trajectory	13
III. A NEW ALGORITHM	15
A. Modified Problem Statement	15
B. Feasible Solution	18
Fixed final time	21
C. Calculation of Lagrange Multipliers	21
Fixed final time	24
D. Improvement of Feasible Solution	24
E. Merging of Switch Points	27
F. Insertion of New Switching Times	29
G. Convergence Issues	29
H. Summary of Algorithm Steps	31
IV. PIECEWISE-LINEAR MODELS	33
A. Linear Model	34
B. Piecewise-Linear Modeling	36
C. Necessary Conditions for Optimality	38
D. Initial Feasible Trajectory	40
E. Calculation of Lagrange Multipliers	41
F. Improvement of Feasible Trajectory	43
V. DEMONSTRATIVE EXAMPLE	45
A. Problem Statement	45
B. Nonexistence of Singular Arc	46
C. Initial Feasible Solution	47
D. Calculation of Lagrange Multipliers	47
E. Optimality of Initial Feasible Solution	49
F. Linear Approximation	51
G. Piecewise-Linear Approximation	53
H. Additional Control Variable	55

Page

VI. APPLICATION TO TURBOFAN CONTROL 60
A. Engine Description. 60
B. Engine Models 62
C. Model Accuracy. 68
D. Steady State Performance. 72
E. Transient Performance 74
Statement of the problem. 76
Results 77
F. Comparison of Nonlinear and Piecewise-Linear Responses 88
G. Comparison of Minimum Time and BOM Control Responses Using the Nonlinear Simulation. 107
H. Suboptimal Control. 116

VII. CONCLUSIONS 121

APPENDIXES
A: OPTIMIZATION WITH STATE VARIABLE INEQUALITY CONSTRAINTS . . 125

B: DERIVATION OF LAGRANGE MULTIPLIER FUNCTIONS FOR FEASIBLE SOLUTION 133

C: MODEL ORDER REDUCTION 139

D: THREE-STATE LINEAR MODELS 142

E: COMPUTER PROGRAM LISTINGS 147

REFERENCES. 163

LIST OF TABLES

Table		Page
I	Five State Linear Model	65
II	Equilibrium Values of Problem Variables	66
III	Eigenvalues and Eigenvectors of Five State Model. . . .	66
IV	Three-State Linear Model.	67
V	Steady-State Performance.	72

LIST OF ILLUSTRATIONS

Figure		Page
5.1	Switching function for initial feasible trajectory. . . .	50
5.2	Initial feasible trajectory	52
5.3	Lagrange multipliers for approximate model.	57
5.4	Switching function for control v	58
6.1	Sketch of F100 engine	61
6.2	Steady-state prediction accuracy.	69
6.3	Acceleration from PLA = 24 degrees to intermediate thrust. Optimum IGV and HVS.	78
6.4	Acceleration from PLA = 24 degrees to intermediate thrust. IGV and HVS, scheduled ±7 degrees.	83
6.5	Terminal error versus acceleration time	87
6.6	Time required to accelerate to intermediate thrust. Terminal error, 0.05.	89
6.7	Comparison of nonlinear and piecewise-linear results. Acceleration from PLA = 24 degrees to intermediate thrust. IGV and HVS, scheduled ±7 degrees.	90
6.8	Comparison of nonlinear and piecewise-linear results. Acceleration from PLA = 36 degrees to intermediate thrust. IGV and HVS, scheduled ±7 degrees.	95
6.9	Comparison of nonlinear and piecewise-linear results. Acceleration from PLA = 36 degrees to intermediate thrust. IGV and HVS, scheduled	99
6.10	Comparison of nonlinear and linear results for 3 percent fuel-flow step.	105
6.11	Comparison of minimum time and BOM control. Acceleration from PLA = 24 degrees to intermediate thrust.	108
6.12	Comparison of minimum time and BOM control. Acceleration from PLA = 36 degrees to intermediate thrust.	112
6.13	Terminal error versus acceleration time. Optimal and suboptimal control.	118

Figure | Page

6.14 Time to accelerate to intermediate thrust. Optimal and suboptimal control 120

A1 Switching function and control profile 131

A2 Optimal trajectory 132

LIST OF SYMBOLS

A_{noz}	nozzle exit area, sq ft
a	scalar function in performance index (2.1)
b	$(r \times 1)$ vector function in performance index (2.1)
C	$(r \times 1)$ vector function of active constraints
c_i	scalar path inequality constraint function in (2.3)
D	$(r \times r)$ matrix function of active constraints
d_i	$(r \times 1)$ vector path inequality constraint function in (2.3)
E	constant path inequality constraint limit
e_{ij}	scalar path constraint limits
F	$(n \times n)$ constant system matrix
FTIT	fan turbine inlet temperature, °R
f	$(n \times 1)$ vector of system functions
G	$(n \times r)$ constant control distribution matrix
g	$(n \times r)$ matrix of control distribution functions
H	variational Hamiltonian
HVS	compressor variable vane position, deg
h	constant vector
I	identity matrix
I_j	distance functions
IGV	inlet guide vane position, deg
J	performance index
J^*	modified performance index, appendix B
M	$(n \times 1)$ vector
m	modal coordinates
N	square matrix

N	speed, rpm
n	number of states
P	$(n \times 1)$ vector
PLA	power lever angle, deg
PS3	combustor static pressure, psi
p	number of terminal state constraints
P_{t7}	augmentor pressure, psi
Q	matrices defined by (3.11)
q	number of path inequality constraints
q_i	vectors defined by (3.10)
R	matrices defined by (3.11)
r	number of controls
r_i	vectors defined by (3.10)
S_{jk}	model switching functions
SMCOMP	compressor surge margin
SMFAN	fan surge margin
s	order of state variable inequality constraint
T	thrust, lbf
T	$(n \times n)$ diagonalizing transformation matrix
TIT	turbine inlet temperature, °R
t	time
u	$(r \times 1)$ control vector
W	$(n \times n)$ weighting matrix
w	number of segments
w_a	airflow, lbm/sec
w_f	combustor fuel flow, lbm/hr

x	$(n \times 1)$ state vector
y	output variable
α_{jk}	vectors defined by (4.17)
β	matrix used in model order reduction
β_{jk}	scalars defined by (4.17)
γ_x, γ_y	control distribution parameters
ε	jump parameter
η	scalar variable
Λ	$(n \times n)$ block-diagonal system matrix
Λ	solution matrix defined by (3.7)
λ	$(n \times 1)$ undetermined Lagrange multiplier vector
μ_i	scalar undetermined Lagrange multiplier
ν	$(p \times 1)$ undetermined parameter vector
ρ_i	undetermined Lagrange multipliers, appendix B
τ	dummy integration variable
Φ	transition matrix
ϕ	scalar function of terminal conditions in (2.1)
ψ_i	scalar terminal constraint function

Operators:

$d(\ )$	differential of ( )
$\frac{d(\ )}{d(\ )}$	total derivative
$\min(\ )$	minimize ( )
$\mathrm{sgn}(\ )$	signum of ( )
$\delta(\ )$	variation of
$\frac{\partial(\ )}{\partial(\ )}$	partial derivative

$\Delta(\ )$	change in ( )
$\sum$	summation
$\lvert\ \rvert$	absolute value

Subscripts:

comp	compressor
e	equilibrium
f	final
fan	fan
fe	feasible
min	minimum
opt	optimum
s	model switching point
ss	steady state
sw	switching point used during gradient improvement
0	initial

Superscripts:

(i)	solution number, eq. (3.5)
T	transpose of a vector or matrix
$\circ$	time derivative
-1	inverse of a square matrix
$(\ )^-$	just before ( )
$(\ )^+$	just after ( )
$\hat{}$	predicted value

CHAPTER I. INTRODUCTION

A. Motivation

Modern, high-performance turbojet and turbofan engines are generally equipped with one or more variable geometry features in order to provide maximum propulsive efficiency over a range of engine power settings and flight conditions. For example, the J-85 engine (a one-spool turbojet used in the F5 aircraft) has variable inlet guide vanes, and variable bleeds in three stages of its eight-stage compressor. The TF30 engine (a two-spool turbofan, used in the F111 and F14 aircraft) has variable bleeds in the low and high compressors. The F100 engine (a two-spool turbofan, used in the F15 and F16 aircraft) has variable fan inlet guide vanes and variable compressor stator vanes. Each of these engines also has a variable-area exhaust nozzle and an afterburner. Variable area turbines, although not yet in operational use, have been tested on technology demonstrator engines.

Propulsive efficiency is probably the most important measure of an aircraft engine's performance. However, another important measure is the time required to accelerate from one thrust level to a higher thrust level. Engine acceleration is one of the functions of the engine control system, and may be accomplished via open-loop scheduling or closed-loop control. For each of the three engines referred to above, engine accelerations are accomplished by controlling fuel flow. The variable geometry features are kept on their steady-state schedules during the acceleration.

In this report, minimum-time acceleration histories are computed for the F100 turbofan engine. Four control variables, i.e., fuel flow, exhaust nozzle area, inlet guide vane position, and compressor stator vane position, are utilized.

B. Related Work

In recent years, linear-quadratic regulator theory has been developed for the design of multi-input, multi-output control systems. An account of the theory and application is given for example in reference 1. Use of the theory has been facilitated by computer programs such as those described in references 2 and 3, which rapidly and efficiently calculate the optimal feedback control gains, given the system description and performance index. This theory has been applied recently to the design of control systems for aircraft gas turbine engines. In addition to the design of regulators, the problem of minimizing acceleration time has also been considered.

Michael and Farrar (refs. 4 and 5) apply linear quadratic regulator theory to the design of controls for the F401 turbofan engine. The nonlinear system equations are linearized about five different equilibrium points, and linear system descriptions are obtained. The resulting linear models have five state and five control variables. At each equilibrium point, a quadratic performance index intended to minimize acceleration time is formulated, and feedback control gains are determined. A nonlinear feedback control law is developed by curvefitting the resulting control gains as a function of compressor speed.

Weinberg (ref. 6) applies linear-quadratic regulator theory to the design of controls for the F100 engine. He shows that this engine

can be adequately represented by three state variables - fan speed, compressor speed, and augmentor pressure. Four control variables are utilized, and linearized engine models are obtained at two equilibrium points. The problem of minimizing acceleration time is considered, and control system gains are derived by conducting small perturbation optimizations at each of two equilibrium points, using a quadratic performance index. The control gains are switched at a fixed value of fan speed, rather than varied in a continuous manner as in references 4 and 5.

In reference 7, Sevich and Beattie consider the minimization of acceleration time for a turbojet engine, using fuel flow and exhaust nozzle area as control variables. They use a quadratic performance index to approximate a minimum time solution, as in references 4 to 6. However, they use a nonlinear engine model, rather than a series of linear models. The result is an open-loop optimal trajectory. The controls are assumed to be piecewise constant, and the performance index is minimized by using a conjugate gradient search technique.

DeHoff et al. (ref. 8) use linear-quadratic theory to design controls for the F100 engine. The control gains are generated using linear models with five state variables and four control variables at several equilibrium points. Principal emphasis is on the regulator design. Although acceleration control is considered, there is no specific attempt at minimizing acceleration time.

References 4 through 8 all make use of integral quadratic performance indices, in which both state and control deviations from some desired trajectory are penalized. The coefficients of the penalty terms are adjusted in an attempt to minimize acceleration time. How-

ever, none of these reports can claim their final histories produce truly minimum-time accelerations.

Minimum-time trajectory optimization has been considered by many investigators for many years. Athans and Falb (ref. 9) give a good account of the literature dealing with time optimal systems in their chapter 7. However, nearly all of their discussion is concerned with problems having only a single control variable. Furthermore, the systems are assumed to be linear and time invariant, and the control limits are not dependent on the state or time. It is shown that the optimal control for such problems is bang-bang, i.e., the control always operates at either the upper or the lower limit.

Wolske (ref. 10) considered the problem of fuel-optimal control of a dynamic system which is nonlinear in the state and linear in the control. The controls are assumed to be bounded in magnitude, and the resulting optimal control is bang-bang. The problem is solved by linearizing about a nominal history, which is neither optimal nor feasible (i.e., it does not satisfy the terminal constraints). The optimality condition and terminal constraints are expressed as linear inequalities, and linear programming techniques are used to improve the solution until a feasible optimum is attained.

C. Contributions

In this report, an algorithm is developed for solution of optimal control problems which are nonlinear in the state variables, and linear in the control variables. Specifically, the problem considered is to minimize a performance index subject to satisfaction of the system dynamic equations, a set of terminal constraints (the number of which may be less than or equal to the number of states) and path inequality

constraints. The performance index and system equations and path constraints are all linear in the control variables.

It is shown that the optimal control is bang-bang, except for possible singular arcs which are not considered. The algorithm requires that a nominal bang-bang solution be found that satisfies the system dynamic equations and terminal constraints. Once such a feasible solution has been found, influence functions are generated which determine if the necessary conditions for optimality have been satisfied. If not, additional control switches are added. Nonlinear optimization (gradient search) techniques are then used to vary the control switching times in order to improve the solution. The nonlinear optimization technique described in reference 11 is used to generate the numerical results presented in this report.

The algorithm presented herein converts an optimal control problem with path inequality constraints and terminal constraints into an unconstrained parameter optimization problem. This is accomplished in two steps. First, the bang-bang nature of the optimal control is used to express the possible optimal trajectories in terms of the switching times between regions of different control strategy. At this point, the original problem has been converted into a parameter optimization problem with equality constraints (terminal constraints). Then, the equality constraints are satisfied by using an equal number of the switching times as iteration variables. This procedure results in an unconstrained parameter optimization problem with a reduced number of parameters, and is similar to the reduced gradient algorithm discussed in reference 12.

The algorithm is then used to find minimum time acceleration histories for the F100 engine, a two-spool turbofan engine used to power the F15 and F16 aircraft. A piecewise-linear engine model having three states and four controls is used to obtain the minimum time solutions. The linear models used in this report were obtained by linearization of a nonlinear model at five equilibrium points, and were taken from reference 13. The linear model which applies at a given time in the trajectory is determined by calculating a normalized "distance" from the current state to the state at each of the equilibrium points; the linear model associated with the closest equilibrium point is then used. Linear state/control constraints which correspond to speed, temperature, pressure, and mechanical control limits are considered. Minimum time solutions are obtained, and the resulting control histories are used as inputs to a nonlinear computer simulation of the F100 engine (ref. 14) to verify the accuracy of the piecewise linear solution.

A suboptimal closed-loop control mode is also developed, which gives performance which closely approximates the open loop results.

Use of the piecewise linear model allows optimal solutions to be obtained with the expenditure of less than one percent of the computer time which is required when a detailed, nonlinear model is used, such as in reference 7. Furthermore, the solutions obtained in this report are truly minimum time solutions to the piecewise linear problem, rather than approximations to minimum time solutions to the nonlinear problem, as in references 4 to 7.

In addition to the transient results, the linear models and con-

straint equations are used to find the control settings which minimize steady-state specific fuel consumption.

D. Organization of the Report

The dynamic optimization problem is defined in chapter II, and necessary conditions for an optimal solution are stated. The algorithm is presented in chapter III. First, the initial feasible solution is defined and discussed. Next, it is shown how to calculate the sensitivity functions (Lagrange multiplier functions) corresponding to the feasible solution. Finally, improvement of the feasible solution is discussed. Chapter IV derives the applicable equations for piecewise linear systems. In chapter V, a detailed comparison of exact and piecewise linear solutions to a particular nonlinear problem is made. One and two control variable problems are discussed. Chapter VI presents the results obtained for the minimization of acceleration time for the F100 engine. Finally, conclusions are drawn and recommendations for future research are made in chapter VII.

CHAPTER II. A NONLINEAR OPTIMAL CONTROL PROBLEM, LINEAR IN CONTROL

In this chapter, the optimal control of a dynamic system which is nonlinear in the state and linear in the control is considered. First, the problem is defined, including the performance criterion, system equations, path constraints, and terminal constraints. Then, necessary conditions for optimality are derived. The derivation of the optimal control strategy is similar to that presented in textbooks on modern optimal control, such as reference 15. This derivation is included here because the nature of the resulting optimal control strategy motivates the development of the new algorithm presented in chapter III.

A. Problem Statement

We consider a fairly general dynamic optimization problem, which is subject to one important restriction - the performance index, system equations and path constraints are all linear functions of the control variables. As will be shown later, this leads to a bang-bang solution. We wish to find the vector control history $u(t)$ which minimizes the scalar functional

$$J = \phi[x(t_f),t_f] + \int_{t_0}^{t_f} [a(x,t) + b^T(x,t)u]dt \qquad (2.1)$$

subject to the vector system differential equations

$$\dot{x} = f(x,t) + g(x,t)u \qquad (2.2)$$

and path inequality constraints

$$c_i(x,t) + d_i^T(x,t)u \leq 0 \qquad i = 1,2, \ldots ,q \qquad (2.3)$$

The initial state and time are assumed to be specified, i.e.,

$$x(t_0) = x_0$$

while the terminal state and time are subject to the p terminal constraints $(p \leq n + 1)$

$$\psi_i[x(t_f), t_f] = 0 \qquad i = 1,2, \ldots, p \leq (n + 1) \qquad (2.4)$$

In the above, x is the $(n \times 1)$ state vector, and u is the $(r \times 1)$ control vector. The functions ϕ, a, and c_i are scalar functions of x and t, while b and d_i are vector functions of dimension $(r \times 1)$. The vector function f and matrix function g have dimension $(n \times 1)$ and $(n \times r)$, respectively. The terminal time t_f may be either fixed or free. In fact, if $a = b = 0$ and $\phi = t_f$, the performance index in (2.1) is simply $J = t_f$.

The path constraints (2.3) serve to bound the allowable values of the control. A path constraint is said to be active if $c_i + d_i^T u = 0$; it is said to be inactive if $c_i + d_i^T u < 0$. If, for a particular path constraint, c_i is constant and d_i has only one nonzero, constant component, then that path constraint is simply a physical control limit. On the other hand, if all components of d_i are equal to zero, the control does not appear explicitly in the path constraint; such constraints are called state variable inequality constraints. In the main body of this report, it is assumed that there are no state variable inequality constraints. However, the theory and numberical algorithm are extended to include state variable inequality constraints in appendix A.

If, for given values of x and t, the jth component of $d_i(x,t)$ is positive, then the ith constraint serves as an upper bound for the jth control variable. Similarly, if the jth component of $d_i(x,t)$ is

negative, the ith constraint is a lower bound for the jth control variable. It will be assumed that sufficient constraints are imposed so that each of the r control variables is bounded above and below for all possible values of x and t. If this is the case, then nc control impulses are allowed.

B. Necessary Conditions for a Local Minimum

Using the techniques employed in reference 15, a Hamiltonian function is defined as

$$H \triangleq a(x,t) + b^T(x,t)u + \lambda^T[f(x,t) + g(x,t)u] + \sum_{i=1}^{q} \mu_i[c_i(x,t) + d_i^T(x,t)u] \tag{2.5}$$

where λ and μ are undetermined Lagrange multiplier vector functions of time, having dimension $(n \times 1)$ and $(q \times 1)$, respectively.

In terms of H, necessary conditions for J to be a local minimum are

$$\dot{\lambda}^T = -\frac{\partial H}{\partial x} \tag{2.6a}$$

$$\frac{\partial H}{\partial u} = 0 \tag{2.6b}$$

and

$$\begin{aligned} \mu_i &\geq 0 \quad \text{if} \quad c_i + d_i^T u = 0 \\ \mu_i &= 0 \quad \text{if} \quad c_i + d_i^T u < 0 \end{aligned} \tag{2.6c}$$

The Lagrange multipliers must satisfy the following terminal conditions.

$$\lambda^T(t_f) = \nu^T \frac{\partial \psi}{\partial x_f}[x(t_f),t_f] + \frac{\partial \phi}{\partial x_f}[x(t_f),t_f] \tag{2.7}$$

where ν is a $(p \times 1)$ undetermined parameter vector. If the terminal time is not specified, another necessary condition which applies is

$$H(t_f) = -\frac{\partial\phi[x(t_f),t_f]}{\partial t_f} - \nu^T \frac{\partial\psi[x(t_f),t_f]}{\partial t_f} \tag{2.8}$$

For the present problem, equations (2.6a, b, and c) may be written explicitly as

$$\dot{\lambda}^T = -\frac{\partial a}{\partial x} - \frac{\partial b^T}{\partial x} u - \lambda^T \frac{\partial f}{\partial x} - \lambda^T \frac{\partial g}{\partial x} u - \sum_{i=1}^{q} \mu_i \frac{\partial c_i}{\partial x} \tag{2.9a}$$

$$b^T + \lambda^T g + \sum_{i=1}^{q} \mu_i d_i^T = 0 \tag{2.9b}$$

$$\begin{aligned} \mu_i &= 0 \quad \text{if} \quad c_i + d_i^T u < 0 \\ \mu_i &\geq 0 \quad \text{if} \quad c_i + d_i^T u = 0 \end{aligned} \tag{2.9c}$$

The optimal control must satisfy (2.9b and c) and constraints (2.3). For given x and t, the functions b, c, d, g, and λ are all constant. Therefore, the determination of the optimal u (for each x and t) is simply a linear programming problem, which can be readily solved by using the Simplex method (ref. 16). Except for singular arcs (to be discussed shortly), the optimal control is always determined by r active constraints from (2.3). The optimization problem is simply to find the r constraints which satisfy (2.9b and c) and (2.3).

The r active constraints change from time to time along the trajectory. When a change of constraints occurs, the control variables jump discontinuously from one boundary to another. Such control is re-

ferred to as bang-bang control, and the points at which the jumps occur are called junction points.

C. Singular Arcs

The optimal control can usually be uniquely determined from (2.9b and c) and (2.3). However, if H is constant along an active constraint boundary, i.e., if $b^T + \lambda^T g \equiv \eta d_i^T$ where η is a real variable, then the control is not uniquely determined along that constraint boundary. This situation is illustrated in sketch (a) for a two control variable problem.

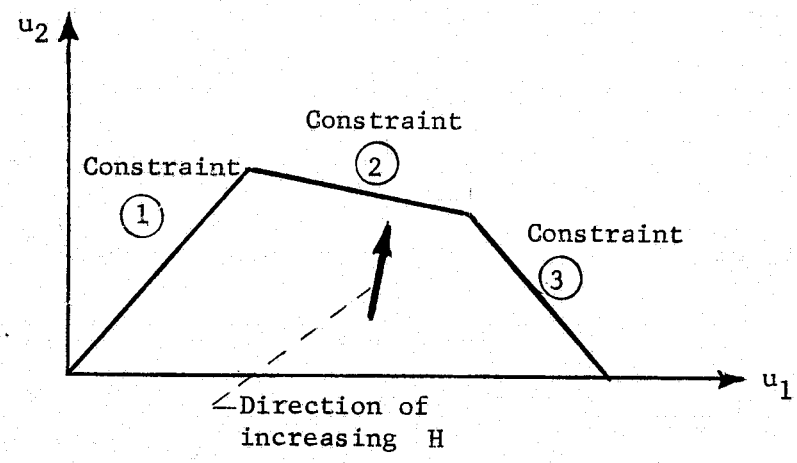

In the sketch, H is constant along constraint 2 and it is not clear whether to use constraint 1 or constraint 3 (or neither) as the other active constraint. Furthermore, if $(b^T + \lambda^T g) = 0$ (all components zero) the control is totally indeterminate.

It is sometimes possible to find minimizing solutions for which some or all of the controls u are not determinate from (2.9b and c) and (2.3) for a finite time period; the corresponding trajectory segments are called <u>singular arcs</u>. On singular arcs, the control is de-

termined from the requirement that the time derivatives of $(b^T + \lambda^T g - \eta d_i^T)$, as well as $(b^T + \lambda^T g - \eta d_i^T)$ itself, must be identically zero. To determine the control u, successive time derivatives of $(b^T + \lambda^T g - \eta d_i^T)$ are taken until the control appears explicitly.

It is difficult to determine general conditions for the existence and minimality of singular arcs. Nevertheless, each individual problem should be examined for the possibility of minimizing singular arcs, and this practice will be followed in this report in the example problem to be discussed later. However, in the algorithm to be described in chapter III, it will be assumed that the minimizing solution is nonsingular.

D. Determination of Optimal Trajectory

We now assume that the problem is nonsingular, and the linear programming problem is solved to yield the active constraints and the optimal control. If we assume that the active constraints are constraints 1 through r and form these into a vector-matrix representation, i.e.,

$$C = \begin{pmatrix} c_1 \\ c_2 \\ \cdot \\ \cdot \\ \cdot \\ c_r \end{pmatrix}, \qquad D^T = \begin{pmatrix} d_1^T \\ d_2^T \\ \cdot \\ \cdot \\ d_r^T \end{pmatrix}$$

then we can solve for the optimal control from

$$u = -D^{-T}C \tag{2.10}$$

where the superscript $(-T)$ denotes the inverse of the transpose. Also, equation (2.9b) can be rewritten using vector-matrix representation for the active constraints as

$$b^T + \lambda^T g + \mu^T D^T = 0$$

and this equation can be solved for μ to yield

$$\mu = -D^{-T}(b + g^T\lambda) \tag{2.11}$$

Substitution of (2.10) and (2.11) into (2.2) and (2.9a) results in a simpler version of (2.2) and (2.9a).

$$\dot{x} = f - gD^{-T}C \tag{2.12}$$

$$\dot{\lambda}^T = -\frac{\partial}{\partial x}(a - b^T D^{-T}C) - \lambda^T \frac{\partial}{\partial x}(f - gD^{-T}C) \tag{2.13}$$

CHAPTER III. A NEW ALGORITHM

Necessary conditions for the optimal control of a dynamic system which is nonlinear in the state and linear in the control were derived in Chapter II. It was shown that except for singular arcs, the optimal control (r variables) is always determined by r active constraint boundaries. In Chapter III, the nature of the optimal control strategy derived in Chapter II is used as the basis for a new algorithm for the solution of such optimization problems.

First, a feasible solution is obtained which satisfies all path and terminal constraints, and for which the controls always lie along r constraint boundaries. The Euler Lagrange equations are not utilized in the determination of this feasible solution; it may or may not be a local minimum. Then, it is shown that the Lagrange multiplier time history can be easily and uniquely calculated from this feasible solution. The necessary conditions for a local minimum may be calculated as functions of the Lagrange multipliers. If the initial feasible solution does not satisfy the necessary conditions, the control history is modified, and nonlinear optimization (gradient search) techniques are used to improve the solution.

A. Modified Problem Statement

In chapter II it was shown that except for singular arcs, the optimal control variables (r variables) are always determined by an equal number of active constraints at all points along an optimal tra-

jectory. The problem is to find which constraints are active, as a function of time. It will be assumed that the optimal trajectory consists of a number of segments. For each segment, the control variables are determined by a set of r active constraints. The optimal control problem stated in (2.1) to (2.4) is solved by finding the optimal values of the switching times, i.e., the times at which the active constraints switch from one set to another.

The modified optimal control problem can be stated as follows: It is desired to find the values of the w switching times,

$$\{t_i,\ i = 1, \ldots, w\}$$

which minimize the scalar functional

$$J = \phi[x(t_f), t_f] + \int_{t_0}^{t_f} [a(x,t) + b^T(x,t)u]dt$$

while satisfying the vector system differential equations

$$\dot{x} = f(x,t) + g(x,t)u$$

and terminal constraints

$$\psi_i[x(t_f), t_f] = 0 \qquad i = 1, \ldots, p \leq (n + 1)$$

During time interval

$$t_{i-1} \leq t \leq t_i$$

the control is given by

$$u = -D_i^{-T} C_i$$

in accordance with (2.10).

The above modified problem is a parameter optimization problem with equality constraints, which might be easier to solve than the

original optimal control problem. However, it should be emphasized that the number of segments in an optimal trajectory, and the active constraint sets for each of the segments, are not known in advance.

The problem statement can be further modified into an unconstrained parameter optimization problem by using the reduced gradient method, as presented in reference 12. To accomplish this, the switching time set is partitioned into two subsets, having p and $(w - p)$ members, respectively. The p members of the first subset are considered as dependent variables, in the following sense: Whenever some of the switching times in the second subset are varied, the values of the p terminal constraints will change from their converged values. The values of the p switching times in the first subset are then used as iteration variables in order to reconverge the terminal constraints to the desired final values. In this way, the problem is converted into the following form: Find the values of the $(w - p)$ switching times

$$\left\{t_i,\ i = (p + 1), \ldots, w\right\}$$

which minimize the scalar functional

$$J = \phi[x(t_f),t_f] + \int_{t_0}^{t_f} [a(x,t) + b^T(x,t)u]dt$$

while satisfying the vector system differential equations

$$\dot{x} = f(x,t) + g(x,t)u$$

where, during time interval

$$t_{i-1} \leq t \leq t_i$$

the control is given by

$$u = -D_i^{-T} C_i$$

The above unconstrained parameter optimization problem may be solved by using any of a number of nonlinear optimization techniques available, such as those discussed in reference 12. The results presented in this report were obtained by using the parameter optimization technique reported in reference 11.

B. Feasible Solution

In order for a trajectory to be a local minimum solution to (2.1), equations (2.12) and (2.13) of Chapter II must be satisfied, and the control must satisfy constraints (2.3) and optimality conditions (2.9b and c). In addition, terminal constraints (2.4) and (2.7) must be satisfied, and equation (2.8) must be satisfied if the terminal time t_f is free. In developing the algorithm for the solution of this problem, it will be assumed initially that t_f is free. Later, we will show how to modify the algorithm for the case in which t_f is specified.

We define a feasible solution as one which satisfies the system differential equations (2.2) and the terminal constraints (2.4), and where the control $u(t)$ is consistent with the necessary conditions for optimality - that is, the control is determined by r of the path constraints (2.3) at all points along the trajectory. It is not necessary that the control be determined by the same r constraints at all points along the trajectory - in fact, we will usually require the control to be determined by several different constraint sets, as

will be seen shortly. Such a trajectory may or may not be a local minimum solution for the performance index (2.1).

In order to obtain a feasible solution, there are p terminal constraints (eqs. (2.4)) which must be satisfied. In general, there must be p degrees of freedom available in order to satisfy the p terminal constraints. In order to provide these degrees of freedom, it will be assumed that there are at least p segments in the trajectory. For each segment, the control is determined by choosing the r constraints which are active. The set of active constraints may be chosen arbitrarily for the first segment; for each succeeding segment, one of the active constraints should be different than any which was utilized in the preceding segments. The durations of p of the segments are variable, and provide the p degrees of freedom necessary to satisfy the p terminal constraints.

The choice of the constraints to be active for the various trajectory segments should be made carefully. There is no guarantee that a solution exists for arbitrary choice of the active constraints, or for any choice of active constraints, for that matter. Also, some of the constraints assumed to be inactive in the initial feasible solution may be violated. In this case, different active constraints must be chosen.

The combination of p degrees of freedom and p terminal constraints is known as a multipoint boundary value problem, and must generally be solved iteratively. Two widely used classes of methods for solution of such problems are Newton-Raphson methods and gradient methods. Both of these methods are widely discussed in the literature

(see, for example, refs. 12 and 17) and will not be discussed here. However, both methods require initial guesses for the values of the p degrees of freedom, and partial derivatives of the terminal constraints with respect to the degrees of freedom. Equations for calculation of the required partial derivatives are derived below.

Suppose, for example, that initial guesses are made for $(p - 1)$ of the junction times t_i, and for t_f. The choice of these times is sufficient to determine a reference trajectory, and values of the p terminal constraints ψ_j.

If one of the t_i is altered slightly, the state at t_i is changed by

$$dx(t_i) = [\dot{x}(t_i^-) - \dot{x}(t_i^+)]dt_i$$

The effect of changes in the t_i on the terminal constraints may therefore be obtained by integration of

$$\frac{d}{dt}\left(\frac{\partial x}{\partial t_i}\right) = \frac{\partial}{\partial x}(f - gD^{-T}C)\frac{\partial x}{\partial t_i} \qquad i = 1, 2, \ldots, (p - 1) \tag{3.1a}$$

from $t = t_i$ to $t = t_f$, with initial conditions

$$\frac{\partial x}{\partial t_i} = \dot{x}(t_i^-) - \dot{x}(t_i^+), \; t = t_i \tag{3.1b}$$

The $\partial\psi_j/\partial t_i$ are then calculated from

$$\frac{\partial\psi_j}{\partial t_i} = \frac{\partial\psi_j}{\partial x_f}\frac{\partial x_f}{\partial t_i} \tag{3.2a}$$

Also, we have

$$\frac{\partial\psi_j}{\partial t_f} = \frac{\partial\psi_j}{\partial x_f}\dot{x}(t_f) \tag{3.2b}$$

Fixed final time. - It was assumed in the above discussion that the terminal time t_f is free. If t_f is fixed, then the duration of the final segment does not provide a degree of freedom. Therefore, there must be at least $(p + 1)$ segments for p terminal constraints, and the durations of p of the segments provide the necessary degrees of freedom.

C. Calculation of Lagrange Multipliers

We consider first the case in which the terminal time is free. Suppose a feasible solution has been found. We will show that the Lagrange multipliers λ and μ can be uniquely calculated, as a function of time. Once the multipliers have been calculated, the necessary conditions for optimality can be checked. If the necessary conditions are not satisfied, an iterative improvement scheme is used in order to find a local minimum solution.

Let the ith trajectory segment have initial time t_{i-1} and final time t_i. The control for the ith segment was determined by a set of r active constraints, and the control just prior to t_i is denoted by $u(t_i^-)$. Just after $t = t_i$, the control is determined by different active constraints, and is given by $u(t_i^+) \neq u(t_i^-)$. It is shown in appendix B that the Hamiltonian must be continuous at $t = t_i$. Therefore, we must have

$$\left[b^T(t_i) + \lambda^T g(t_i)\right]\left[u(t_i^+) - u(t_i^-)\right] = 0 \qquad i = 1, 2, \ldots, (p - 1) \tag{3.3}$$

where the notation $g(t_i)$ is shorthand for

$$g(t_i) \triangleq g[x(t_i), t_i]$$

Equation (3.3) must be satisfied at each of the (p - 1) junction points which are varied in order to satisfy the terminal constraints. Also, as shown in appendix B, the terminal λ and H must be given by (2.7) and (2.8).

$$\lambda^T(t_f) = \nu^T \frac{\partial\psi(t_f)}{\partial x_f} + \frac{\partial\phi}{\partial x_f}$$

$$H(t_f) = -\frac{\partial\phi(t_f)}{\partial t_f} - \nu^T \frac{\partial\psi(t_f)}{\partial t_f}$$

If we use (2.5) for H, and substitute for u and λ from (2.10) and (2.7), respectively, the above equation is converted to

$$\nu^T \frac{d\psi}{dt}(t_f) + \frac{d\phi(t_f)}{dt_f} + a(t_f) + b^T(t_f)D^{-T}(t_f)C(t_f) = 0 \qquad (3.4)$$

Equations (3.3) and (3.4) give p equations which must be satisfied, and there are p multipliers which may be varied. Thus, we have a multipoint boundary value problem, similar to that which must be solved iteratively to determine a feasible trajectory. However, in the present case, iterative solution is not required. Instead we can solve for the parameters ν as follows:

First, we find (p + 1) backward solutions of the $\dot{\lambda}$ equation (2.13) for $\nu^T = (0, \ldots, 0)$, $\nu^T = (1, 0, \ldots, 0)$, $\nu^T = (0, 1, 0, \ldots, 0), \ldots, \nu^T = (0, 0, \ldots, 0, 1)$ where

$$\lambda^T(t_f) = \frac{\partial\phi}{\partial x_f} + \nu^T \frac{\partial\psi}{\partial x_f}$$

These backward solutions are called

$$\lambda^{(0)}(t), \lambda^{(1)}(t), \ldots, \lambda^{(p)}(t) \qquad (3.5)$$

Then $\lambda(t)$ is given by

$$\lambda(t) = \lambda^{(0)}(t) + \Lambda(t)\nu \tag{3.6}$$

where $\Lambda(t)$ is defined as

$$\Lambda(t) \triangleq [\lambda^{(1)}(t) \vdots \ldots \vdots \lambda^{p}(t)] \tag{3.7}$$

There are $(p - 1)$ equations for the continuity of H:

$$[u(t_i^+) - u(t_i^-)]^T[b(t_i) + g^T(t_i)\lambda^{(0)}(t_i) + g^T(t_i)\Lambda(t_i)\nu] = 0$$

$$i = 1, 2, \ldots, (p - 1) \tag{3.8}$$

and at t_f, we must have

$$a(t_f) - b^T(t_f)D^{-T}(t_f)C(t_f) + \frac{d\phi}{dt}(t_f) + \left[\frac{d\psi}{dt}(t_f)\right]^T \nu = 0 \tag{3.9}$$

These equations may be put in matrix form as follows:

Define vectors r_i and q_i and matrices Q and R by

$$q_i^T \triangleq [u(t_i^+) - u(t_i^-)]^T g^T(t_i)\Lambda(t_i) \qquad i = 1, \ldots, (p - 1)$$

$$r_i^T \triangleq [u(t_i^+) - u(t_i^-)]^T[b(t_i) + g^T(t_i)\lambda^{(0)}(t_i)]$$

$$q_p^T \triangleq \left(\frac{d\psi(t_f)}{dt}\right)^T \tag{3.10}$$

$$r_p^T \triangleq a(t_f) + b^T(t_f)D^{-T}(t_f)C(t_f) + \frac{d\phi}{dt}(t_f)$$

$$Q \triangleq \begin{pmatrix} q_1^T \\ - - - \\ \vdots \\ - - - \\ q_p^T \end{pmatrix} \qquad R \triangleq \begin{pmatrix} r_1^T \\ - - - \\ \vdots \\ - - - \\ r_p^T \end{pmatrix} \tag{3.11}$$

Then ν may be calculated from

$$\nu = -Q^{-1}R \tag{3.12}$$

Once the ν are known, (2.7) can be used to calculate $\lambda^T(t_f)$, and $\lambda(t)$ can be obtained by integrating (2.13) backward in time, or by using (3.6).

Fixed final time. - In the above development, it was assumed that the terminal time t_f is free. In the event that t_f is fixed, the equations for calculation of ν are easily modified. In this case, (3.4) is not applicable. Instead, there are p of equations (3.8), instead of $(p - 1)$, since there are $(p + 1)$ segments for this case. The p equations (3.8) are sufficient to calculate the p parameters, ν.

D. Improvement of Feasible Solution

The Lagrange multipliers can be used to determine if the necessary conditions for optimality are satisfied by the initial feasible solution. The optimal control is obtained as a function of time by finding active constraints which result in satisfying (2.9b and c) and (2.3), using $x(t)$ and $\lambda(t)$ as determined from the feasible solution. If $u_{opt}(t)$ as determined in this manner is identical to the control time history $u_{fe}(t)$ utilized in the feasible solution, then the initial feasible solution satisfies the necessary conditions for an optimal solution, and no further calculations need be made. On the other hand, if $u_{opt}(t)$ differs from $u_{fe}(t)$ for even a portion of the trajectory, then the feasible solution is not a local minimum.

Suppose, for example, the control $u_{opt}(t)$ differs from $u_{fe}(t)$ during trajectory segment k. Then the performance index (2.1) can be

improved by splitting segment k into two parts, and using control as follows.

$$u(t) = u_{opt}(t), \qquad t_{k-1} \leq t \leq t_{sw}$$
$$u(t) = u_{fe}(t), \qquad t_{sw} \leq t \leq t_k \tag{3.13}$$

where t_{sw} should be chosen to be only slightly greater than t_{k-1}, so that the modified trajectory differs only slightly from the initial feasible trajectory. Because of the modified control history, the new trajectory will not satisfy the p terminal constraints (2.4). Therefore, the original p junction times should be adjusted, while holding t_{sw} fixed, so that the terminal constraints are satisfied.

During the time interval from t_{k-1} to t_{sw}, the control has been changed (from that of the initial feasible trajectory) from $u_{fe}(t)$ to $u_{opt}(t)$. Therefore, the state at t_{sw} is changed (to first order) by

$$\Delta x_{sw} \cong g(t_{sw})[u_{opt}(t_{sw}) - u_{fe}(t_{sw})](t_{sw} - t_{k-1}) \tag{3.14}$$

The effect of this change on the terminal conditions ψ_j is determined from

$$\Delta\psi_j = \frac{\partial\psi_j}{\partial x_f}\Delta x(t_f) \tag{3.15}$$

where $\Delta x(t_f)$ is obtained by integration of

$$\frac{d}{dt}(\Delta x) = \frac{\partial}{\partial x}(f - gD^{-T}C)(\Delta x) \tag{3.16}$$

from $t = t_{sw}$ to $t = t_f$, with initial conditions given by (3.14).

The change in the ψ_j must be canceled by appropriate changes in the t_i. Therefore, we must have

$$\Delta\psi_j + \frac{\partial\psi_j}{\partial t_i}\Delta t_i = 0$$

which may be solved for Δt_i to give

$$\Delta t_i = -\left(\frac{\partial\psi_j}{\partial t_i}\right)^{-1}\Delta\psi_j \tag{3.17}$$

Equation (3.17) is applied repeatedly in an iterative manner until the terminal constraints are satisfied to sufficient accuracy so that further iteration is not required.

Once a modified trajectory has been obtained and the terminal constraints satisfied, the Lagrange multiplier time history may be calculated for the modified trajectory in the same manner as it was calculated for the initial feasible trajectory. From the Lagrange multipliers, the gradient of the performance index with respect to the switching time, i.e., $\partial J/\partial t_{sw}$ can be obtained. It is shown in appendix B that

$$\frac{\partial J}{\partial t_{sw}} = H(t_{sw}^-) - H(t_{sw}^+) = \lambda^T(t_{sw})g(t_{sw})[u(t_{sw}^-) - u(t_{sw}^+)] + b^T(t_{sw})[u(t_{sw}^-) - u(t_{sw}^+)] \tag{3.18}$$

The set of all such switching points t_{sw} and corresponding gradients, can be used in conjunction with a nonlinear search technique (see refs. 12 or 17 for a general discussion of nonlinear search techniques, or ref. 11 for the particular search technique used to obtain the results presented in this report) to search for the values of t_{sw} such that the gradient vector $\partial J/\partial t_{sw}$ is equal to, or nearly equal to, zero.

E. Merging of Switch Points

In this report, optimal solutions are found by searching for the values of a number of control switching times which minimize a performance index and satisfy terminal constraints. These switching times divide regions of different control action, in which different path inequality constraints are active. In addition to the number of such control regions, the order in which these regions occur (timewise) must be specified initially. However, during the course of the search for an optimal solution, the switching times do not necessarily remain in the originally specified order.

Suppose, for example, the set of switching times for the initial feasible solution is given by $\{t_i, i = 1, \ldots, w \geq p\}$ and $t_0 < t_1 < \ldots < t_w < t_f$. The values of p of the switching times are varied in order to satisfy the terminal constraints, while the remaining $(w - p)$ switching times are varied to minimize the performance index. During the search for an optimal solution, there are three possible situations which can arise which affect the order and/or number of switch points. These are: (1) t_1 becomes less than t_0; (2) t_w becomes greater than t_f; (3) t_k becomes greater than t_{k+1} where $1 \leq k \leq (w - 1)$.

Cases (1) and (2) may be handled in an identical manner. It is tentatively assumed that segment 1 (or segment $(w + 1)$) is not required, and the search is restarted with one less segment. Once this reduced-segment search has converged, the necessary conditions for optimality are checked, and the segment which had been eliminated is reinstituted if necessary (along with other additional segments, as appropriate).

The segment which was eliminated may have been one of the p segments used to satisfy the terminal constraints. In this case, one of the remaining segments which had been used to minimize the performance index must be used instead to satisfy the terminal constraints.

The procedure followed if case (3) is encountered involves several possibilities, and can result in a change of active constraints or a loss of one or two switching times. It was stated earlier that at each switching time, one of the active constraints changes. For definiteness, let the active constraint from segment k which is inactive in segment $(k + 1)$ be denoted by constraint a. Also, let constraint b denote the new active constraint for segment $(k + 1)$.

Similarly, let constraint c denote the active constraint from segment $(k + 1)$ which is inactive in segment $(k + 2)$, and let constraint d denote the new active constraint in segment $(k + 2)$. Clearly, $a \neq b$, $c \neq d$, $a \neq c$, and $b \neq d$, but b and c, and/or a and d, may be the same. The several possibilities are as follows:

(3.1) $b \neq c$, $a \neq d$. For this case, if t_k and t_{k+1} become equal and interchange, then the active constraints for segment $(k + 1)$ become a and d, instead of b and c. No segments are eliminated.

(3.2) $b = c$, $a \neq d$. For this case, if t_k and t_{k+1} become equal, segment $(k + 1)$ and switching time t_{k+1} are eliminated.

(3.3) $b = c$, $a = d$. For this case, if t_k and t_{k+1} become equal, segments k and $(k + 2)$ merge into one, and segments k and $(k + 1)$, and switching times t_k and t_{k+1} are both eliminated.

F. Insertion of New Switching Times

Suppose a local minimum solution has been found for a particular set of switching times $\{t_i, i = 1, \ldots, w \geq p\}$. As discussed earlier, the next step is to determine if the necessary conditions for a local minimum solution have been satisfied. If not, new switching times are added, and a new search for a local minimum is undertaken. The new switching times are added in the region in which the necessary conditions are violated. Initially, the new switching times are inserted at times exactly equal to existing switching times. In this way, new segments having new active constraints are added, but with zero time duration.

For example, suppose an initial feasible solution is found having w segments, and it is discovered that the necessary conditions for a local minimum are not satisfied during segment k. Then a new segment and corresponding switching time are added during segment k. Initially, the new switching time is placed at $t_{w+1} = t_{k-1}$ so that the new segment starts at t_{k-1} and has zero duration. A segment having zero duration cannot alter the trajectory or performance index; therefore, we have

$$J(t_1, \ldots, t_w, t_{w+1} = t_{k-1}) = J(t_1, \ldots, t_w)$$

i.e., the performance index is continuous with respect to insertion of new switching times.

G. Convergence Issues

It is highly desirable that one be able to demonstrate in advance that a particular search will always converge to a solution which satisfies the necessary conditions for a local minimum. There

are several properties which the algorithm must have in order to assure such convergence. First, the algorithm must be setup as a descent algorithm. That is, each trial solution must have a smaller performance index than the preceding solution. This descent property is possessed by most available nonlinear optimization techniques, including the one used herein (ref. 11). Additionally, both the algorithm and the performance index must be continuous functions of their arguments, in this case the switching times.

It is clear that the performance index is a continuous function of the switching times so long as the switching times do not intersect, and no switching points are deleted or inserted. It remains to be shown that the performance index is continuous even when switching times intersect, and/or switching times are added or deleted.

When switching times intersect, the algorithmic search is terminated. As discussed previously, the intersection may result in the deletion of zero, one or two switching points. In any case, the deleted switching times correspond to segments having zero duration at the time of intersection. Since segments of zero duration do not affect the trajectory or performance index, it can be concluded that the performance index is continuous with respect to switching time deletions. After the deletion of switching times, the search is restarted with the appropriate number of switching times.

Switching times may also be added after a search is completed if it is discovered that the necessary conditions for a local minimum solution have not been satisfied. This possibility has been discussed previously. It was shown that the performance index is continuous

with respect to such switching time additions because the new switching times are added in such a manner as to create segments of zero duration initially.

The one required property which unfortunately is not possessed is continuity of the algorithm. Whenever switching times are added or deleted, the number of arguments changes, and it can be shown that the algorithm is discontinuous under such conditions. Because of this, convergence to a solution which satisfies the necessary conditions for a local minimum cannot be guaranteed. Nevertheless, such convergence is assured if no switching time insertions or deletions are encountered. Furthermore, convergence to a solution which satisfies the necessary conditions for a local minimum will be attained in most instances even if switching time insertions or deletions are encountered during the search.

H. Summary of Algorithm Steps

It is useful to summarize the steps which are followed in the determination of an optimal solution, using the algorithm presented herein:

(1) An initial feasible solution must be found. The number of segments $w \geq p$ is selected, and the r active constraints for each segment are chosen. The p segments which are varied in order to satisfy the p terminal constraints are also chosen. The initial feasible solution is obtained by iterating on the p variable switching times until the p terminal constraints are satisfied to desired accuracy. (2) The Lagrange multipliers corresponding to the initial feasible solution are calculated by using the procedure described in

Chapter III. The necessary conditions for optimality are calculated from functions of the Lagrange multipliers. (3) If the necessary conditions for optimality are not satisfied, additional control segments are added (if required) and the values of the (w - p) switching times are used in conjunction with a parameter optimization (gradient search) procedure to improve the initial feasible solution.

CHAPTER IV. PIECEWISE-LINEAR MODELS

An important special case of the problem considered in chapters II and III is when the performance index, system equations and path constraints are all linear in both the state and the control. This case occurs frequently in practice because linear approximations to complex dynamic systems are readily available. Furthermore, solutions to linear problems are easier and less costly to obtain because the system and Euler-Lagrange equations may be represented by transition matrices.

If the actual system is only slightly nonlinear, a single linear approximation to the nonlinear system may suffice over the full operating range. However, if greater accuracy is desired and/or the actual system is very nonlinear, a series of linear models may be used, each of which is obtained by linearizing about a different equilibrium point. Linear equations are still used to describe the system at each state point, but the coefficients in the linear model vary from point to point. Such a model is called a piecewise linear model.

In this chapter, linear and piecewise linear models will be considered. Although the development of chapters II and III is fully applicable to this problem, significant results for the linear problem will be repeated here because of the importance of this special case. The one-piece linear model will be considered first; then, the piecewise linear model will be considered.

A. Linear Model

The problem to be considered is to find the control $u(t)$ which minimizes the functional

$$J = \phi[x(t_f), t_f] + \int_{t_0}^{t_f} (a^T x + b^T u)\,dt \tag{4.1}$$

subject to the system differential equations

$$\dot{x} = Fx + Gu + h \tag{4.2}$$

and path inequality constraints

$$c_i^T x + d_i^T u + e_i \leq 0 \qquad i = 1, 2, \ldots, q \tag{4.3}$$

Here, the vectors a, b, c_i, d_i, and h, and the matrices F and G, are all constant. The terminal constraints on the state are given by (2.4). The Hamiltonian for the linear problem is

$$H = a^T x + b^T u + \lambda^T(Fx + Gu + h) + \sum_{i=1}^{q} \mu_i (c_i^T x + d_i^T u + e_i) \tag{4.4}$$

and the resulting Euler-Lagrange equations are

$$\dot{\lambda}^T = -a^T - \lambda^T F - \sum_{i=1}^{q} \mu_i c_i^T \tag{4.5}$$

The Lagrange multipliers must satisfy terminal conditions (2.7) and (2.8). The optimal control is determined from

$$b^T + \lambda^T g + \sum_{i=1}^{q} \mu_i d_i^T = 0 \tag{4.6}$$

where

$$\mu_i \begin{cases} > 0 & \text{if} \quad c_i^T x + d_i^T u + e_i = 0 \\ = 0 & \text{if} \quad c_i^T x + d_i^T u + e_i < 0 \end{cases}$$

We assume, as in chapter II, that the solution is nonsingular and the active constraints and optimal control have been determined from (4.6) and (2.3). The active constraints are formed into matrices as follows:

$$C = \begin{pmatrix} c_1^T \\ --- \\ \\ --- \\ c_r^T \end{pmatrix} \qquad D^T = \begin{pmatrix} d_1^T \\ --- \\ \\ --- \\ d_r^T \end{pmatrix}$$

and the optimal control is given by

$$u = -D^{-T}Cx \tag{4.7}$$

The multipliers μ are given by

$$\mu = -D^{-1}(b + G^T\lambda) \tag{4.8}$$

Substitution of (4.7) and (4.8) into (4.2) and (4.5) results in

$$\dot{x} = (F - GD^{-T}C)x + h \tag{4.9}$$

$$\dot{\lambda}^T = -(a^T - b^T D^{-T}C) - \lambda^T(F - GD^{-T}C) \tag{4.10}$$

Determination of the feasible trajectory and Lagrange multipliers proceeds exactly as in chapter III. However, the sensitivity vectors defined in (3.1) and (3.5) as well as solutions to the system equations and Euler-Lagrange equations, may be represented by transition matrices because the equations are linear. For example, (3.1) becomes

$$\frac{d}{dt}\left(\frac{\partial x}{\partial t_i}\right) = (F - GD^{-T}C)\left(\frac{\partial x}{\partial t_i}\right)$$

which has the general form

$$\frac{dP}{dt} = M + NP; \qquad P(0) = P_0 \tag{4.11}$$

where P and M are $(n \times 1)$ vectors and N is an $(n \times n)$ matrix. The solution of (4.11) is given by

$$P(t) = \Phi(t)P_0 + \int_0^t \Phi(t - \tau)M\, dt \tag{4.12}$$

or

$$P(t) = \Phi(t)P_0 + N^{-1}[\Phi(t) - I]M$$

where

$$\dot{\Phi} = N\Phi$$

with initial condition

$$\Phi(0) = I$$

Also, $\Phi(t)$ may be calculated from

$$\Phi(t) = T\Lambda(t)T^{-1}$$

where

$$\Lambda(t) = \mathrm{diag}\left[e^{\lambda_1 t}, \ldots, e^{\lambda_n t}\right]$$

λ_i is the ith eigenvalue of N, and the ith column of T is the ith eigenvector of N.

B. Piecewise-Linear Modeling

The desirability of using linear equations to model a system is obvious. Nevertheless, the actual system may be so nonlinear that a linear system description is not sufficiently accurate over the full

range of interest. In such cases, it is possible to increase model accuracy while retaining the advantages of linear modeling by using a piecewise-linear system model.

Suppose, for example, the nonlinear system is linearized about a number of equilibrium points. In the neighborhood of each equilibrium point, we have

$$\dot{x} = F_j(x - x_{ej}) + G_j(u - u_{ej}) \tag{4.13}$$

where x_{ej} and u_{ej} are the equilibrium values of state and control at the equilibrium point j. The system matrices F_j and G_j also differ, in general, for each equilibrium point. The path constraints may also be linearized about each equilibrium point to yield

$$c_{ij}^T(x - x_{ej}) + d_{ij}^T(u - u_{ej}) + e_{ij} \leq 0 \qquad i = 1, 2, \ldots, q \tag{4.14}$$

The path constraint vectors c_{ij} and d_{ij} also differ for each equilibrium point.

With a piecewise linear model, the system is described by linear equations at each state point, but the linear system coefficients vary from one point to another. A question that arises is which equilibrium model applies best for a given state, x? It is natural to choose the equilibrium point which is closest to x in some sense. Since the various states do not necessarily have the same physical dimension, a normalized distance function is used to determine which equilibrium point is closest. For a given state x, the distance functions

$$I_j = (x - x_{ej})^T W (x - x_{ej}) \tag{4.15}$$

are calculated for each equilibrium point j, and the equilibrium point is chosen for which I_j is a minimum.

Since the I_j are continuous functions of x, model switches (say, from j to k) occur when $I_j = I_k$ or

$$(x - x_{ej})^T W(x - x_{ej}) = (x - x_{ek})^T W(x - x_{ek})$$

Simplification of this expression results in

$$2(x_{ek}^T - x_{ej}^T)Wx = x_{ek}^T W x_{ek} - x_{ej}^T W x_{ej}$$

If we define

$$S_{jk} \triangleq \alpha_{jk}^T x - \beta_{jk} \tag{4.16}$$

where

$$\alpha_{jk}^T \triangleq 2\left(x_{ek}^T - x_{ej}^T\right)W \tag{4.17}$$

and

$$\beta_{jk} \triangleq x_{ek}^T W x_{ek} - x_{ej}^T W x_{ej}$$

then, switches between equilibrium models j and k occur at

$$S_{jk} = 0 \tag{4.18}$$

Although (4.16) is linear in x, iterative solution is generally required to find the switching points, since x is not a linear function of time.

C. Necessary Conditions for Optimality

The problem to be solved is to minimize

$$J = \phi[x(t_f), t_f] + \int_{t_0}^{t_f} (a^T x + b^T u)\,dt$$

subject to the system differential equations

$$\dot{x} = F_j(x - x_{ej}) + G_j(u - u_{ej})$$

and path inequality constraints

$$c_{ij}^T(x - x_{ej}) + d_{ij}^T(u - u_{ej}) + e_{ij} \leq 0$$

$$i = 1, 2, \ldots, q$$

where the linear model index j is determined from

$$\min_j (x - x_{ej})^T W (x - x_{ej})$$

At switching points between models j and k, we have

$$S_{jk} = \alpha_{jk}^T x - \beta_{jk}$$

where α_{jk} and β_{jk} are defined by (4.17). The Hamiltonian is defined as

$$H = a^T x + b^T u + \lambda^T [F_j(x - x_{ej}) + G_j(u - u_{ej})]$$

$$+ \sum_{i=1}^{q} \mu_i [c_{ij}^T (x - x_{ej}) + d_{ij}^T (u - u_{ej}) + e_{ij}]$$

and the Euler-Lagrange equations are

$$\dot{\lambda}^T = -a^T - \lambda^T F_j - \sum_{i=1}^{q} \mu_i c_{ij}^T$$

where the model index j is the same function of time as determined by integration of the system equations. In addition, it is shown in reference 15 that the Lagrange multipliers are discontinuous at model switching points, the jump in λ being given by

$$\lambda(t_s^+) = \lambda(t_s^-) + \varepsilon\alpha_{jk} \tag{4.19}$$

where t_s is the time at which the model subscript changes from j to k. Furthermore, since the switching time is not specified a priori, the Hamiltonian must be continuous at $t = t_s$. Therefore, we must have

$$b^T u(t_s^+) + [\lambda(t_s^-) + \varepsilon\alpha_{jk}]^T \dot{x}(t_s^+) = b^T u(t_s^-) + \lambda^T(t_s^-)\dot{x}(t_s^-) \tag{4.20}$$

which gives

$$\varepsilon = \frac{\lambda^T(t_s^-)[\dot{x}(t_s^-) - \dot{x}(t_s^+)] + b^T[u(t_s^-) - u(t_s^+)]}{\alpha_{jk}^T \dot{x}(t_s^+)} \tag{4.21}$$

The equations (4.6) for determination of u, the equations (4.7) and (4.8) for u and μ, and the equations (4.9) and (4.10) for the working forms of the system and Euler-Lagrange equations, all apply to the piecewise-linear model, but with the appropriate model subscript j added.

D. Initial Feasible Trajectory

Calculation of the initial feasible trajectory proceeds in the same manner as in chapter III, except that the model switches must be made at the appropriate times. Also, the calculation of the partial derivatives $\partial\psi_j/\partial t_i$ in (3.2) must be modified. Suppose the junction time t_i is perturbed slightly and there is a model switching time $t_s > t_i$. Since t_s is determined by satisfying (4.18), the change in t_i causes t_s to change. Therefore, the change in t_i not only affects the ψ_j directly as in (3.2), but also indirectly through the effect of a change in t_s on ψ_j.

Specifically, a change in t_i causes $x(t_s)$ to change by

$$dx(t_s) = \frac{\partial x_s}{\partial t_i} dt_i \tag{4.22}$$

where $\partial x_s/\partial t_i$ is obtained by integration of (3.1) from t_i to t_s. The resulting change in the model switching function S is

$$dS = \alpha^T dx(t_s) = \alpha^T \frac{\partial x_s}{\partial t_i} dt_i \tag{4.23}$$

This change in S must be canceled by a change in t_s. Therefore, we have

$$dS = \alpha^T \frac{\partial x_s}{\partial t_i} dt_i + \alpha^T \dot{x}(t_s^-) dt_s = 0$$

from which it follows that

$$\frac{\partial t_s}{\partial t_i} = - \frac{\alpha^T \frac{\partial x_s}{\partial t_i}}{\alpha^T \dot{x}(t_s^-)} \tag{4.24}$$

Therefore, $\partial\psi_j/\partial t_i$ is given by

$$\frac{\partial \psi_j}{\partial t_i} = \frac{\partial \psi_j}{\partial x_f} \left[\frac{\partial x_f}{\partial t_i} - \frac{\partial x_f}{\partial t_s} \left(\frac{\alpha^T \frac{\partial x_s}{\partial t_i}}{\alpha^T \dot{x}(t_s^-)} \right) \right] \tag{4.25}$$

E. Calculation of Lagrange Multipliers

The procedure for calculating the Lagrange multipliers corresponding to the initial feasible solution differs from that employed in chapter III, because of the jumps which occur in the multipliers at model switching times, as given by (4.19) to (4.21). For simplicity, we consider the case in which there is a single model switching point. The procedure which will be derived can be extended to the case of multiple model switches. At a model switching point, we have

$$\lambda^T(t_s^+) = \lambda^T(t_s^-) + \varepsilon\alpha_{jk} \tag{4.19}$$

As in chapter III, the value of H must be continuous at the $(p - 1)$ variable junction points, $t = t_1, \ldots, t_{p-1}$. In addition, for final

time free, equation (3.4) must also be satisfied.

Except at t_s, the requirement for continuity of H is achieved by satisfying (3.3). The requirement for continuity of H at $t = t_s$ requires special consideration because of the change in the system equations, and can be expressed as

$$\Delta H = b^T[u(t_s^+) - u(t_s^-)] + \lambda^T(t_s^-)[\dot{x}(t_s^+) - \dot{x}(t_s^-)] + \varepsilon\alpha_{jk}^T\dot{x}(t_s^+) \qquad (4.26)$$

In order to solve for ε and the p values of ν, we find $(p + 2)$ backward solutions of the $\dot{\lambda}$ equation (2.13). The first $(p + 1)$ of these solutions are identical to (3.5); $\lambda^{(p+1)}(t)$ is obtained by integrating (2.13) backward, starting at $t = t_s$, with initial conditions

$$\lambda^{(p+1)}(t_s) = -\alpha_{jk}$$

By superposition, $\lambda(t)$ is given by

$$\lambda(t) = \lambda^{(0)}(t) + \Lambda(t)\nu + \varepsilon\lambda^{(p+1)}(t) \qquad (4.27)$$

The $(p + 1)$ equations for the determination of ε and ν are given by

$$[u(t_i^+) - u(t_i^-)]^T[b(t_i) + g^T(t_i)\lambda^{(0)}(t_i) + g^T(t_i)\Lambda(t_i)\nu$$

$$+ g^T(t_i)\lambda^{(p+1)}(t)\varepsilon] = 0 \qquad i = 1, \ldots, (p - 1) \qquad (4.28)$$

$$[u(t_s^+) - u(t_s^-)]^T b(t_s) + [\dot{x}(t_s^+) - \dot{x}(t_s^-)]^T[\lambda^{(0)}(t_s) + \Lambda(t_s)\nu]$$

$$+ \dot{x}(t_s^+)^T\alpha_{jk}\varepsilon = 0 \qquad (4.29)$$

$$a(t_f) - b^T(t_f)D^{-T}(t_f)C(t_f) + \frac{d\phi}{dt}(t_f) + \left[\frac{d\psi}{dt}(t_f)\right]^T \nu = 0$$

(4.30)

The calculation of ν and ε proceeds exactly as in (3.10) to (3.12) and will not be repeated here.

F. Improvement of Feasible Trajectory

Equations (3.14) to (3.17) used to reconverge the trajectory at each iteration of the improvement phase must also be modified because of the variable model switching times. Suppose there is a model switching time such that $t_{sw} < t_s$. Then, if t_{sw} is modified, the effect on the model switching function S is given by

$$\Delta S = \alpha^T \Delta x(t_s) \tag{4.31}$$

where $\Delta x(t_s)$ is obtained by integration of (3.16) from t_{sw} to t_s, with initial conditions given by (3.14). The change in S must be canceled by a change in t_s. The result is

$$\Delta t_s = \frac{-\alpha^T \Delta x(t_s)}{\alpha^T \dot{x}(t_s^-)} \tag{4.32}$$

The terminal conditions ψ_j are altered due to the direct effect of the change in t_{sw}, and indirectly due to the change in t_s. The total change in ψ_j is given by

$$\Delta\psi_j = \frac{\partial\psi_j}{\partial x_f}\left[\Delta x(t_f) - \frac{\partial x_f}{\partial t_s}\frac{\alpha^T \Delta x(t_s)}{\alpha^T \dot{x}(t_s^-)}\right] \tag{4.33}$$

where $\Delta x(t_f)$ is obtained by integration of (3.16) from t_{sw} to t_f, with initial conditions given by (3.14), and $\partial x_f/\partial t_s$ is obtained by integrating (3.1a) subject to initial conditions (3.1b), for $t_i = t_s$.

The change in ψ_j must be canceled by appropriate changes in the t_i. As in (3.17), this results in

$$\Delta t_i = -\left(\frac{\partial \psi_j}{\partial t_i}\right)^{-1} \frac{\partial \psi_j}{\partial x_f} \left[\Delta x(t_f) - \frac{\partial x_f}{\partial t_s} \frac{\alpha^T \Delta x(t_s)}{\alpha^T \dot{x}(t_s^-)}\right] \tag{4.34}$$

CHAPTER V. DEMONSTRATIVE EXAMPLE

The ideas developed in chapters II through IV are illustrated in this chapter with the aid of numerical examples. First, a problem will be solved in which the system equations are nonlinear in the state and linear in the control. The possibility of minimizing singular arcs will be discussed. Next, the same problem will be solved by using one- and two-piece linear approximations to the original system equations. Solutions will be obtained for two different sets of terminal state constraints, and both one and two control variable problems will be solved.

A. Problem Statement

Consider the problem of finding $u(t)$ which transfers the system

$$\begin{aligned} \dot{x} &= -x^2 + u \\ \dot{y} &= -4y + u \end{aligned} \tag{5.1}$$

subject to the control limits $|u| \leq 2$ from initial conditions $(x_0,y_0) = (1,1)$ to terminal conditions $(x_f,y_f) = (0,0)$ in minimum time.

We have in (2.1), (2.3), and (2.4)

$$\begin{aligned} \phi &= t_f, & a &= b = 0 \\ c_1 &= -2, & d_1 &= -1 \\ c_2 &= -2, & d_2 &= 1 \\ \psi_1 &= x_f, & \psi_2 &= y_f \end{aligned} \tag{5.2}$$

The Hamiltonian (2.5) is

$$H = \lambda_x(-x^2 + u) + \lambda_y(-4y + u) + \mu_1(-2 - u) + \mu_2(-2 + u) \quad (5.3)$$

and the Euler Lagrange equations are

$$\begin{aligned} \dot{\lambda}_x &= 2\lambda_x x \\ \dot{\lambda}_y &= 4\lambda_y \end{aligned} \quad (5.4)$$

The control is determined from

$$\min_u (\lambda_x + \lambda_y)u \quad (5.5)$$

which results in

$$u = -2 \operatorname{sgn}(\lambda_x + \lambda_y) \quad (5.6)$$

The terminal conditions on the Lagrange multipliers are

$$\begin{aligned} \lambda(t_f) &= \nu \\ H(t_f) &= -1 \end{aligned} \quad (5.7)$$

B. Nonexistence of Singular Arc

The optimal control is determined from (5.6) unless $(\lambda_x + \lambda_y) \equiv 0$. In this case, the control is determined by successively differentiating $(\lambda_x + \lambda_y)$ with respect to time until the control appears explicitly. This procedure results in

$$\begin{aligned} \frac{d}{dt}(\lambda_x + \lambda_y) &= 2\lambda_x x + 4\lambda_y = 0 \\ \frac{d^2}{dt^2}(\lambda_x + \lambda_y) &= 2\lambda_x x^2 + 2\lambda_x u + 16\lambda_y = 0 \end{aligned} \quad (5.8)$$

Simultaneous solution of $(\lambda_x + \lambda_y) = 0$ and (5.8) results in two possibilities for a singular arc. First, we may have $x = 2$ and $u = 4$. However, this is not possible, since we must have $|u| \leq 2$. The second

possibility is that $\lambda_x \equiv \lambda_y \equiv 0$. In this case, we would have $H = 0$ and since the system is autonomous, $H \equiv 0$. However, this is inconsistent with $H(t_f) = -1$ in (5.7). Therefore, there can be no singular arc for this problem.

C. Initial Feasible Solution

Since there are two terminal constraints and the terminal time is free, the initial feasible trajectory must have two segments. The only possible control for these segments is $u = \pm 2$. Therefore, we assume tentatively that the optimal control history is given by

$$\begin{aligned} u &= -2, \qquad 0 \le t \le t_1 \\ u &= 2, \qquad t_1 \le t \le t_f \end{aligned} \tag{5.9}$$

with t_1 and t_f to be determined such that $x_f = y_f = 0$. The state equations (5.1) can be integrated in closed form when (5.9) is used as the control. The result is

$$\begin{aligned} x(t_1) &= \frac{1 - \sqrt{2}\tan\sqrt{2}\,t_1}{1 + \frac{1}{\sqrt{2}}\tan\sqrt{2}\,t_1} \\ y(t_1) &= -\frac{1}{2}\left(1 - e^{-4t_1}\right) + e^{-4t_1} \end{aligned} \tag{5.10}$$

Iterative solution of (5.10) for t_1 and t_f such that $x(t_f) = y(t_f) = 0$ results in

$$t_1 = 0.56, \qquad t_f = 0.69$$

D. Calculation of Lagrange Multipliers

For this problem, we have $\partial\phi/\partial x = 0$ and $\partial\psi/\partial x = I$. Therefore, $\lambda(t_f) = \nu$. We must integrate (5.4) backward with three sets of initial conditions $-\lambda^{(0)}(t_f) = \begin{pmatrix}0\\0\end{pmatrix}$, $\lambda^{(1)}(t_f) = \begin{pmatrix}1\\0\end{pmatrix}$, $\lambda^{(2)}(t_f) = \begin{pmatrix}0\\1\end{pmatrix}$ in order to

find $\Lambda(t_1)$ and $\lambda^{(0)}(t_1)$. Equations (5.4) may be integrated in closed form as follows:

$$\left.\begin{aligned} \lambda_y(t) &= \lambda_y(t_f)e^{4(t-t_f)} \\ \lambda_x(t) &= \frac{-2\lambda_x(t_f) - 2\lambda_y(t_f) - \lambda_y(t)[-4y(t) + 2]}{-x^2(t) + 2} \end{aligned}\right\} \quad t \geq t_1$$

Therefore, we obtain

$$\lambda^{(0)}(t_1) = \begin{pmatrix} 0 \\ 0 \end{pmatrix}, \qquad \lambda_1(t_1) = \begin{pmatrix} 1.035 \\ 0 \end{pmatrix}, \qquad \lambda_2(t_1) = \begin{pmatrix} 0 \\ 0.595 \end{pmatrix}$$

Equations (3.8) and (3.9) give

$$4 \quad (1,1) \begin{pmatrix} 1.035 & 0 \\ 0 & 0.595 \end{pmatrix} \begin{pmatrix} \nu_1 \\ \nu_2 \end{pmatrix} = 0$$

and

$$(2,2) \begin{pmatrix} \nu_1 \\ \nu_2 \end{pmatrix} = -1$$

which can be expanded to give

$$1.035\ \nu_1 + 0.595\ \nu_2 = 0$$

$$\nu_1 + \nu_2 = -0.5$$

Solving for ν_1 and ν_2 yields

$$\nu_1 = 0.676, \qquad \nu_2 = -1.176$$

Therefore, from (5.7) we have

$$\lambda_x(t_f) = 0.676, \qquad \lambda_y(t_f) = -1.176 \tag{5.11}$$

From this problem, the state equations and Euler-Lagrange equations can be integrated in closed form. The result is

$$\left.\begin{aligned}
\lambda_y(t) &= -1.176\, e^{4(t-t_f)} \\
\lambda_x(t) &= \frac{-1 - \lambda_y(t)[-4y(t) + 2]}{-x^2(t) + 2} \\
x(t) &= \frac{-0.252 + 1.414 \tanh \sqrt{2}\,(t - t_1)}{1 - 0.178 \tanh \sqrt{2}\,(t - t_1)} \\
y(t) &= 0.5\left[1 - e^{-4(t-t_1)}\right] - 0.340\, e^{-4(t-t_1)}
\end{aligned}\right\} \quad t_1 \le t \le t_f \qquad (5.12)$$

$$\left.\begin{aligned}
\lambda_y(t) &= -0.699\, e^{4(t-t_1)} \\
\lambda_x(t) &= \frac{1 - \lambda_y(t)[4y(t) + 2]}{x^2(t) + 2} \\
x(t) &= \frac{1 - 1.414 \tan \sqrt{2}\, t}{1 + 0.707 \tan \sqrt{2}\, t} \\
y(t) &= -0.5(1 - e^{-4t}) + e^{-4t}
\end{aligned}\right\} \quad 0 \le t \le t_1 \qquad (5.13)$$

E. Optimality of Initial Feasible Solution

The initial feasible trajectory was obtained under the tentative assumption that the optimal $u(t)$ is given by (5.9). According to (5.6), this control strategy is optimal only if

$$\begin{aligned}
\lambda_x + \lambda_y &> 0, \qquad 0 \le t \le t_1 \\
\lambda_x + \lambda_y &< 0, \qquad t_1 \le t \le t_f
\end{aligned} \qquad (5.14)$$

To determine if this is the case, $(\lambda_x + \lambda_y)$ is calculated as a function of time from (5.12) and (5.13). The result is plotted in figure 5.1, and shows that for this problem, the necessary conditions for opti-

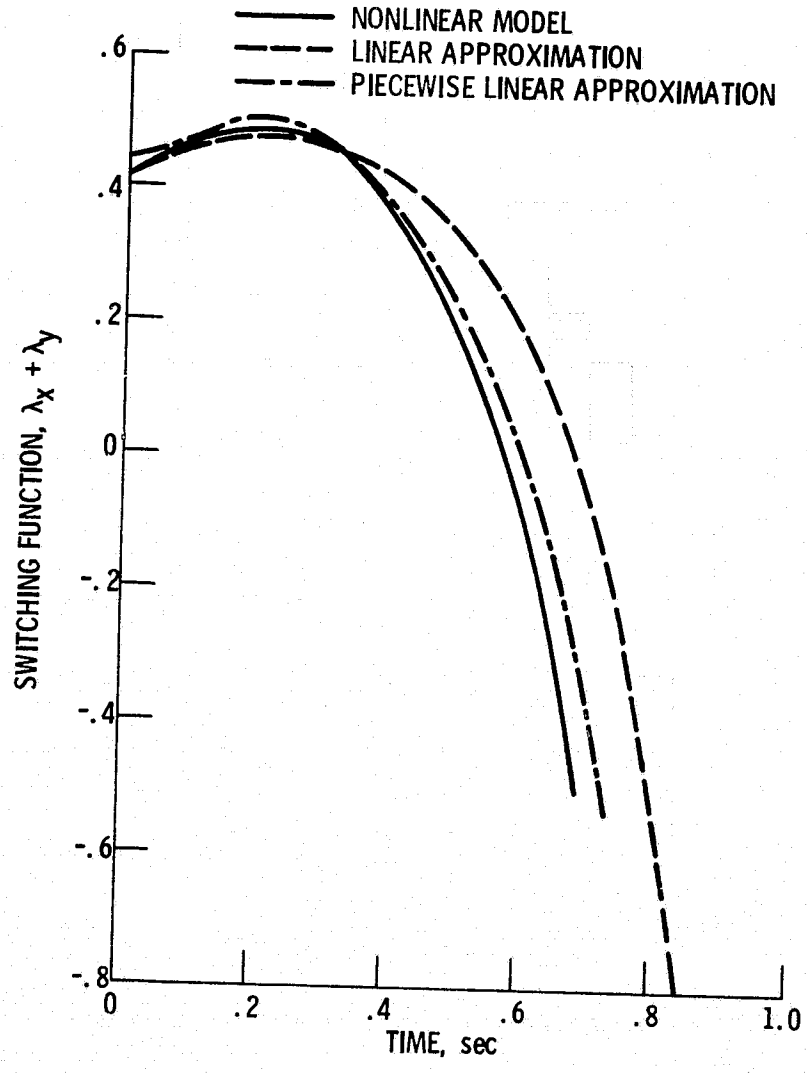

Figure 5.1. - Switching function as a function of time for initial feasible trajectory.

mality are satisfied by the initial feasible trajectory. Therefore, no further improvement needs to be made. The optimal trajectory, $x(t)$ and $y(t)$, is shown in figure 5.2.

F. Linear Approximation

The nonlinear system equations (5.1) may be approximated by linear equations. Actually, since the $\dot{y}$ equation is already linear, only the $\dot{x}$ equation needs to be approximated. If we choose to linearize the $\dot{x}$ equation about $x = 0.5$, the result is

$$\begin{aligned} \dot{x} &\cong -2x\Big|_{x=0.5} (x - 0.5) + (u - 0.25) \\ &= -x + u + 0.25 \end{aligned} \tag{5.15}$$

For this linearized model, the Hamiltonian is

$$H = \lambda_x(-x + u + 0.25) + \lambda_y(-4y + u) + \mu_1(-2 - u) + \mu_2(-2 + u) \tag{5.16}$$

and the Euler-Lagrange equations are

$$\begin{aligned} \dot{\lambda}_x &= \lambda_x \\ \dot{\lambda}_y &= 4\lambda_y \end{aligned} \tag{5.17}$$

As previously, the initial feasible trajectory is obtained by assuming (5.9) is the optimal control strategy. Solution of the resulting boundary value problem for t_1 and t_f yields

$$t_1 = 0.68, \qquad t_f = 0.827$$

The solution of equation (3.7) is given by

$$\Lambda(t_1) = \begin{pmatrix} 0.863 & 0 \\ 0 & 0.555 \end{pmatrix}$$

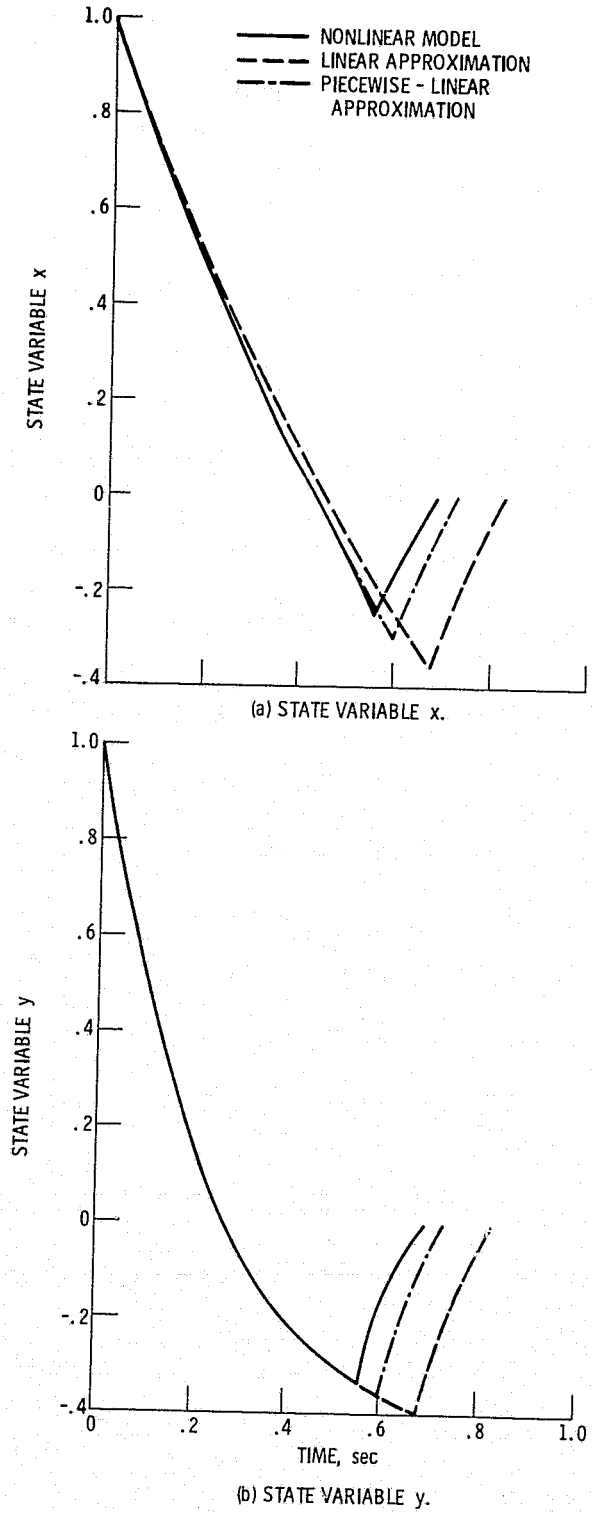

(a) STATE VARIABLE x.

(b) STATE VARIABLE y.

Figure 5.2. - Initial feasible trajectory for example problem.

and equations (3.8) and (3.9) are evaluated to give

$$\nu_1 = 1.163, \qquad \nu_2 = -1.808$$

from which it follows that

$$\lambda_x(t_f) = 1.163, \qquad \lambda_y(t_f) = -1.808$$

Since the boundary conditions are known, the system and Euler-Lagrange equations can be integrated to give x, y, λ_x, and λ_y as functions of time. The switching function $(\lambda_x + \lambda_y)$ is shown in figure 5.1, and the optimal trajectory is shown in figure 5.2. As was the case when the nonlinear equations were used, the initial feasible trajectory is a local minimum in the present case also.

G. Piecewise-Linear Approximation

Comparison of the nonlinear and approximate linear results in figures 5.1 and 5.2 shows that the linear approximation does not give a very accurate representation of the nonlinear system for the present problem. The approximation may be improved by using a piecewise linear model, as described in chapter IV. If we choose $x = 0.25$ and $x = 0.75$ as the equilibrium values about which linear models will be derived, the resulting linear models are

$$\begin{aligned} \mathring{x} &= -\frac{x}{2} + u + \frac{1}{16} \left(\text{valid near} \quad x = \frac{1}{4}\right) \\ \mathring{x} &= -\frac{3}{2}x + u + \frac{9}{16} \left(\text{valid near} \quad x = \frac{3}{4}\right) \end{aligned} \tag{5.18}$$

Since the $\dot{y}$ equation is linear, the weighting matrix W in (4.15) is chosen to be

$$W = \begin{pmatrix} 1 & 0 \\ 0 & 0 \end{pmatrix} \tag{5.19}$$

This choice of W results in a model switching function (see (4.16) and (4.17)) of

$$S = x - \frac{1}{2} \tag{5.20}$$

The Euler-Lagrange equations are

$$\begin{aligned} \dot{\lambda}_x &= \frac{1}{2}\lambda_x, & x &\leq 0.5 \\ \dot{\lambda}_x &= \frac{3}{2}\lambda_x, & x &\geq 0.5 \\ \dot{\lambda}_y &= 4\lambda_y \end{aligned} \tag{5.21}$$

At the model switching point, there is a jump discontinuity in λ_x:

$$\lambda_x(t_s^+) = \lambda_x(t_s^-) + \varepsilon \tag{5.22}$$

where ε is determined from (4.20)

$$\varepsilon = \frac{\lambda_x(t_s^-)\left[-\frac{3}{2}(0.5) + \frac{9}{16} + \frac{1}{2}(0.5) - \frac{1}{16}\right]}{-\frac{1}{2}(0.5) + 2 + \frac{1}{16}}$$

Which results in $\varepsilon = 0$ for this problem.

Based on the earlier solutions presented in figures 5.1 and 5.2, it appears that the model switch will take place prior to the change of control at $t = t_1$. Therefore, we assume that $t_s < t_1$ and look for a feasible solution with control given by (5.9). Solution of the multipoint boundary value problem gives

$$t_s = 0.197, \qquad t_1 = 0.597, \qquad t_f = 0.733$$

The solution of equation (3.7) is

$$\Lambda(t_1) = \begin{pmatrix} 0.934 & 0 \\ 0 & 0.580 \end{pmatrix}$$

and equations (3.8) and (3.9) are solved to give

$$\lambda_x(t_f) = \nu_1 = 0.863, \qquad \lambda_y(t_f) = \nu_2 = -1.390$$

Again, the trajectory and Euler-Lagrange equations are solved as a function of time, and the results are presented in figures (5.1) and (5.2). It can be seen that the two-piece linear model is a good representation of the actual nonlinear system for the present problem.

H. Additional Control Variable

Consider the following problem. Find $u(t)$ and $v(t)$ which transfers the system given by

$$\begin{aligned} \dot{x} &= -x + u + \gamma_x v + 0.25 \\ \dot{y} &= -4y + u + \gamma_y v \end{aligned} \tag{5.23}$$

from initial conditions $(x_0, y_0) = (1,1)$ to terminal conditions $(x_f, y_f) = (0,0)$ in minimum time. The controls are subject to the constraints

$$|u| \leq 2 \qquad \text{and} \quad 0 \leq v \leq 1$$

This problem is identical to the one-piece linear approximation of the original nonlinear example problem, except that there are now two control variables, u and v. The coefficients γ_x and γ_y will be left unspecified temporarily.

Since there are two terminal constraints, the initial feasible trajectory must have two segments. The allowable control strategy for either of the two segments is $u = +2$ or -2 and $v = 0$ or 1. Suppose we choose for our control strategy

$$u = -2 \quad \text{and} \quad v = 0, \qquad 0 \leq t \leq t_1$$
$$u = +2 \quad \text{and} \quad v = 0, \qquad t_1 \leq t \leq t_f \tag{5.24}$$

Since we have chosen $v = 0$ for both segments, the initial feasible trajectory and Lagrange multiplier time histories are identical to those obtained earlier for the one-piece linear model, single control problem. The switching function $(\lambda_x + \lambda_y)$ for control u is shown in figure 5.1, and the trajectory is shown in figure 5.2.

For the present problem, we are interested not only in the optimality of $u_{fe}(t)$, but also in the optimality of $v_{fe}(t)$. The switching function for $v(t)$ is given by $(\gamma_x\lambda_x + \gamma_y\lambda_y)$; for optimal $v(t)$ we must have

$$v = 0 \quad \text{if } (\gamma_x\lambda_x + \gamma_y\lambda_y) > 0$$
$$v = 1 \quad \text{if } (\gamma_x\lambda_x + \gamma_y\lambda_y) < 0 \tag{5.25}$$

The time histories of λ_x and λ_y are shown in figure 5.3. The initial feasible trajectory is a local minimum if the values of γ_x and γ_y are such that $(\gamma_x\lambda_x + \gamma_y\lambda_y) > 0$ for the entire trajectory; for instance, this is the case if $\gamma_x = 1$ and $\gamma_y = 0.5$. On the other hand, if $\gamma_x = 1$ and $\gamma_y = 0.8$, the switching function $(\lambda_x + 0.8\ \lambda_y)$ is shown as a function of time in figure 5.4. For this case, $v = 0$ is the optimal control up to about $t = 0.75$ sec, but the negative value of the switching function for $t > 0.75$ sec indicates that t_f can be reduced if v is increased in this region.

In order to improve the trajectory (decrease the performance index, t_f) a third control segment is added to the trajectory. The third segment is made very short initially, so that the new trajec-

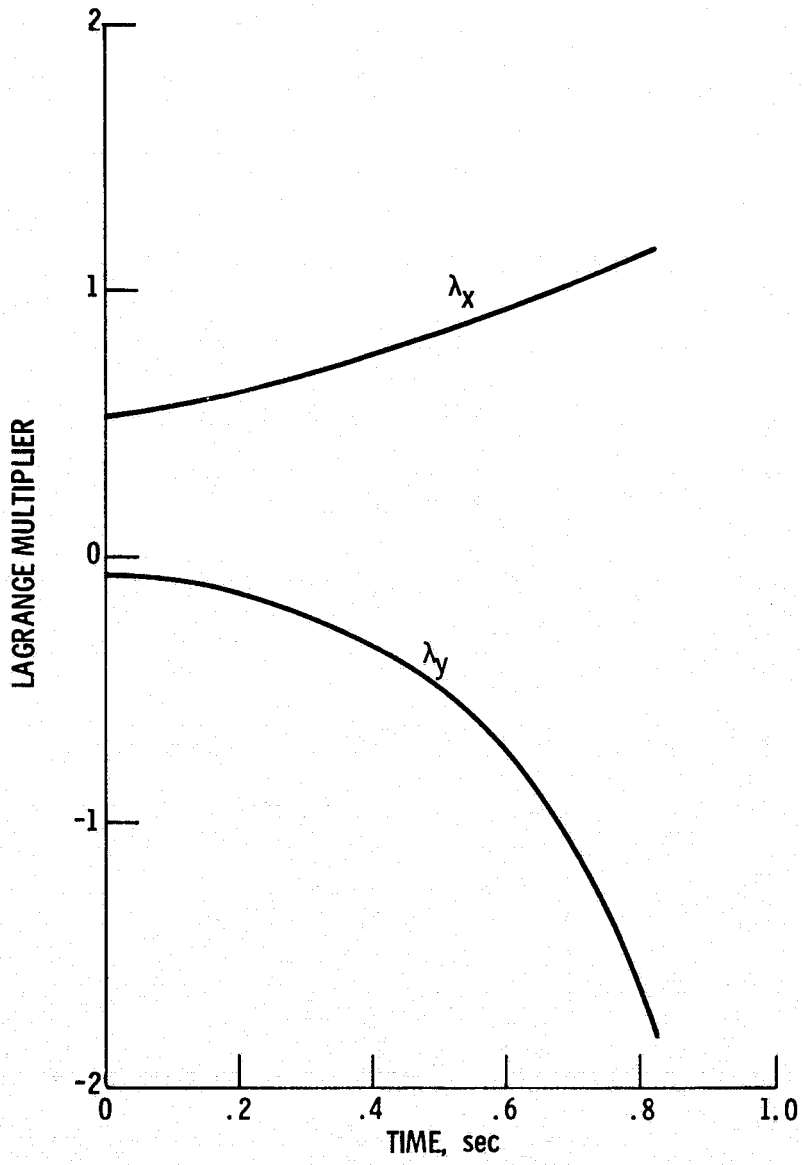

Figure 5.3. - Lagrange multiplier profiles for one-piece approximate model.

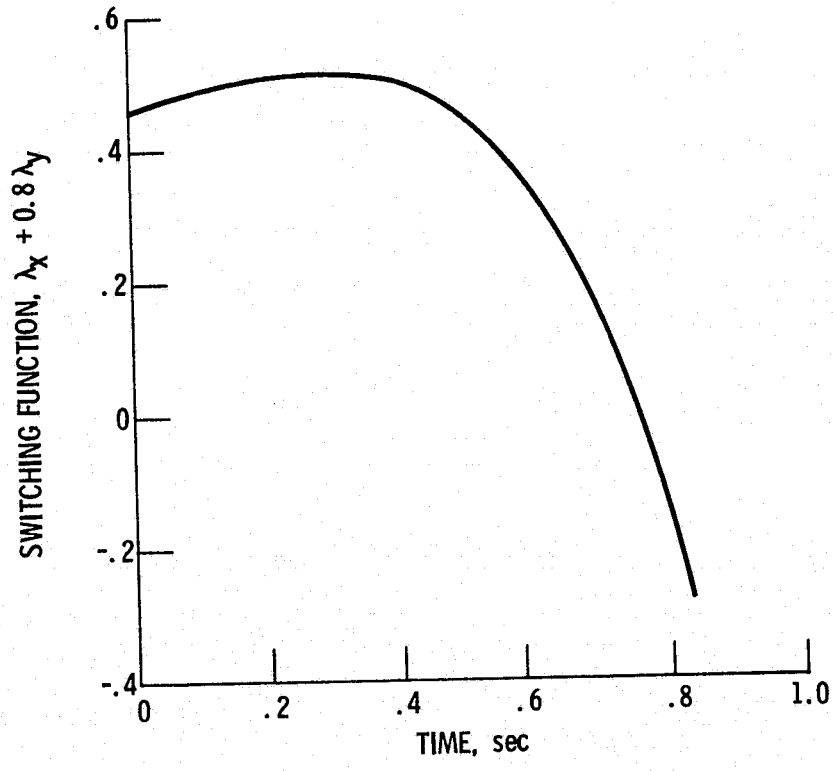

Figure 5.4. - Switching function for control v, $\lambda_x + 0.8\lambda_y$.

tory does not differ substantially from the initial feasible trajectory. Specifically, the control is chosen to be

$$u = -2 \quad \text{and} \quad v = 0, \qquad 0 \leq t \leq t_1$$

$$u = +2 \quad \text{and} \quad v = 0, \qquad t_1 \leq t \leq t_{sw}$$

$$u = +2 \quad \text{and} \quad v = 1, \qquad t_{sw} \leq t \leq t_f$$

where $t_{sw} = 0.8$ is selected, and held fixed while t_1 and t_f are varied to reconverge on the end conditions $x_f = y_f = 0$. The converged values of t_1 and t_f are given by

$$t_1 = 0.68, \qquad t_f = 0.819$$

It can be seen that t_f has been reduced from its value of 0.827 for the initial feasible trajectory. At this point, the Lagrange multiplier time history must be calculated for the new three segment trajectory, and the gradient of the performance index with respect to t_{sw} calculated by using (3.18). A nonlinear search technique such as presented in reference 11 is used to iteratively search for the value of t_{sw} for which t_f is a minimum. When this has been accomplished, the switching functions $(\lambda_x + \lambda_y)$ and $(\lambda_x + 0.8\ \lambda_y)$ should be examined once again to determine if t_f can be further reduced by including additional control segments in the trajectory.

CHAPTER VI. APPLICATION TO TURBOFAN CONTROL

In this chapter, the algorithm described in chapters III and IV is used to find optimal trajectories for an F100 aircraft turbofan engine. Specifically, values of the control variables are found as a function of time, which minimize the terminal error for a fixed-time acceleration, while adhering to the engine constraints. This is equivalent to minimizing acceleration time for a fixed terminal error. A suboptimal, closed loop control mode is also developed. Finally, the problem of minimizing steady-state specific fuel consumption is considered.

A. Engine Description

The following description of the F100 engine is taken largely from reference 18. The Pratt & Whitney F100 engine (fig. 6.1) is an axial, mixed-flow, augmented, twin-spool, low-bypass-ratio turbofan. A single inlet is used for both the fan airflow and engine core airflow. Airflow leaving the fan is separated into two streams: one stream passing through the engine core and the other stream passing through the annular fan duct. A three-stage fan is connected by a through-shaft to the two-stage, low-pressure turbine. A ten-stage compressor is connected by a hollow shaft to the two-stage, high-pressure turbine. The fan has variable, trailing-edge inlet guide vanes, which are positioned by the engine control system as a function of fan corrected speed to maintain fan stability at low speeds. The

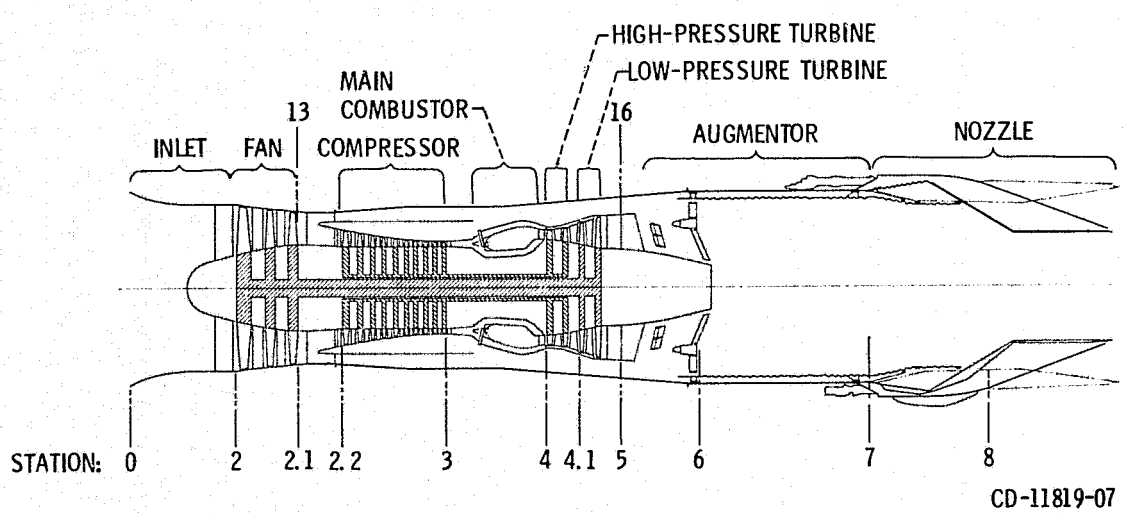

Figure 6.1. - Schematic representation of F100-PW-100 augmented turbofan engine.

compressor has a variable inlet guide vane followed by two variable stator vanes; the vanes are positioned as a function of compressor corrected speed. The engine core and fan duct streams combine in an augmentor and are discharged through a variable convergent-divergent nozzle.

The fuel control system meters fuel to the main combustor, as a function of power lever angle (PLA), compressor speed, fan discharge temperature and compressor discharge static pressure. Augmentor fuel flow is metered as a function of PLA, fan discharge temperature, and compressor discharge static pressure. Exhaust nozzle area is controlled so as to maintain a desired engine airflow during augmented operation.

B. Engine Models

Pratt & Whitney Aircraft (P&WA) has developed a detailed dynamic simulation of the F100 engine using a digital computer (ref. 14). The simulation includes overall performance maps of the engine components, variable gas properties, and Reynolds number effects in order to provide good steady-state accuracy over the range of power settings and flight conditions. Factors such as fluid momentum, mass and energy storage and rotor inertias are included to provide transient capability. A detailed simulation of the engine's control system is also included. In addition to transient capability, the simulation also has the capability to solve iteratively for equilibrium operating points for specified flight conditions and power lever angle.

A drawback to the use of detailed dynamic simulations on a digital computer is that they require large amounts of computer time to

obtain transient solutions. A requirement of several minutes of digital computer time per second of real time is typical. Szuch and Seldner (ref. 18) developed a hybrid computer simulation of the F100 engine which runs in real time. This simulation is useful for development and checkout of engine control system hardware and software. Some simplification is made in the hybrid model in order to allow the real time capability. Nevertheless, steady-state and transient results presented in reference 18 compare favorably both with the detailed P&WA digital simulation and with a limited amount of experimental data.

Because of the virtual impossibility of using nonlinear feedback control theory for realistic systems, control software is usually developed using linear models. For turbofan control system design, nonlinear dynamic simulations such as references 14 and 18 are linearized about various equilibrium conditions, and linear models obtained. This process produces equations of the form

$$\dot{x} = F(x - x_e) + G(u - u_e) \tag{6.1}$$

where x_e and u_e are equilibrium values of state and control, respectively. Other engine variables which are not modeled as states are also of interest. Such variables will be called outputs, and denoted by y. The linearized output equations are given by

$$y = y_e + C(x - x_e) + D(u - u_e) \tag{6.2}$$

If the outputs have upper (or lower) bounds which must not be exceeded, then combined state/control path inequality constraints of the form

$$y_e + C(x - x_e) + D(u - u_e) - y_{max} \leq 0$$
$$y_{min} - y_e - C(x - x_e) - D(u - u_e) \leq 0 \qquad (6.3)$$

are produced. Mechanical limits on the control variables also have the general form of (6.3) with $C = 0$.

The engine simulations of references 14 and 18 contain 16 and 17 state variables, respectively. Therefore, the state vector x in (6.1) has dimension 16 or 17, depending on which simulation is used to obtain the linear model. It is preferable to conduct control system studies by using lower-order models, if possible. Fortunately, in the present case, most of the eigenvalues (natural frequencies) of the system matrix F are considerably larger than the lowest eigenvalues. Therefore, quasi-steady approximation may be used to reduce the order of the system. A quasi-steady approximation technique which preserves the lower eigenvalues exactly, and also retains the desired states, is presented in appendix C.

In a recent contractual effort under joint Air Force/NASA sponsorship (ref. 8), Systems Control Inc. (SCI) used linear quadratic regulator theory to design controls for the F100 engine. Linear models having 16 states and reduced models having 5 states were provided to SCI by P&WA for a number of equilibrium points at different flight conditions and PLA's. Some of these linear models are given in reference 13.

Five of the five-state equilibrium models from the P&WA/SCI study, equally spaced along the sea-level-static (SLS) operating line, are used in the present report. The normalized linear model for

PLA = 67 degrees is shown in table I. The 67 degree power lever setting is typical of subsonic cruise; PLA is 20 degrees at idle, and 83 degrees at maximum nonaugmented thrust (also referred to as intermediate). The normalized equilibrium values of the states, controls, and outputs are given in table II, along with the definitions of these variables.

TABLE I. - FIVE-STATE LINEAR MODEL

[Sea level static, PLA = 67°]

$$F = \begin{pmatrix} -4.20 & 0.877 & -0.645 & 1.22 & 0.892 \\ -0.353 & -5.63 & -0.335 & -0.416 & .813 \\ 19.2 & -13.1 & -7.38 & -0.257 & 4.74 \\ 6.28 & -21.9 & -3.02 & -30.2 & 3.22 \\ 71.0 & 456 & 39.2 & -1.06 & -147 \end{pmatrix}$$

$$G = \begin{pmatrix} -0.573 & -0.0349 & -0.103 & -0.000639 \\ .976 & -0.0212 & -0.0256 & -0.00591 \\ 2.11 & -7.50 & .702 & .0138 \\ 32 & -0.281 & -0.174 & .0351 \\ 129 & 2.86 & 3.32 & 0.109 \end{pmatrix}$$

$$C = \begin{pmatrix} 0.856 & -0.666 & 0.154 & -0.0335 & 0.222 \\ 2.09 & 0.0292 & -0.0194 & 0.196E-3 & -0.00131 \\ 0.0531 & -0.349 & -0.0498 & .527E-3 & .0521 \\ 7.40 & 2.31 & -1.38 & .0148 & -0.0963 \\ -4.90 & 23.7 & .776 & .874E-2 & -3.62 \end{pmatrix}$$

$$D = \begin{pmatrix} 0.216 & -0.0135 & 0.0294 & -0.614E-4 \\ .210 & .0432 & .0799 & -0.560E-3 \\ .498 & -0.468E-2 & -0.303E-2 & .392E-3 \\ 1.65 & .139 & -0.669 & -0.438E-2 \\ 4.55 & .327 & -0.0187 & -0.107 \end{pmatrix}$$

In order to determine if the fifth-order models could be further reduced, the eigenvalues and eigenvectors of the fifth-order models were calculated. The results are presented in table III for PLA = 67 degrees. The eigenvectors are the columns of the symmetry transformation T as defined in appendix C. It can be seen that there

TABLE II. - EQUILIBRIUM VALUES OF PROBLEM VARIABLES

[Sea level static, PLA = 67°]

$$x_e = \begin{pmatrix} \text{Fan speed, } N_{fan}\text{, 100 rpm} \\ \text{Compressor speed, } N_{comp}\text{, 100 rpm} \\ \text{Augmentor pressure, Pt7, 0.1 psi} \\ \text{Fan turbine inlet temperature, FTIT, 10° R} \\ \text{Combustor pressure, } P_{s3}\text{, PSI} \end{pmatrix} = \begin{pmatrix} 94.39 \\ 121.70 \\ 330 \\ 187.1 \\ 290 \end{pmatrix}$$

$$u_e = \begin{pmatrix} \text{Combustor fuel flow, } W_f\text{, 100 lbm/hr} \\ \text{Exhaust nozzle area, } A_{noz}\text{, 0.01 ft}^2 \\ \text{Inlet guide vane position, IGV, 0.1 deg} \\ \text{High variable stator position, HVS, 0.01 deg} \end{pmatrix} = \begin{pmatrix} 68.60 \\ 298 \\ -164 \\ 92.2 \end{pmatrix}$$

$$y_e = \begin{pmatrix} \text{Thrust, T, 100 lb} \\ \text{Airflow, } w_a\text{, lbm/sec} \\ \text{Turbine inlet temperature, TIT, 100\%} \\ \text{Fan surge margin, SMFAN (0.001)} \\ \text{Compressor surge margin, SMCOMP (0.001)} \end{pmatrix} = \begin{pmatrix} 105.14 \\ 203 \\ 86.42 \\ 254 \\ 179 \end{pmatrix}$$

TABLE III. - EIGENVALUES AND EIGENVECTORS OF FIVE-STATE MODEL

[Eigenvalues = -3.42, -4.42 ≠ 2.91j, -30.8, -151 (sec^{-1})]

$$T = \begin{pmatrix} -0.0823 & 0.317\pm0j & -0.0463 & 0.00594 \\ -0.118 & 0.0508\pm0.0117j & .0152 & .00574 \\ -0.761 & 1.0\mp1.8j & .0496 & .0326 \\ .0884 & 0.00625\pm0.142j & .997 & .0281 \\ -0.626 & -0.587\mp0.470j & .0392 & -0.999 \end{pmatrix}$$

are three dominant eigenvalues, one real and a complex pair; the other two eigenvalues are at least a factor of six larger. Also, it appears from the T matrix that states four and five (FTIT and Ps3) are closely related to the two larger eigenvalues. Therefore, quasi-steady reduction was performed on the five state system, as described in appendix C, to reduce it to a three state system, with state variables N_{fan}, N_{comp}, and Pt7. It should be noted that these are the same three states used by Weinberg (ref. 6). The reduced three-state linear system matrices are presented in table IV. There are seven outputs for

TABLE IV. - THREE-STATE LINEAR MODEL

[Sea-level static, PLA = 67°]

$$F = \begin{pmatrix} -3.37 & 3.13 & -0.493 \\ -0.130 & -2.87 & -0.072 \\ -21.3 & 1.93 & -6.03 \end{pmatrix} \qquad x_e = \begin{pmatrix} N_{fan} \\ N_{comp} \\ Pt7 \end{pmatrix} = \begin{pmatrix} 94.38 \\ 121.70 \\ 330 \end{pmatrix}$$

$$G = \begin{pmatrix} 1.59 & -0.0354 & -0.0848 & -0.00155 \\ 1.17 & .0165 & -0.00795 & -0.00574 \\ 5.74 & -7.34 & .804 & .0173 \end{pmatrix}$$

$$C = \begin{pmatrix} 0.945 & 0.0511 & 219 \\ 2.09 & .0249 & -0.0198 \\ .0769 & -0.187 & -0.0353 \\ 7.37 & 2.00 & -1.42 \\ -6.54 & 12.3 & -0.245 \\ .351 & -0.465 & -0.0817 \\ .454 & 3.16 & .282 \end{pmatrix} \qquad y_e = \begin{pmatrix} T \\ W_a \\ TIT \\ SMFAN \\ SMCOMP \\ FTIT \\ PS3 \end{pmatrix} = \begin{pmatrix} 105.14 \\ 203 \\ 86.42 \\ 254 \\ 179 \\ 187.1 \\ 290 \end{pmatrix}$$

$$D = \begin{pmatrix} 0.361 & -0.00523 & 0.0342 & 0.807E-4 \\ .210 & .0432 & .0799 & -0.561E-3 \\ .541 & -0.00294 & -0.00191 & .436E-3 \\ 1.59 & .135 & -0.671 & -0.444E-2 \\ 1.53 & .206 & -0.0967 & -0.110 \\ 1.16 & -0.025 & -0.437E-3 & 0.119E-2 \\ .838 & .0335 & .0215 & .819E-3 \end{pmatrix}$$

the three state model, since the variables FTIT and Ps3 now have the role of outputs. The eigensystems for the four other linear models have the same qualitative features as observed in table IV, and the same quasi-steady reduction was performed on these models also.

C. Model Accuracy

A nonlinear model can be approximated by a suitable number of linear models at various equilibrium points. It is of interest to determine how many equilibrium models need to be used for suitable accuracy. One way to do this is to see how well the equilibrium conditions for one model are predicted by adjacent models. For example, if the equilibrium control from model 2 is used in model 1, the predicted equilibrium state for model 2, $\hat{x}_{e2}$, is given by

$$0 = F_1(\hat{x}_{e2} - x_{e1}) + G_1(u_{e2} - u_{e1}) \tag{6.4}$$

which implies

$$\hat{x}_{e2} = x_{e1} - F_1^{-1}G_1(u_{e2} - u_{e1}) \tag{6.5}$$

The error in predicted state is

$$\Delta x = \hat{x}_{e2} - x_{e2} = (x_{e1} - x_{e2}) + F_1^{-1}G_1(u_{e1} - u_{e2}) \tag{6.6}$$

The error in predicted output can be calculated by using u_{e2} and $\hat{x}_{e2}$ from (6.5) in (6.3). The result is

$$\hat{y}_{e2} = y_{e1} + (D_1 - C_1F_1^{-1}G_1)(u_{e1} - u_{e2}) \tag{6.7}$$

The error in predicted output is

$$\Delta y = y_{e2} - \hat{y}_{e2} = (y_{e2} - y_{e1}) + (D_1 - C_1F_1^{-1}G_1)(u_{e2} - u_{e1}) \tag{6.8}$$

The results obtained by using (6.4) and (6.8) with the five linear models are presented in figure 6.2. The true values of the

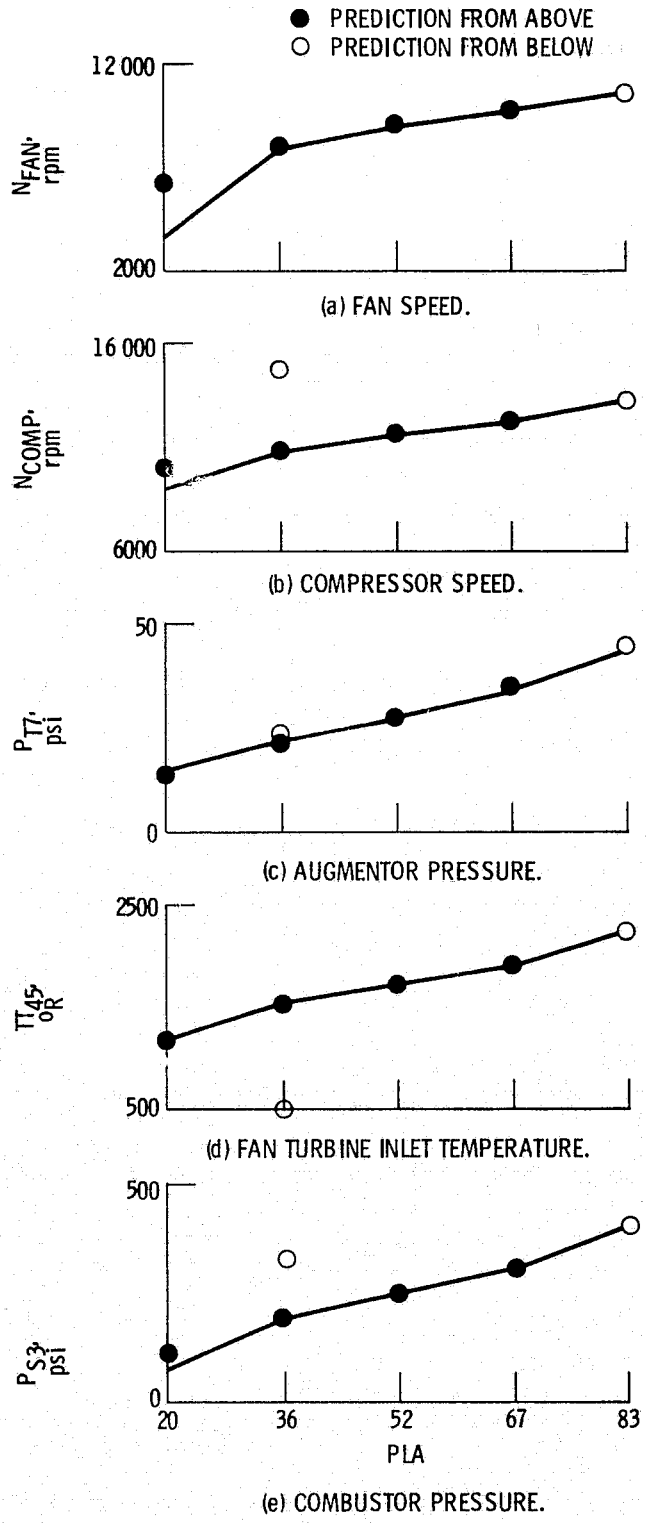

Figure 6.2. - Steady-state prediction accuracy.

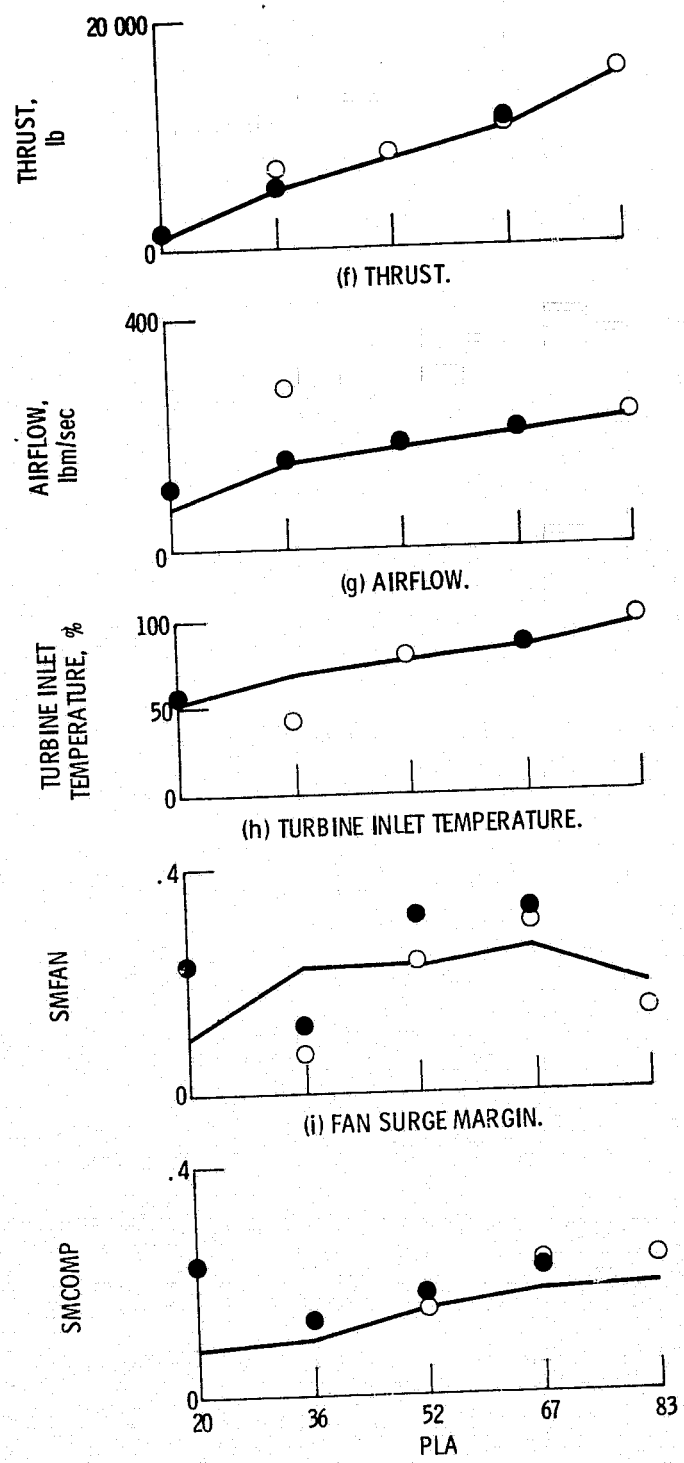

(j) COMPRESSOR SURGE MARGIN.

Figure 6.2. - Concluded.

problem variables (states and outputs) are presented as a function of PLA. The values at the five PLA's are connected by straight lines; however, the true variation between equilibrium data points is not necessarily linear. The predicted problem variables are also shown, as predicted from adjacent equilibrium points both above and below the predicted point.

It can be seen from figure 6.2 that prediction accuracy is generally very good, with several notable exceptions. First, for nearly all of the variables, the idle model (PLA = 20 degrees) does not accurately predict the equilibrium values at PLA = 36 degrees. Also, the model at PLA = 36 degrees does not predict the idle conditions accurately. Both of these results may be explained by the fact that the engine exhaust nozzle and low pressure turbine are unchoked at idle, but become choked a few degrees above idle and remain choked as PLA increases further. Engine dynamic characteristics differ substantially between choked and unchoked conditions. Therefore, there is a large discontinuity in the linear models at the point at which choking occurs.

With the exception of the idle prediction difficulty, all problem variables are accurately predicted over the range of PLA, except for the fan and compressor surge margins. The difficulty in predicting surge margins is due to the fact that surge margin is proportional to the difference between two pressures which are of similar magnitudes. Hence, relatively small errors in the pressures give rise to large errors in the surge margins.

Because of the fact that the engine exhaust nozzle is unchoked only in the near vicinity of idle, and furthermore is choked at all

PLA's at nonzero flight Mach numbers, it was decided to eliminate the idle model from all subsequent calculations. Therefore, the engine will be modeled by using the three-state models (e.g., Table IV) at four equilibrium points: PLA = 36, 52, 67, and 83 degrees.

D. Steady State Performance

Linear models can be used to find the control settings which maximize steady-state performance. For example, suppose we wish to maximize thrust for constant fuel flow - this is equivalent to minimizing specific fuel consumption. The minimization must be accomplished while adhering to the engine constraints and control limits. The minimization will be conducted at PLA = 67 degrees, a typical power setting for subsonic cruise. At this power setting, the only applicable engine constraints are that fan and compressor surge margins should be kept above a safe level, say five percent. In addition, the exhaust nozzle area, inlet guide vanes, and compressor variable vanes must not exceed their mechanical limits.

For given values of u, the equilibrium values of states and outputs are given by (6.5) and (6.7)

$$\begin{aligned} x_{ss} &= x_e - F^{-1}G(u - u_e) \\ y_{ss} &= y_e + (D - CF^{-1}G)(u - u_e) \end{aligned} \tag{6.9}$$

If the performance index and constraints are linear combinations of states, outputs, and controls, a linear programming problem results, which can be solved by using the simplex method (ref. 16).

Results for the maximization of thrust are presented in table V. For all cases, fuel flow is held constant at 6860 lbm/hr. For the

TABLE V. - STEADY-STATE PERFORMANCE

[Sea-level static, PLA = 67°, w_f = 6860 lbm/hr]

	A_{noz}, ft^2	IGV, deg	HVS deg	Thrust, lbf	SMFAN	SMCOMP
Nominal	2.98	-16.4	0.92	10 514	0.25	0.18
Optimum	2.8	5	-40	11 411	.07	.71
Scheduled geometry ±7°	2.8	-9.4	-6.1	10 790	.16	.28

nominal case, the exhaust nozzle area, inlet guide vanes and compressor variable vanes are at their scheduled values; the thrust which results is 10 514 lbf. In the optimum case, A_{noz}, IGV, and HVS are free for optimization, subject to their mechanical limits. The resulting thrust is 11 411 lbf, which represents an increase of about 9 percent over the nominal value. However, it is recognized that the linear models are not necessarily valid over the full range of possible controls. Furthermore, use of optimum values of IGV or HVS could result in violation of flutter boundaries. Therefore, a third case is considered in which the values of IGV and HVS are allowed to deviate by at most 7 degrees from the scheduled values at that power setting. In this case, the thrust is 10 790 lbf, which still represents an increase of more than 2.5 percent from the nominal value.

A possible explanation for the increased thrust achieved by using off-schedule geometry is that the scheduled values of IGV and HVS are based on optimized component performance, rather than optimized overall engine performance.

E. Transient Performance

We now consider the problem of minimizing the time required to accelerate the F100 engine from one equilibrium thrust level to another as rapidly as possible. In solving this problem, a piecewise-linear model of the F100 engine will be used. Specifically, the engine model is given by

$$\dot{x} = F_i(x - x_{ei}) + G_i(u - u_{ei}) \tag{6.10}$$

where the state vector x (three states) and control vector u (four controls) are as defined in table IV. There are also other problem variables of interest, called outputs, which are related to the states and controls by

$$y = C_i(x - x_{ei}) + D_i^T(u - u_{ei}) + y_{ei} \tag{6.11}$$

the index i refers to the equilibrium model number; there are four equilibrium linear models at PLA = 36, 52, 67, and 83 degrees. The 67 degree model is presented in table IV. The linear model which applies at a given time is selected by minimizing the quadratic function

$$T_i = (x - x_{ei})^T W(x - x_{ei}) \tag{6.12}$$

with respect to i; the model whose equilibrium state is "closest" to the actual state at that time is chosen to represent the engine. The function of W in (6.12) is to scale the states to comparable numerical values.

During an acceleration from a part-power condition to intermediate, the engine is first represented by the PLA = 36 degrees model. As the engine accelerates, the model switches successively to the 52, 67, and

83 degree models. The W matrix used in comparing successive PLA models k and (k + 1) in (6.12) is given by

$$W = \begin{pmatrix} \frac{1}{(x_{ek} - x_{e,k+1})_1^2} & 0 & 0 \\ 0 & \frac{1}{(x_{ek} - x_{e,k+1})_2^2} & 0 \\ 0 & 0 & \frac{1}{(x_{ek} - x_{e,k+1})_3^2} \end{pmatrix} \quad (6.13)$$

It should be noted that the components of W defined by (6.13) are different for each successive switch. The normalizing factor for each state has been chosen to be the difference in values of that state from one equilibrium point to the next.

The trajectory must also satisfy path inequality constraints given by

$$c_i^T x + d_i^T u + e_i \leq 0, \qquad i = 1, \ldots, q \qquad (6.14)$$

The coefficients c_i, d_i, and e_i are different for each equilibrium model. Some of the path inequality constraints correspond to engine physical limits, others to control mechanical limits. The following constraints will be assumed for this problem.

(1) Turbine inlet temperature cannot exceed the equilibrium value at intermediate thrust by more than 50 degrees R.

(2) Fan and compressor speeds cannot exceed the equilibrium values at intermediate thrust by more than 50 rpm.

(3) Fan and compressor surge margins must not be less than 5 percent.

(4) Inlet guide vanes, compressor vanes, exhaust nozzle area, and

fuel flow rate must not exceed their limits.

Statement of the problem. - Before developing a precise mathematical statement of the optimization problem to be solved, it is useful to consider first the manner in which the resulting optimal control for minimum-time acceleration (which will be referred to as the transition control) might be implemented in an actual engine. The transition control will be used during acceleration from one equilibrium power setting to another; during near-steady conditions, the Bill-of-Material (BOM)* control (which will be referred to as the regulator) will be used.

In deciding when to transfer authority from the transition controller to the regulator, it must be recognized that the equilibrium conditions at a given PLA are not known precisely; they vary from one engine to another and as a function of operating time for a given engine. Therefore, control authority should be transferred from the transition controller to the regulator when the state vector is in the "vicinity" of the desired state vector rather than when desired values of the states have been achieved precisely. The distance to the desired state vector (terminal error) may be defined as

$$\phi(x_f) = \sqrt{\sum_{i=1}^{3}\left(\frac{x_i - x_{id}}{x_{id}}\right)^2} \tag{6.15}$$

The switch from the transition controller to the regulator would occur

*The BOM control is the standard control system supplied with the engine.

at a fixed value of ϕ, say 0.05 or 0.1

The problem to be solved is stated as follows. Find controls $u(t)$, $0 \leq t \leq t_f$ which minimize $\phi(x_f)$ while satisfying the system equations (6.10) and path constraints (6.14). A sequence of solutions to such problems for different acceleration times may be used to find the minimum-time solution for a given value of terminal error. Necessary conditions for an optimal solution are given in chapter II. The problem is solved by using the new algorithm described in chapters III and IV.

Results. - The problem of minimizing the terminal error for an acceleration from near-idle (PLA = 24 degrees) to intermediate thrust is considered. The engine's exhaust nozzle first becomes choked at PLA = 24 degrees. The final time is specified to be $t_f = 0.75$ second. The problem variables (states, outputs, and controls) for the optimal trajectory are shown in figure 6.3. The state variables N_{fan}, N_{comp}, and Pt7, are shown as functions of time in figure 6.3(a) to (c). It can be seen that the states approach the desired final values smoothly and with no overshoot. The value of the terminal error is $\phi = 0.012$, which results from errors in the states of $\Delta N_{fan} = 15$ rpm, $\Delta N_{comp} = 78$ rpm, and $\Delta P_{t7} = 0.43$ psi.

The outputs are shown as functions of time in figures 6.3(d) to (j). Because of the way in which the outputs are defined in equation (6.11) these variables are in general discontinuous at model switching points and points of discontinuous control.

The optimal control strategy results in the high-pressure turbine inlet temperature having its maximum value for the entire trajectory;

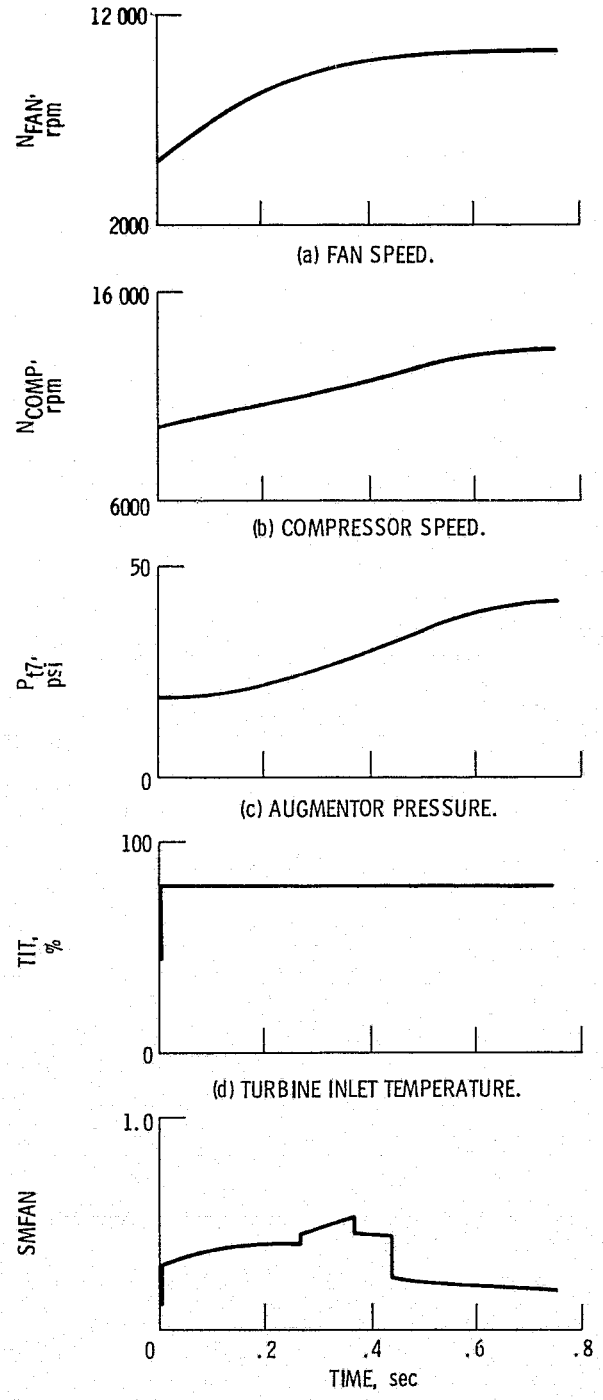

Figure 6.3. - Acceleration from PLA = 24 deg to intermediate thrust. Acceleration time, 0.75 sec.

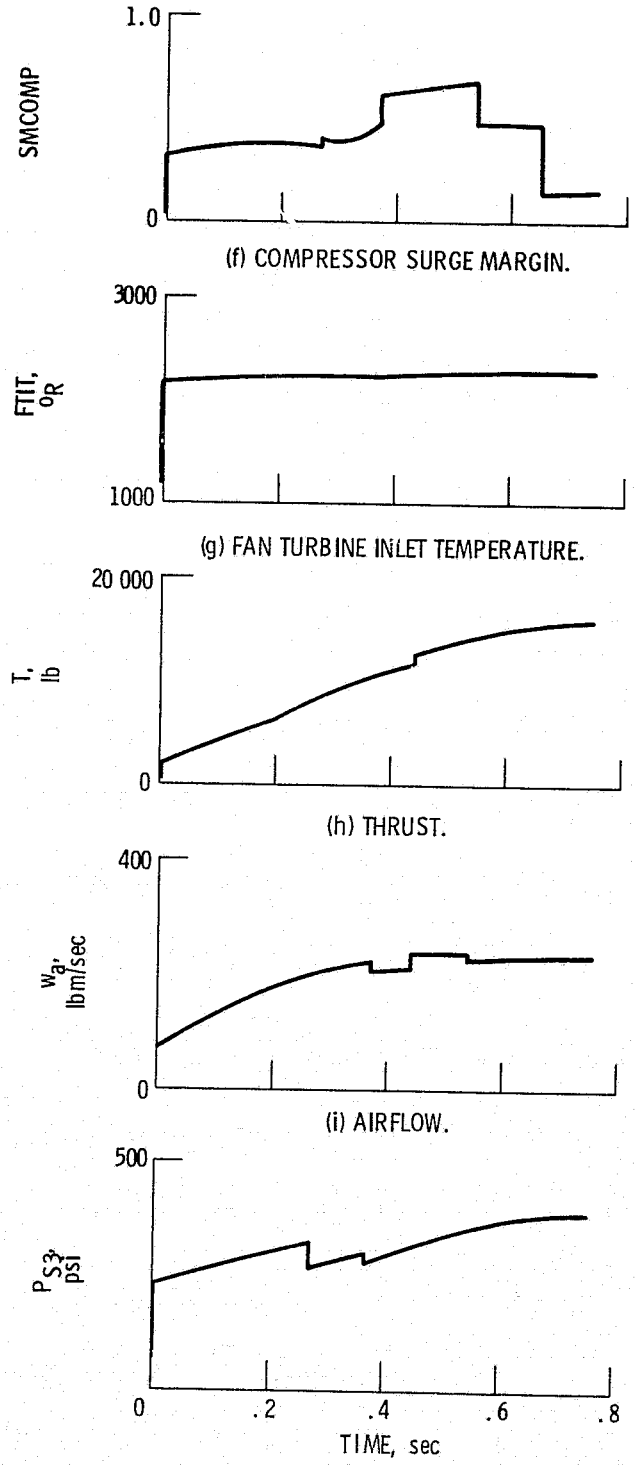

(f) COMPRESSOR SURGE MARGIN.

(g) FAN TURBINE INLET TEMPERATURE.

(h) THRUST.

(i) AIRFLOW.

(j) BURNER PRESSURE.

Figure 6.3 - Continued.

this is shown in figure 6.3(d). Fan and compressor surge margins remain well above acceptable minimums (figs. 6.3(e) and (f)). Low pressure turbine inlet temperature (fig. 6.3(g)) is very nearly constant. Thrust (fig. 6.3(h)) increases smoothly and monotonically with time.

The optimal control histories are shown as a function of time in figures 6.3(k) to (n). Fuel flow jumps at $t = 0$ from its idle value, then increases slowly to maintain constant turbine inlet temperature. The optimal values of A_{noz}, IGV, and HVS are piecewise constant, as required by variational theory (chapter II). Each of these variables has one switch during the trajectory.

Figure 6.3(o) shows the distance from the current state vector to the equilibrium state vector of the current model. The distance is normalized in such a way that the distance between adjacent equilibrium state vectors is unity. It can be seen that the instantaneous distance is always less than unity; this is a good indication of the validity of the piecewise-linear model throughout the entire trajectory.

Although the maximum nozzle area is greater than 6 square feet, nozzle area has been restricted to a range of 2.8 to 3.2 square feet for the present study. This arbitrary upper limit has been imposed because the linear models are not necessarily valid for the full range of allowable control action. It is also recognized that model accuracy may be degraded if IGV and HVS values are far from their scheduled values from the BOM controller. In fact, available test data for the IGV and HVS are limited to about ±7 degrees of the scheduled values. Furthermore, large deviations in IGV and HVS might result

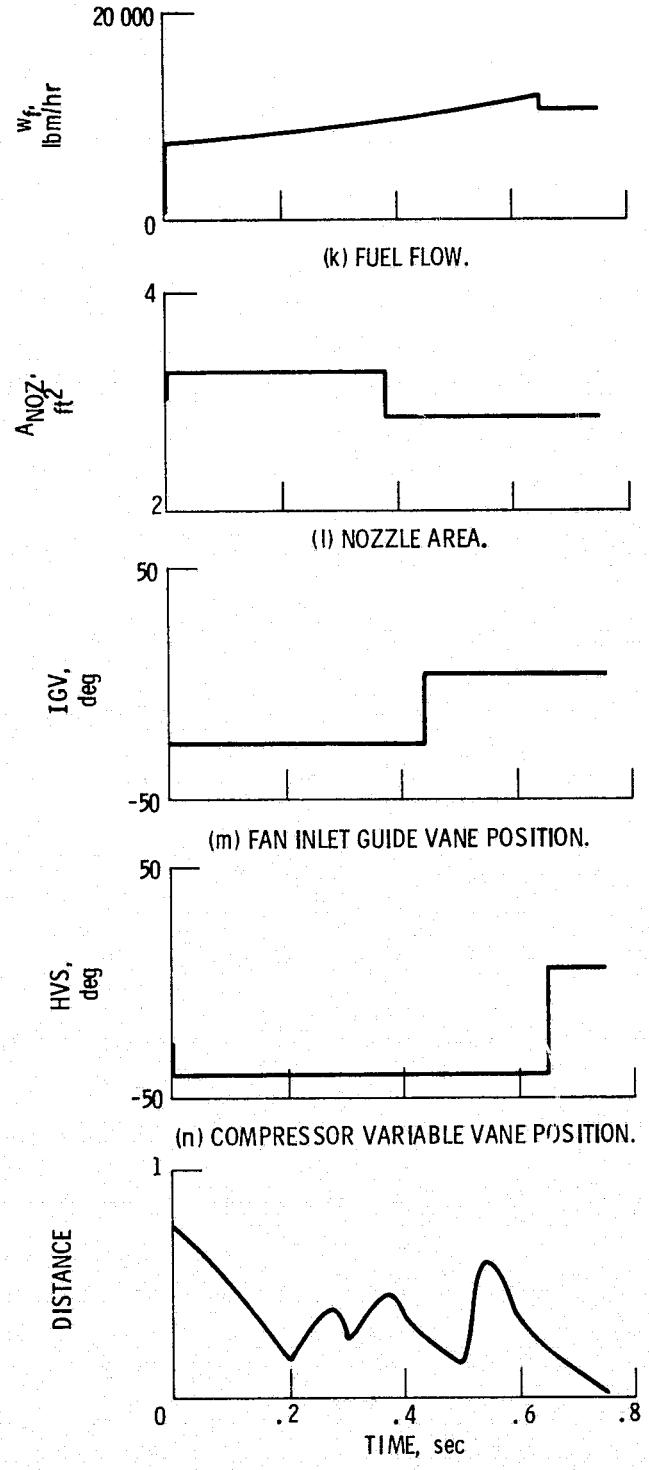

(o) DISTANCE FROM EQUILIBRIUM POINT.

Figure 6.3. - Concluded.

C-2

in flutter boundaries being violated. For these reasons, two additional optimal trajectories were run for $t_f = 0.75$ second. For one of the trajectories, the HVS and IGV were required to have their scheduled values; for the other, IGV and HVS were limited to ±7 degrees from their scheduled values. In addition, optimal trajectories were run for other values of t_f.

Figure 6.4 shows the problem variables as a function of time for the optimal trajectory in which the IGV and HVS were limited to ±7 degrees of the scheduled values. The acceleration time is 0.75 second. For this case, the terminal error is 0.045, compared to a terminal error of 0.012 which is achieved when the IGV and HVS are allowed full variation within their mechanical limits.

It can be seen that the results for this case are qualitatively very similar to those of figure 6.3. Turbine inlet temperature has its maximum value for the entire trajectory, and the state variables increase monotonically to their final values. IGV position (fig. 6.4(m)) is 7 degrees less than the scheduled value up to about 0.56 second; after that time, IGV position is 7 degrees greater than the scheduled value. It is interesting to note that HVS position (fig. 6.4(n)) is 7 degrees less than the scheduled value for the entire trajectory.

Figure 6.5 presents terminal error as a function of acceleration time, t_f, for accelerations from PLA = 24 degrees to intermediate. Results are presented for values of IGV and HVS which are fully optimized, scheduled and scheduled ±7 degrees. The corresponding trajectories have the same characteristics as shown in figures 6.3 and 6.4.

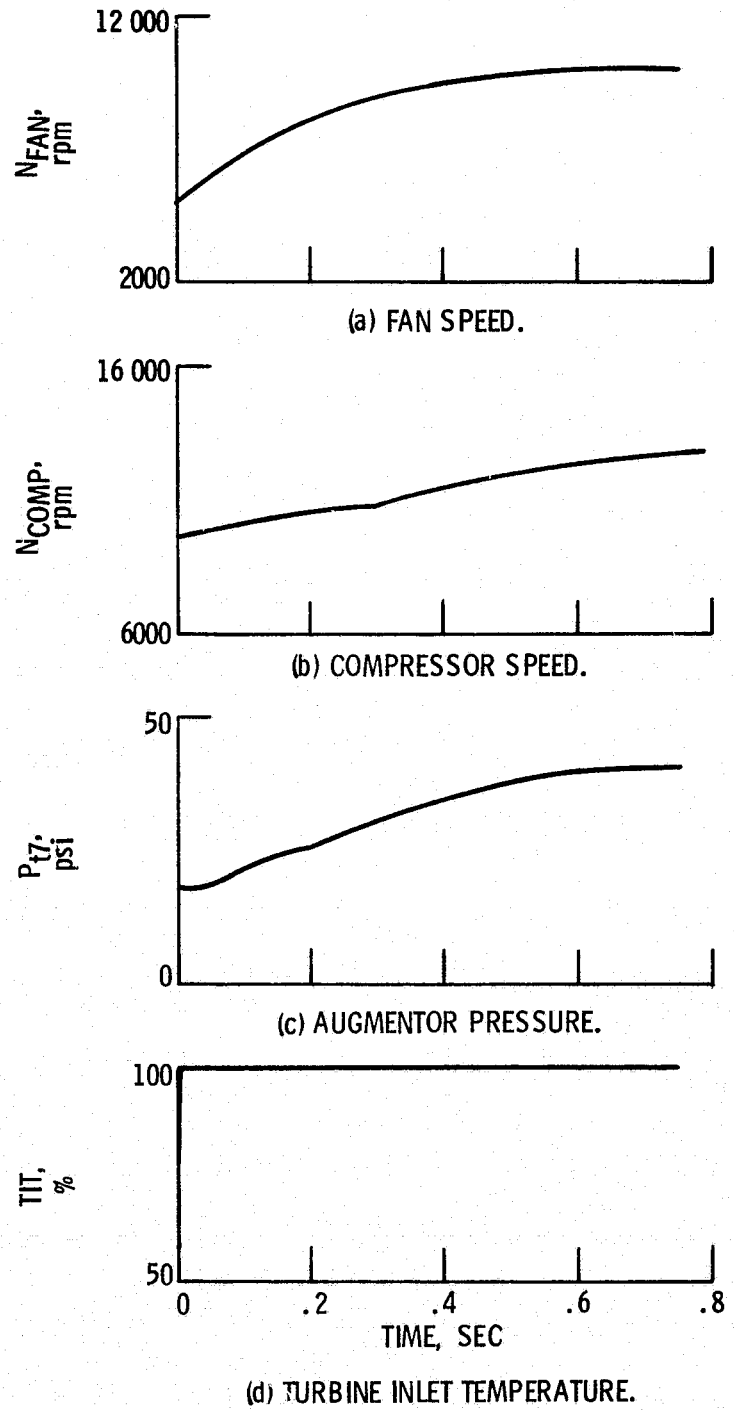

Figure 6.4. - Acceleration from PLA = 24 deg to intermediate thrust. Acceleration time, 0.75 sec. IGV and HVS scheduled ±7 deg.

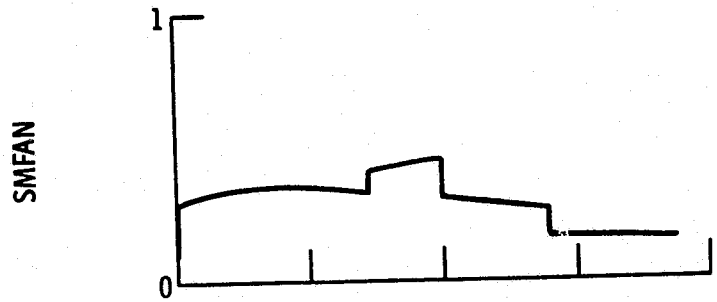

(e) FAN SURGE MARGIN.

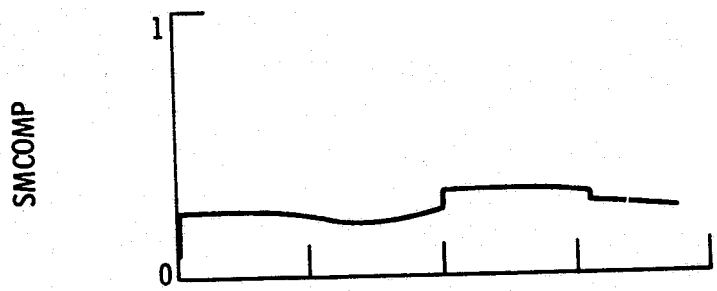

(f) COMPRESSOR SURGE MARGIN.

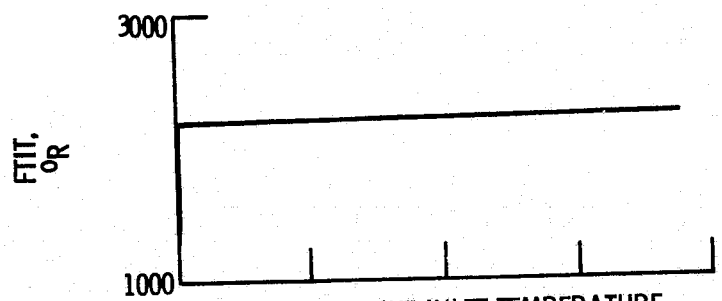

(g) FAN TURBINE INLET TEMPERATURE.

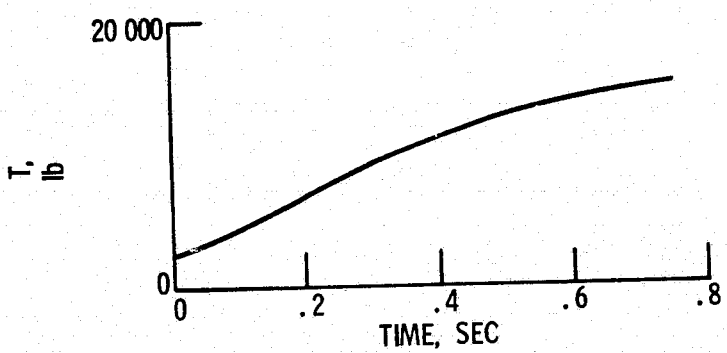

(h) THRUST.

Figure 6.4. - Continued.

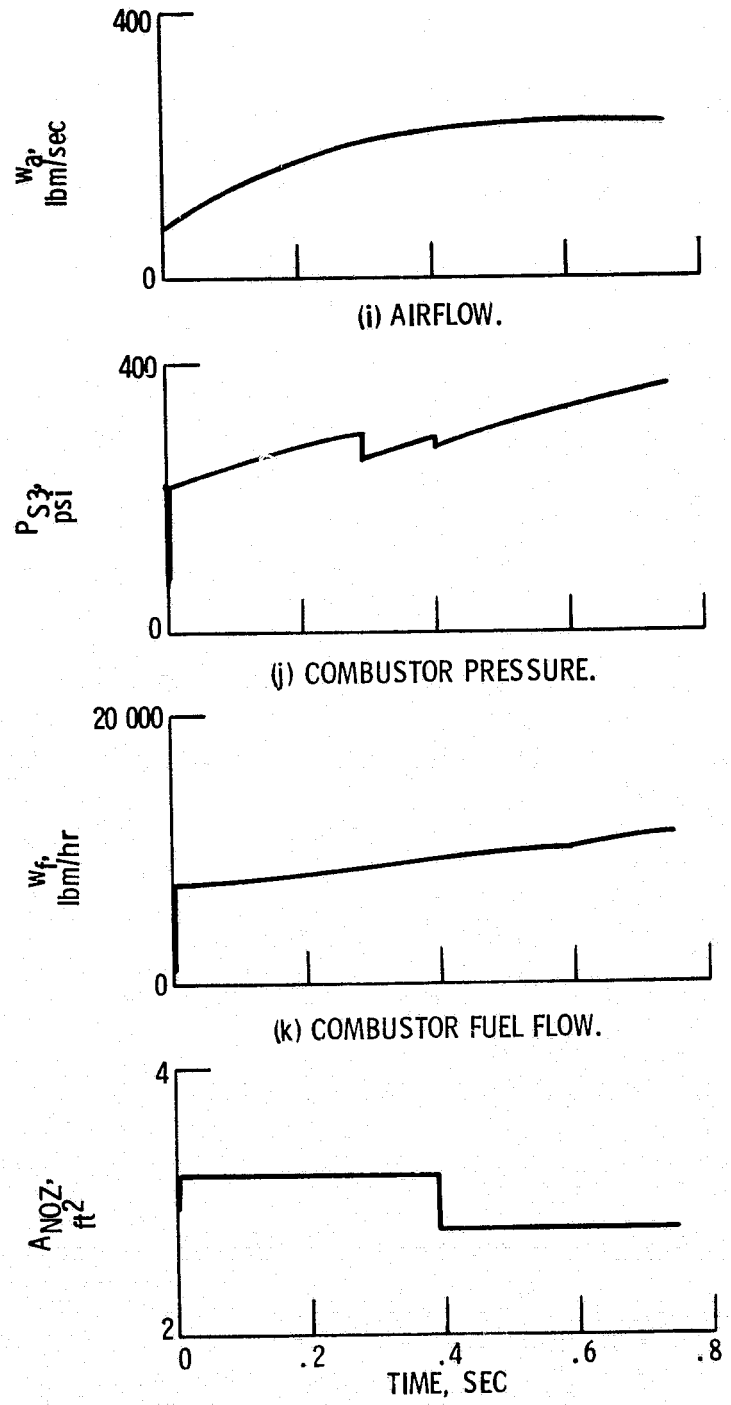

Figure 6.4. - Continued.

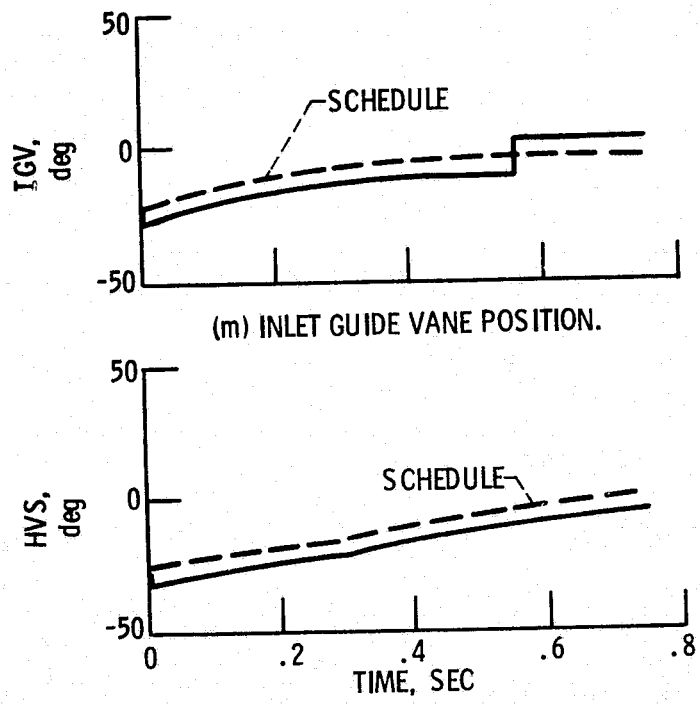

(m) INLET GUIDE VANE POSITION.

(n) COMPRESSOR VARIABLE VANE POSITION.

Figure 6.4. - Concluded.

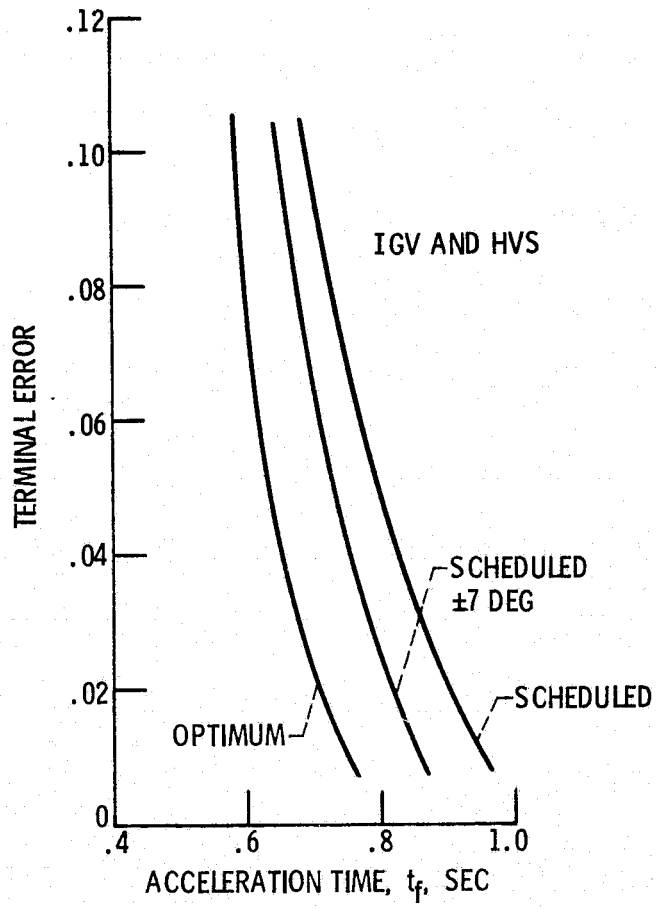

Figure 6.5. - Terminal error versus acceleration time. Part-power (PLA = 24 deg) to intermediate thrust acceleration.

In particular, turbine inlet temperature is kept at its maximum value throughout each of the trajectories.

As discussed earlier, authority might be transferred from the transition controller to the regulator at a fixed value of terminal error. The time required to reach a given terminal error depends on the control strategy used. For example, figure 6.5 shows that a time of 0.80 second is required to reduce the terminal error to 0.05 if scheduled IGV and HVS are used. If IGV and HVS are controlled optimally within scheduled ±7 degree values, the time is reduced to 0.74 second; if fully optimized IGV and HVS are used, t_f is 0.65 second.

The time required to accelerate from other initial values of PLA to intermediate is also of interest. Figure 6.6 presents the time required to accelerate for a terminal error of 0.05 as a function of PLA. Results are presented for scheduled and scheduled ±7 degree values of IGV and HVS.

F. Comparison of Nonlinear and Piecewise-Linear Responses

In figure 6.2, accuracy of the piecewise-linear model was investigated in terms of the ability of the model to predict the values of adjacent equilibrium values of states and outputs. This type of accuracy test is particularly relevant to the ability of the piecewise-linear model to predict values of the control variables for optimal steady-state performance. However, for transient performance prediction, a much better check on model accuracy is achieved by comparison of the nonlinear and piecewise-linear model transient responses for the same control variable time histories.

Figure 6.7 presents a comparison of nonlinear and piecewise-linear

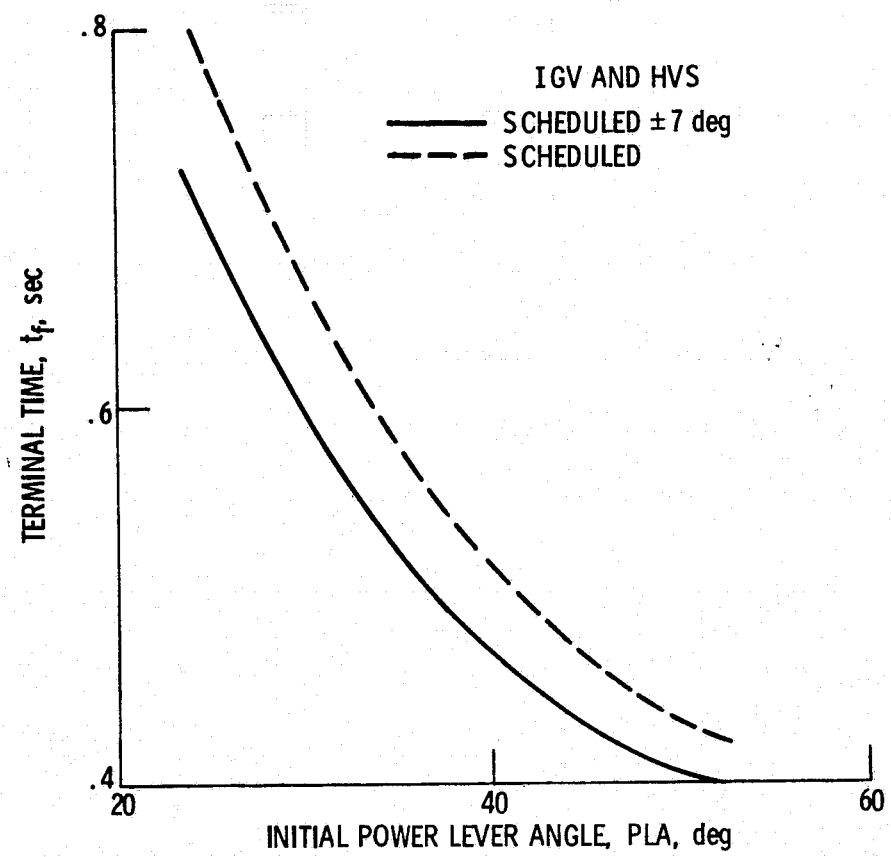

Figure 6.6. - Time required to accelerate to intermediate thrust with a fixed terminal error of 0.05.

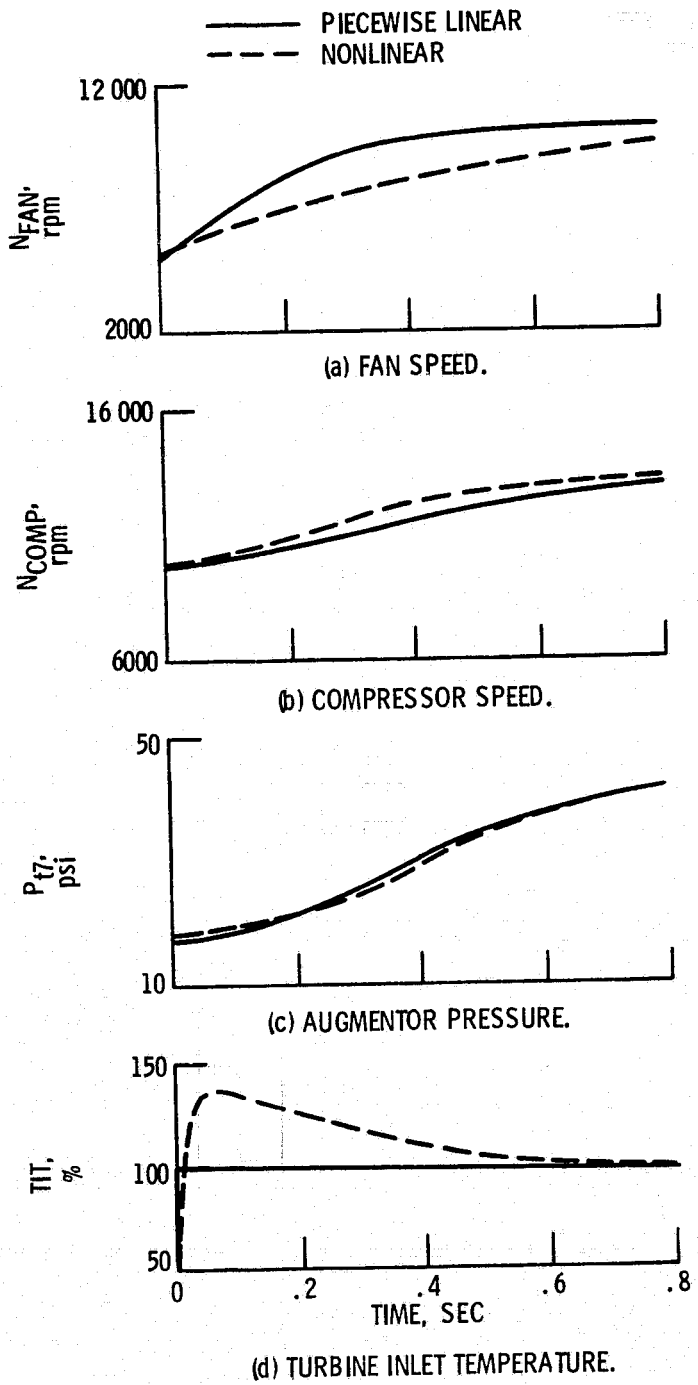

Figure 6.7. - Comparison of nonlinear and piecewise-linear results. Acceleration from PLA = 24 deg to intermediate thrust. Acceleration time, 0.8 sec. IGV and HVS, scheduled ±7 deg.

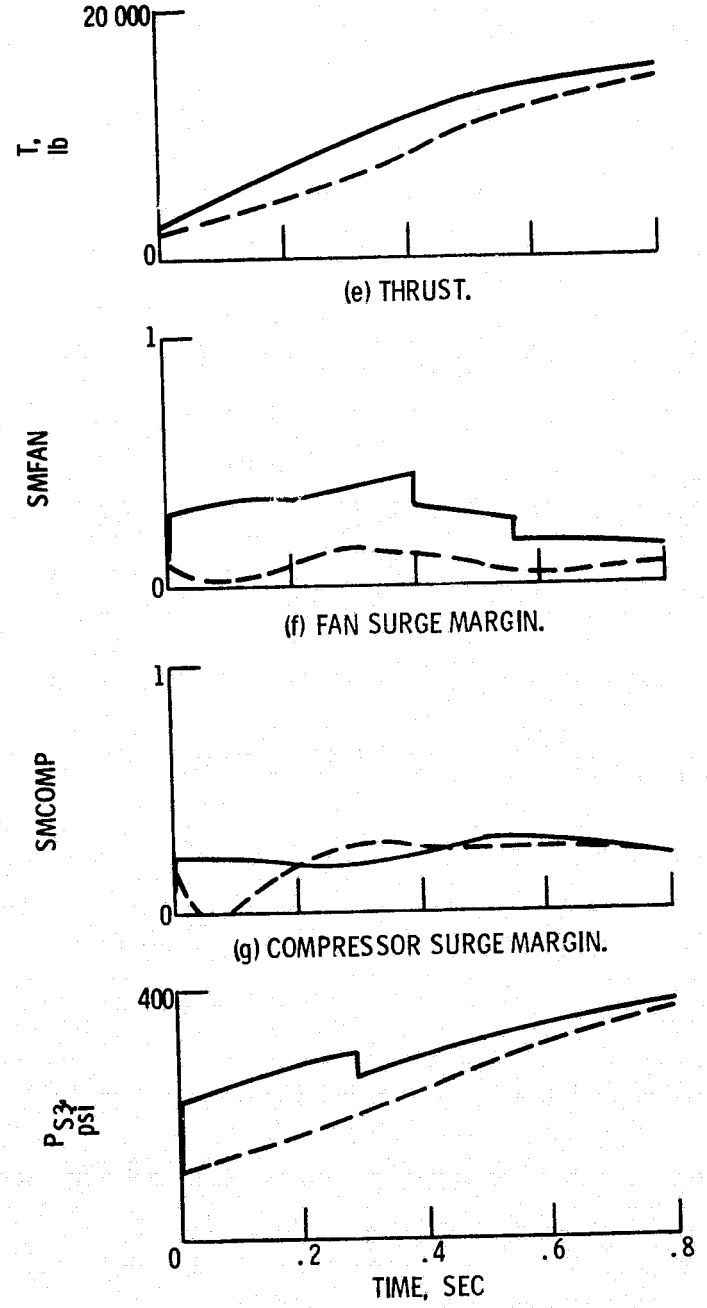

(h) COMBUSTOR PRESSURE.

Figure 6.7. - Continued.

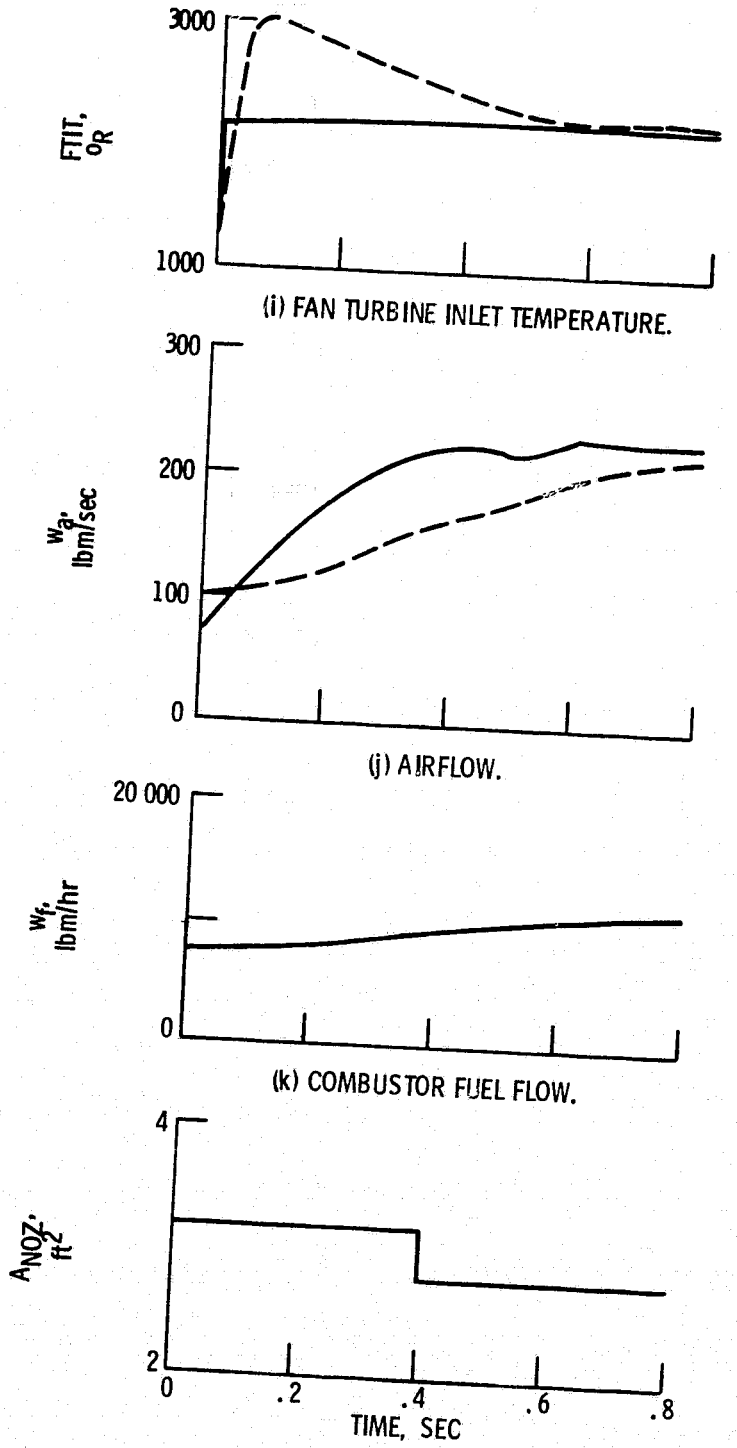

(l) NOZZLE AREA.

Figure 6.7. - Continued.

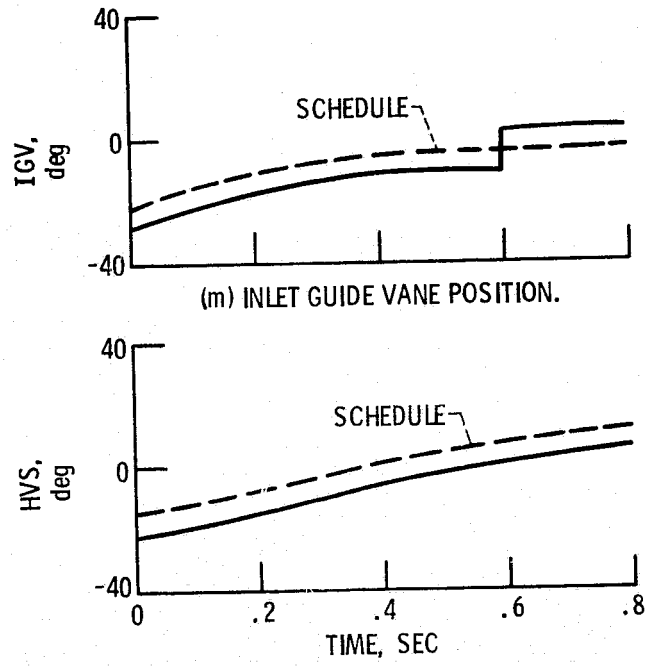

(m) INLET GUIDE VANE POSITION.

(n) COMPRESSOR VARIABLE VANE POSITION.

Figure 6.7. - Concluded.

transient responses. The control variable histories are based on an optimal acceleration from PLA = 24 degrees to intermediate thrust, for a specified acceleration time of 0.8 second. For this case, the values of IGV and HVS were constrained to be within ±7 degrees of the BOM scheduled values. The nonlinear responses were obtained by using the P&WA digital dynamic nonlinear F100 engine simulation (ref. 14). It can be seen that the nonlinear and piecewise-linear responses of compressor speed and augmentor pressure are in good agreement. However, differences are observed in the fan speed responses. Also, there are substantial and important differences in the high-pressure turbine inlet temperature and fan and compressor surge margin responses. The nonlinear results show that the maximum value of the high-pressure turbine inlet temperature is violated by a large amount, and the compressor surges at about 0.06 second. The fan does not surge, but the fan surge margin does fall below the minimum value of 5 percent early in the trajectory.

Additional comparisons of nonlinear and piecewise-linear results are made in figures 6.8 and 6.9. In these two figures, the comparison is based on an acceleration of 0.6 second from PLA = 36 degrees to intermediate thrust. For figure 6.8, the IGV and HVS are limited to scheduled values ±7 degrees, while for figure 6.9, the IGV and HVS take on scheduled values. The results are qualitatively similar to those presented in figure 6.7, but the nonlinear and piecewise linear results do not differ by as much as was observed in figure 6.7. For example, there is no compressor surge in figure 6.8, and neither fan nor compressor surge margin limits are violated in figure 6.9.

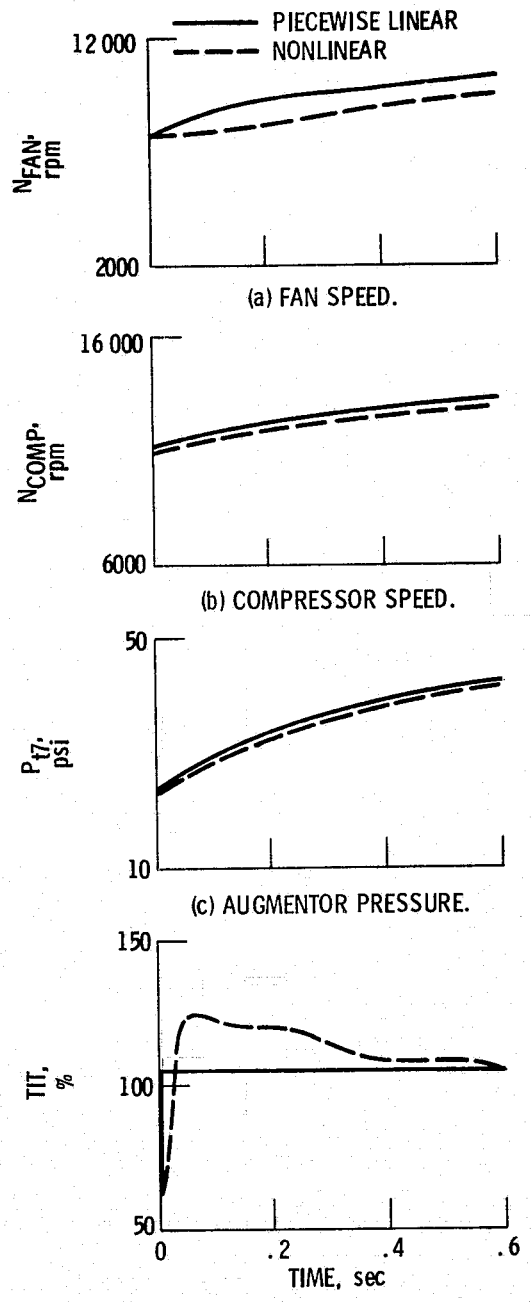

Figure 6.8. - Comparison of nonlinear and piecewise linear results. Acceleration from PLA = 36 deg to intermediate thrust, acceleration time, 0.6 sec. IGV and HVS, scheduled ± 7 deg.

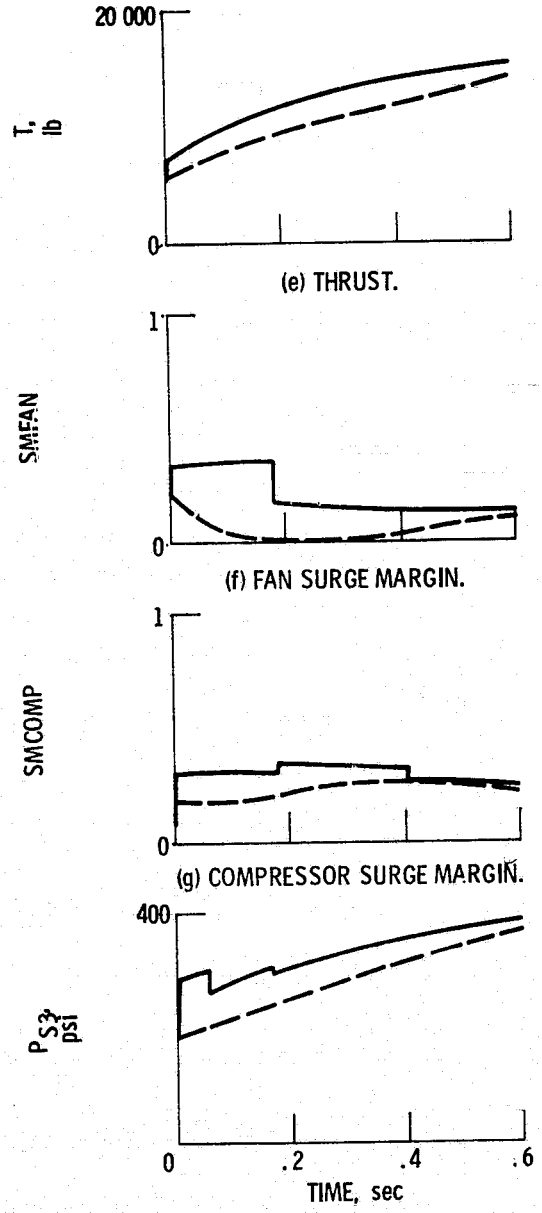

(h) COMBUSTOR PRESSURE.

Figure 6.8. - Continued.

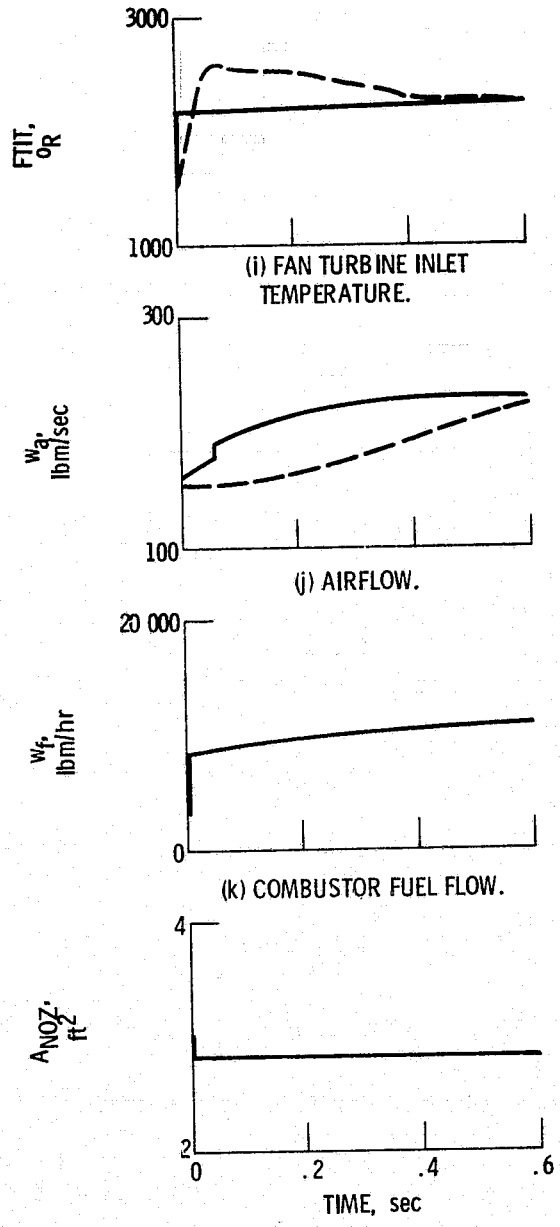

(l) NOZZLE AREA.

Figure 6.8. - Continued.

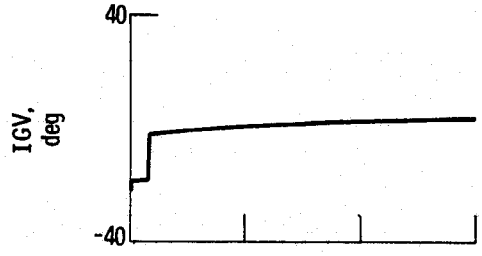

(m) INLET GUIDE VANE POSITION.

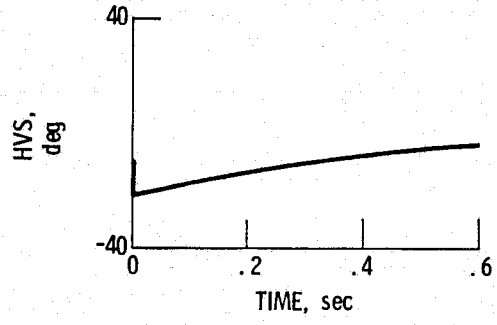

(n) COMPRESSOR VARIABLE VANE POSITION.

Figure 6.8. - Concluded.

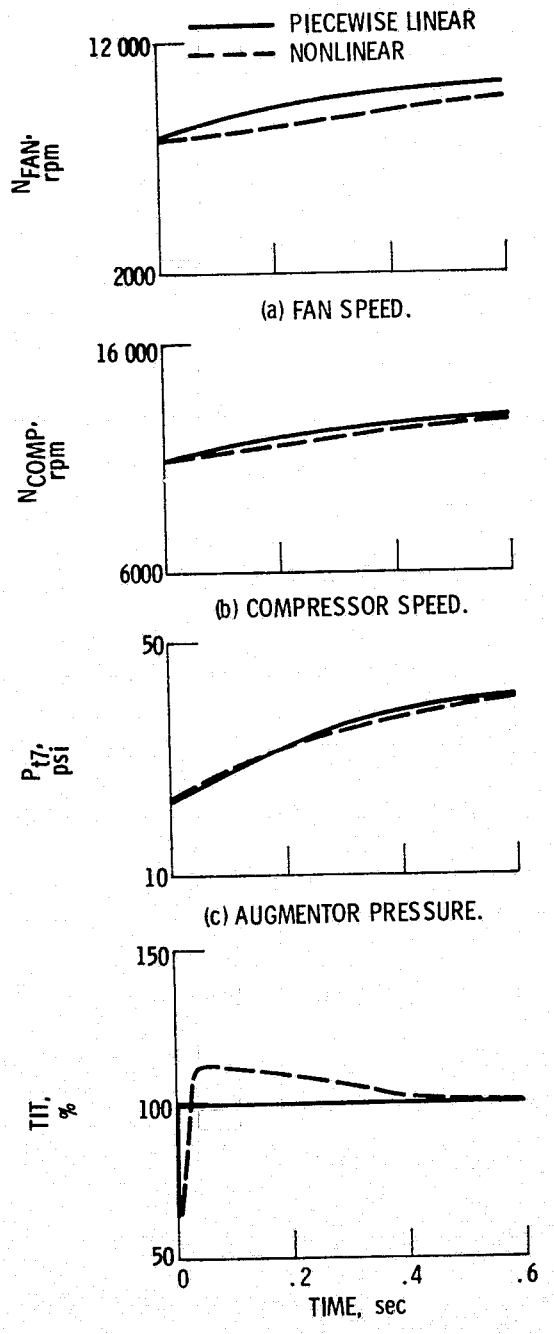

Figure 6.9. - Comparison of nonlinear and piecewise-linear results. Acceleration from PLA = 36 deg to intermediate thrust. Acceleration time, 0.6 sec. IGV and HVS scheduled.

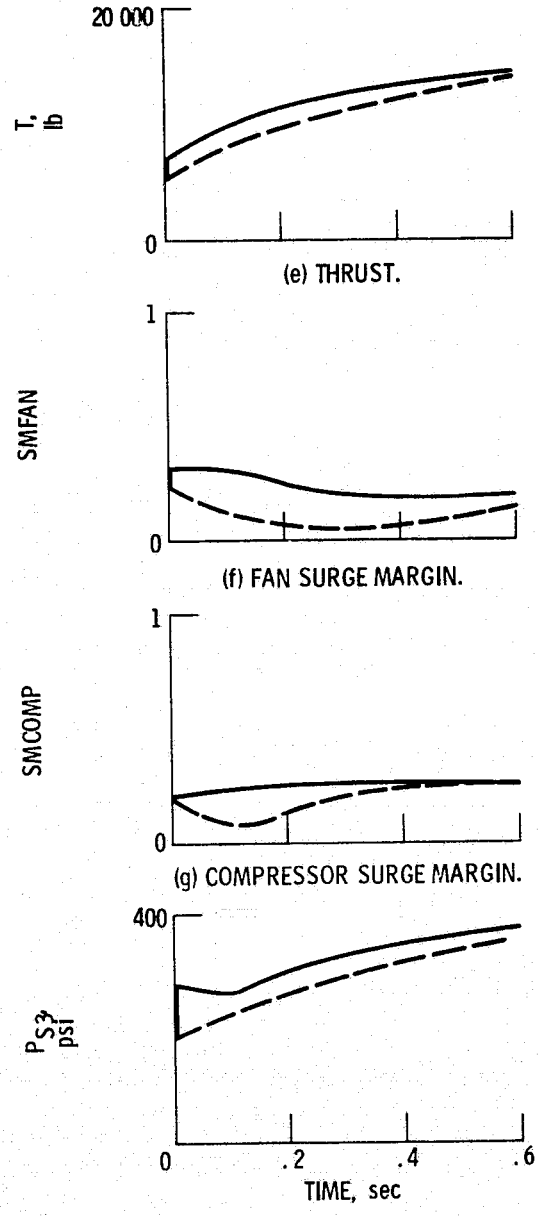

(h) COMBUSTOR PRESSURE.

Figure 6.9. - Continued.

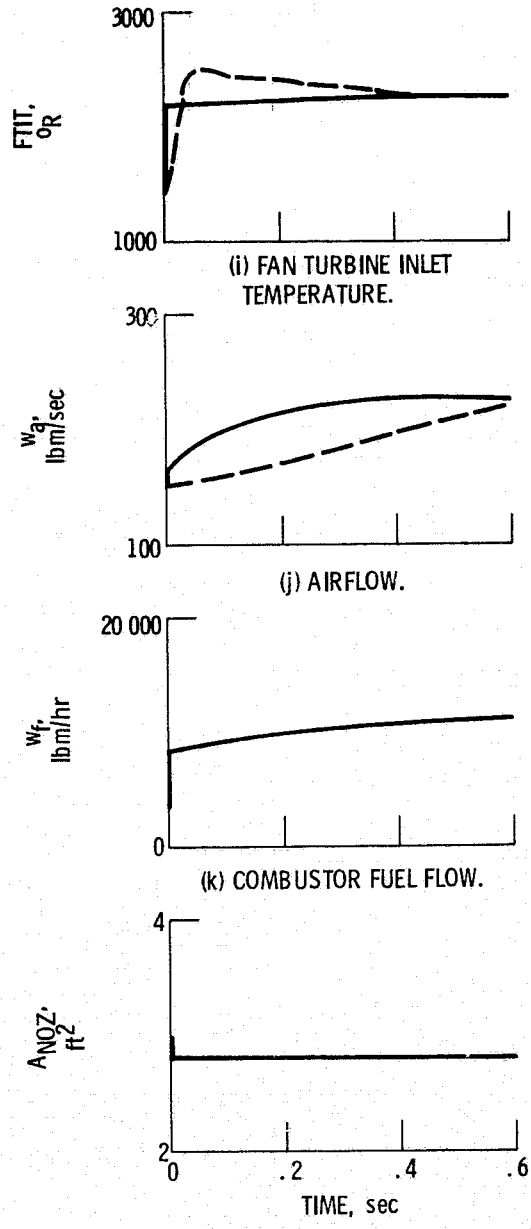

Figure 6.9. - Continued.

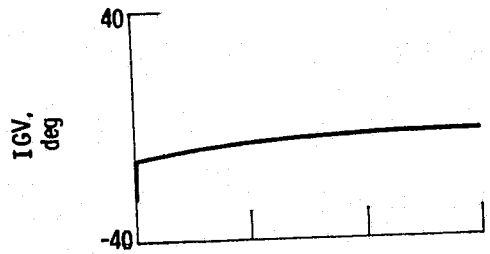

(m) INLET GUIDE VANE POSITION.

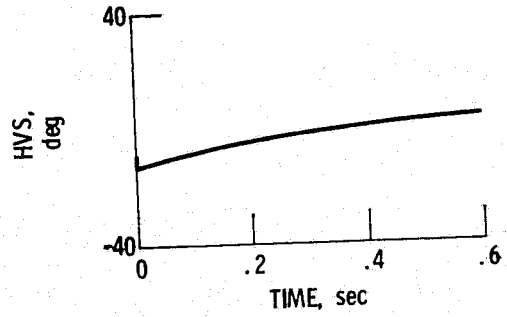

(n) COMPRESSOR VARIABLE VANE POSITION.

Figure 6.9. - Concluded.

There are several possible explanations for the differences between nonlinear and piecewise-linear responses observed in figures 6.7 to 6.9. They are as follows:

(1) The individual linear models may not be good approximations even for small perturbation inputs.

(2) The number of equilibrium linear models may be inadequate to accurately describe the system nonlinearities with respect to the state variables.

(3) There may be substantial nonlinearities with respect to the control variables, which are not included in the piecewise-linear model.

(4) Model reduction from sixteenth to third order may have resulted in modeling inaccuracies.

Items (1) and (4) may be checked by comparison of nonlinear and three and sixteen variable linear transient responses for small-perturbation control inputs. Such a comparison is made in figure 6.10. The equilibrium state and three and sixteen variable linear models correspond to PLA = 52 degrees, and the control input is a small step in combustor fuel flow. Results are presented for fan speed, compressor speed, augmentor pressure, turbine inlet temperature, and fan and compressor surge margins. It can be seen that the linear and nonlinear responses are in good agreement for states compressor speed and augmentor pressure, but are not in good agreement for fan speed. The sixteen-state linear result is in better agreement with the nonlinear result than is the three-state linear result, but neither of the linear results can be considered to be in adequate agreement. Also, the

linear and nonlinear results are in reasonably good agreement for turbine inlet temperature, but the three and sixteen state linear models do not give a good representation of fan or compressor surge margin.

The differences between nonlinear and linear predictions of fan speed and fan and compressor surge margins observed in figure 6.10 are qualitatively similar to those observed in figures 6.7 through 6.9. It appears that a more accurate set of linear models, obtained from small perturbation responses of the nonlinear simulation, would result in more accurate piecewise-linear results. Also, there are substantial differences between the three and sixteen state linear results for several of the variables. The three-state linear models were obtained by modal reduction from five state linear models, which in turn were obtained directly from the nonlinear simulation. Since the three-state models were not obtained by modal reduction from the sixteen-state linear models, no conclusions can be drawn here relative to errors introduced by modal reduction.

Because of the inaccuracy of the linear models, it is not possible to determine conclusively if nonlinearities with respect to states or controls contributed substantially to the differences in the nonlinear and piecewise-linear results observed in figures 6.7 to 6.9. Nevertheless, the relatively good agreement of turbine inlet temperature observed in the small perturbation results (fig. 6.10) as compared to the large turbine inlet temperature errors observed in figures 6.7 to 6.9 suggests strongly that there is a substantial nonlinearity, probably with respect to combustor fuel flow, which would have to be included in the model to achieve accurate results.

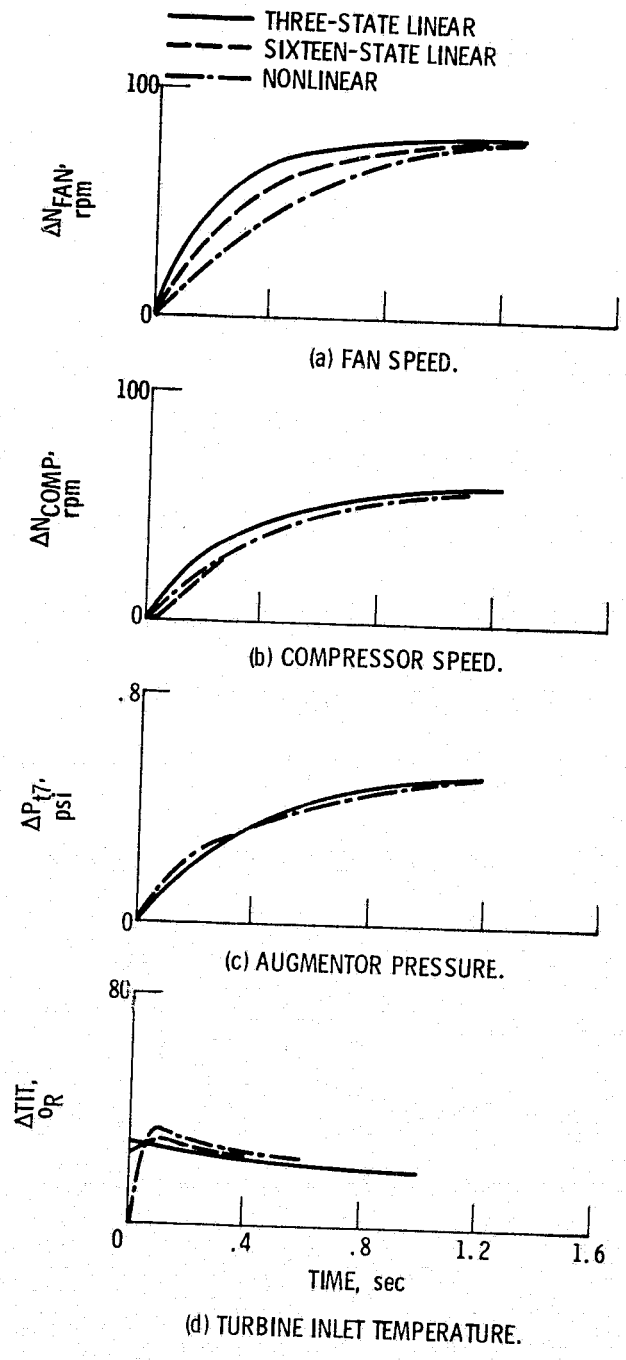

Figure 6.10. - Comparison of nonlinear and three-and-sixteen-state linear model responses to a three percent step in fuel flow. Equilibrium condition, PLA = 52 deg.

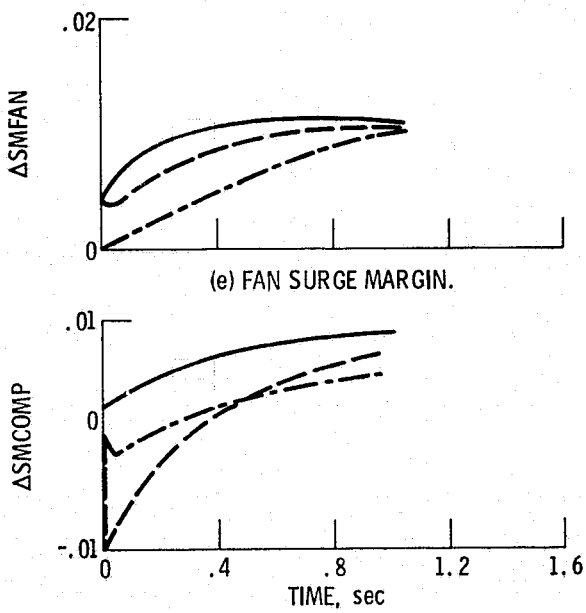

(e) FAN SURGE MARGIN.

(f) COMPRESSOR SURGE MARGIN.

Figure 6.10. - Concluded.

G. Comparison of Minimum Time and BOM Control Responses Using the Nonlinear Simulation

It is of interest to compare the transient responses obtained by using optimal minimum-time strategy with those obtained by using the BOM control. Such comparisons are made in figures 6.11 and 6.12, for accelerations from PLA = 24 degrees to intermediate thrust and from PLA = 36 degrees to intermediate thrust, respectively. For both figures, the minimum time controls were obtained by using the piecewise-linear model with the IGV and HVS constrained to be within ±7 degrees of the BOM scheduled values. However, the data presented in figures 6.11 and 6.12 were obtained by using the minimum-time and BOM controls applied to the nonlinear F100 engine simulation.

The results show that the minimum-time control strategy produces a more rapid acceleration to the vicinity of intermediate thrust. It appears that the principal reason for the improved acceleration is the much more rapid increase in fuel flow, which results in a rapid increase in high-pressure turbine inlet temperature. Naturally, the comparison of performance is invalidated because of the violation of constraints which occurs. Nevertheless, it seems highly probable that substantial improvement in acceleration time can be made without violation of engine constraints since the high-pressure turbine inlet temperature (figs. 6.11(d) and 6.12(d)) increases very slowly when the BOM control is used. Some compromise between the optimal control based on the piecewise-linear model and the BOM control would probably yield improved accelerations without violating the turbine inlet temperature limit.

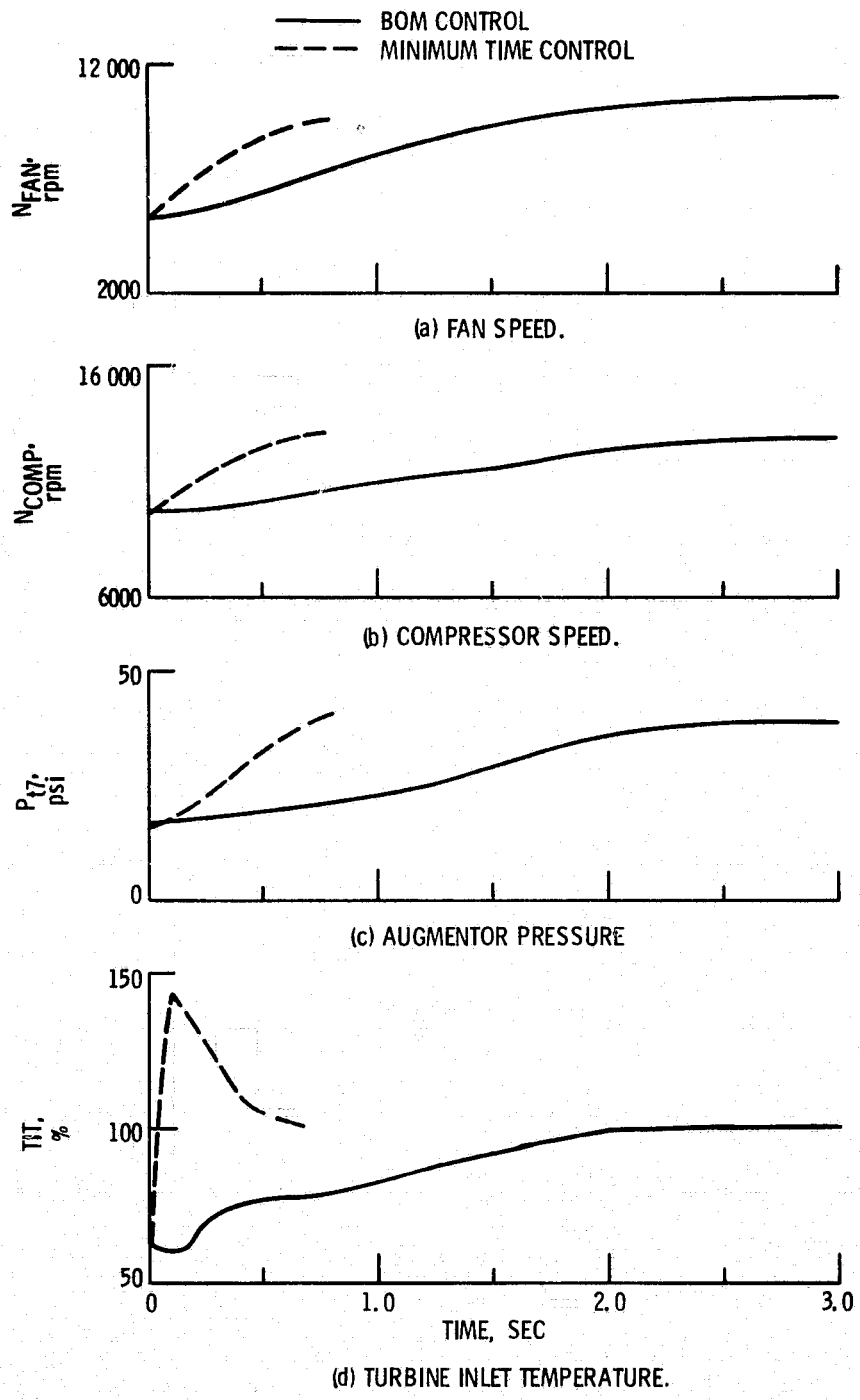

Figure 6.11. - Comparison of trajectories for minimum time and BOM control. Acceleration from PLA = 24 deg to intermediate thrust. Nonlinear simulation.

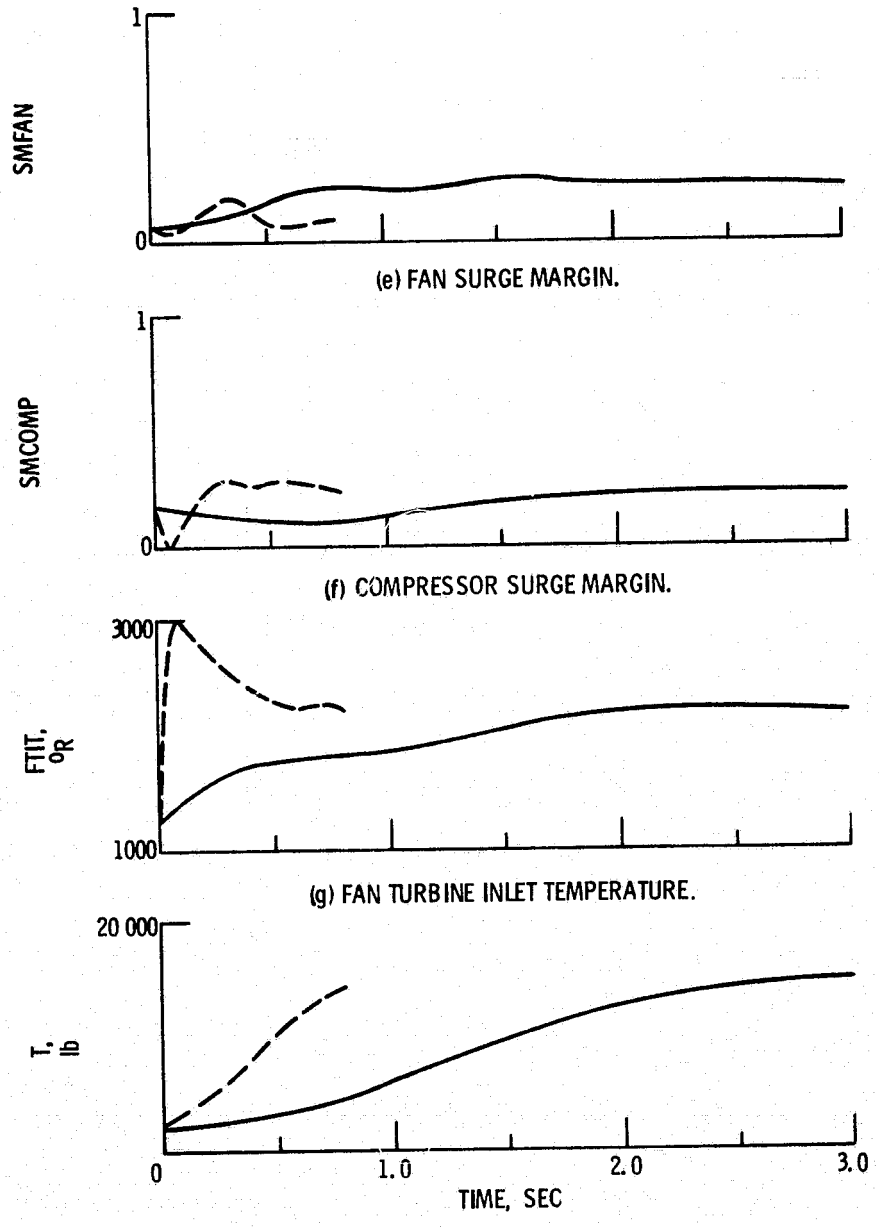

(e) FAN SURGE MARGIN.

(f) COMPRESSOR SURGE MARGIN.

(g) FAN TURBINE INLET TEMPERATURE.

(h) THRUST.

Figure 6.11. - Continued.

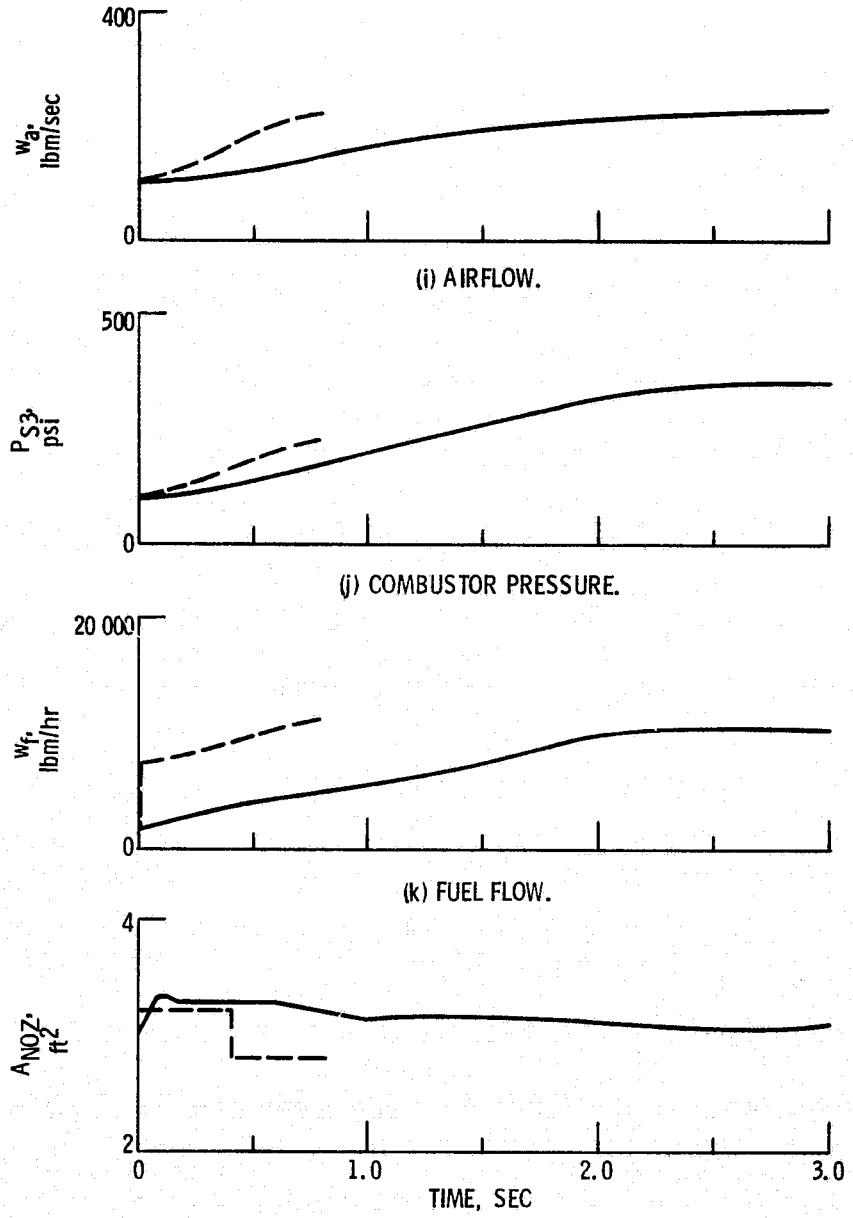

Figure 6.11. - Continued.

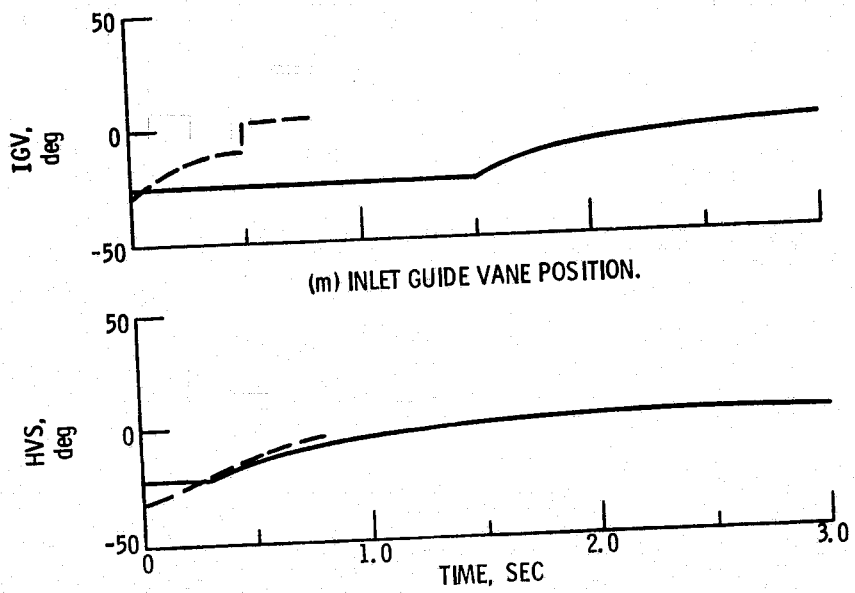

(m) INLET GUIDE VANE POSITION.

(n) COMPRESSOR VARIABLE VANE POSITION.

Figure 6.11. - Concluded.

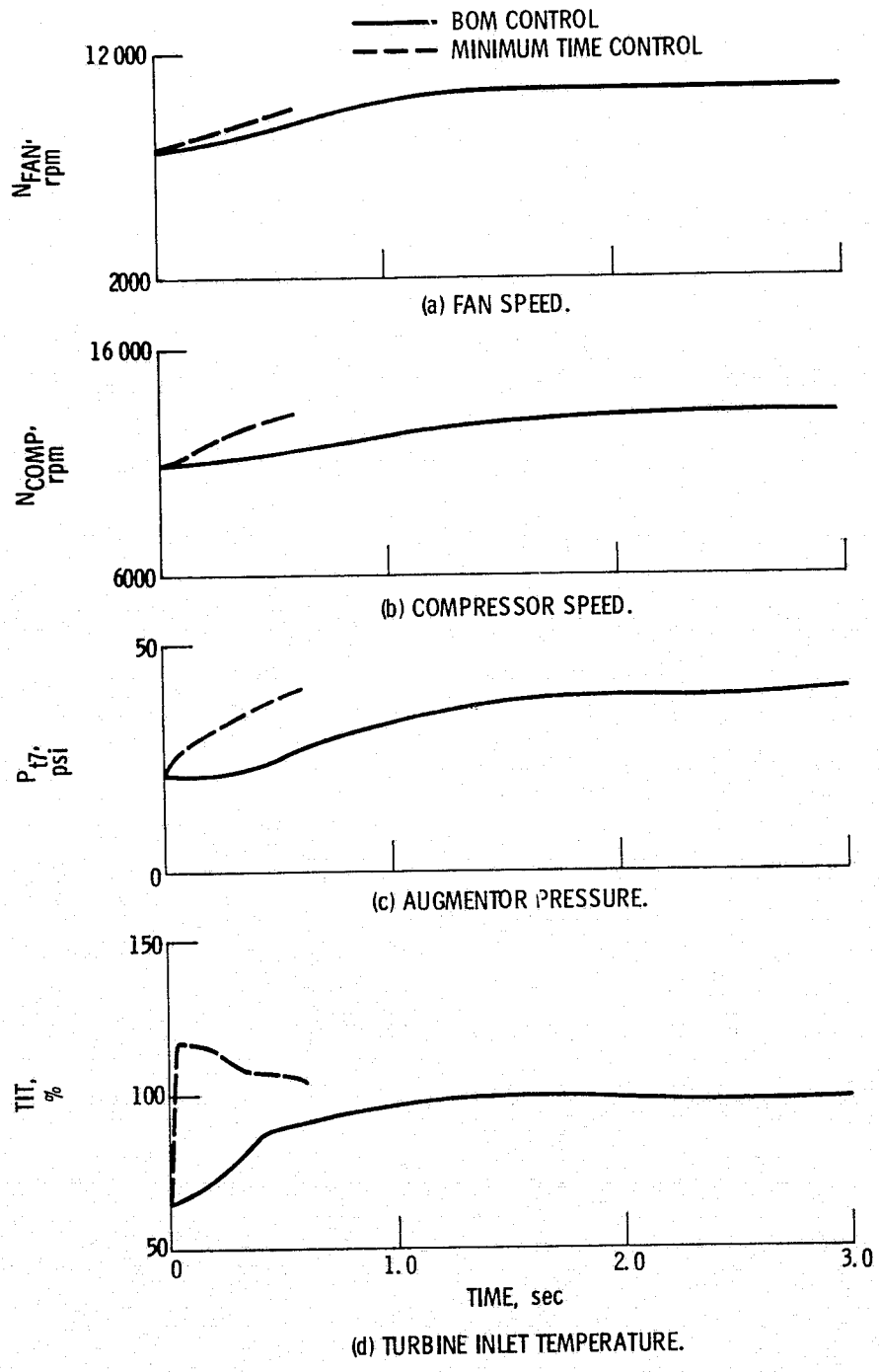

Figure 6.12. - Comparison of trajectories for minimum time and BOM control. Acceleration from PLA = 36 deg to intermediate thrust, nonlinear simulation.

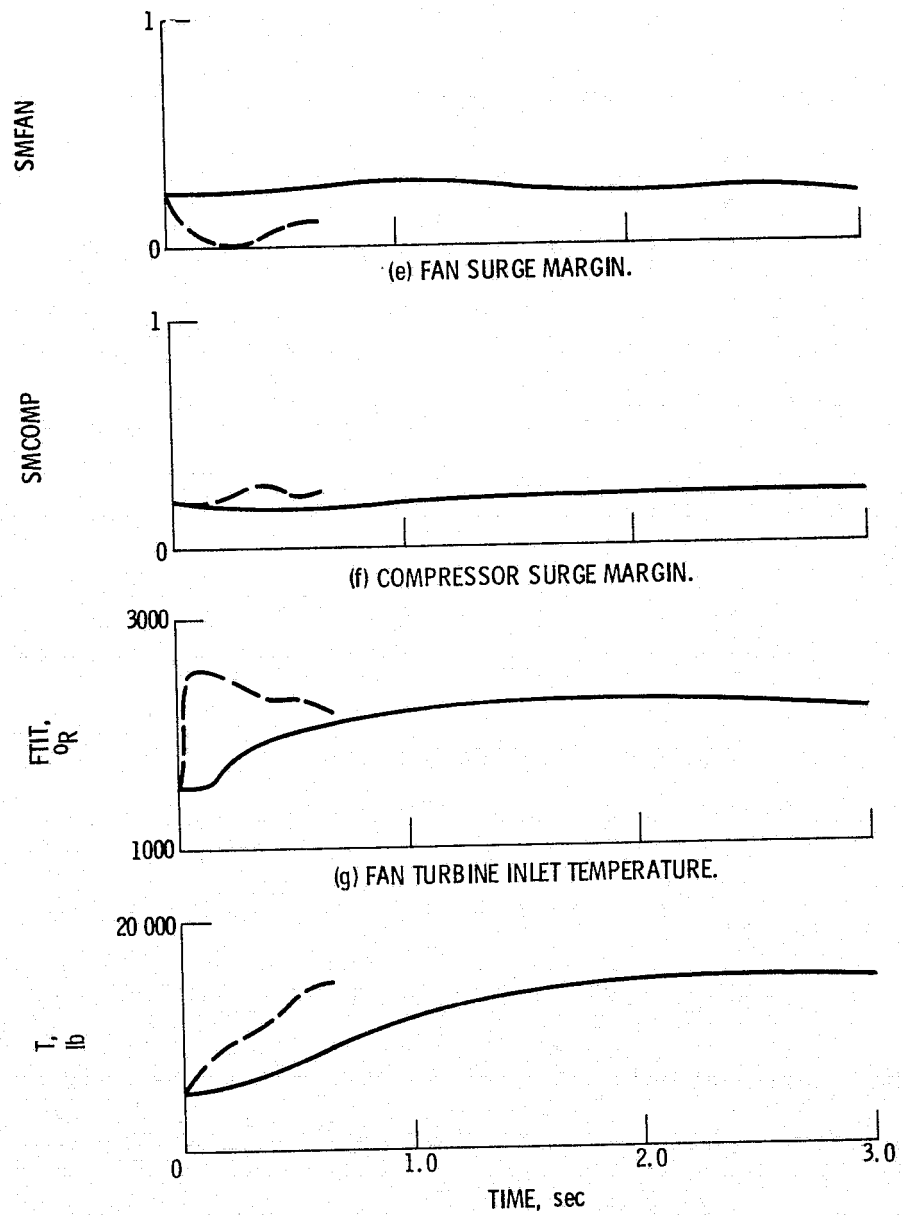

(e) FAN SURGE MARGIN.

(f) COMPRESSOR SURGE MARGIN.

(g) FAN TURBINE INLET TEMPERATURE.

(h) THRUST.

Figure 6.12. - Continued.

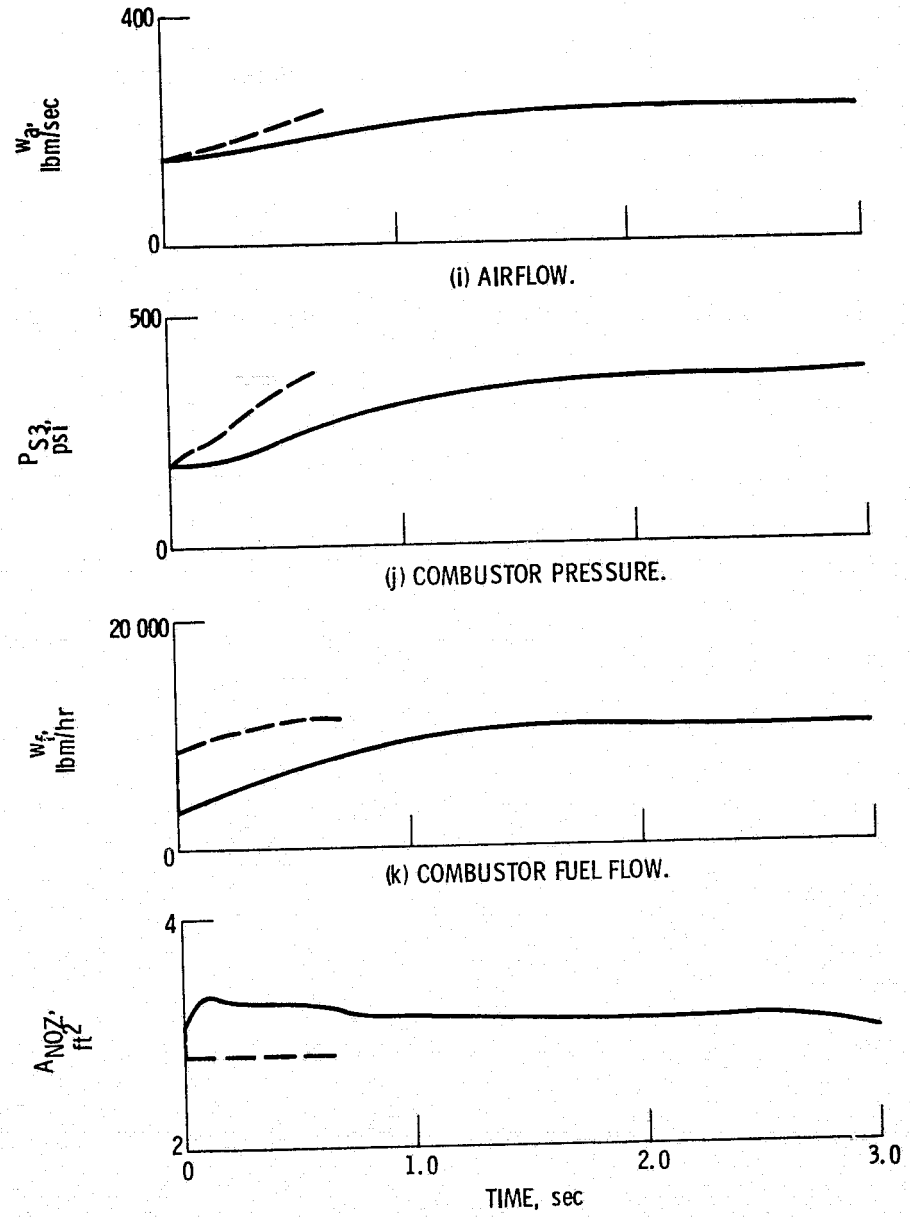

(l) NOZZLE AREA.

Figure 6.12. - Continued.

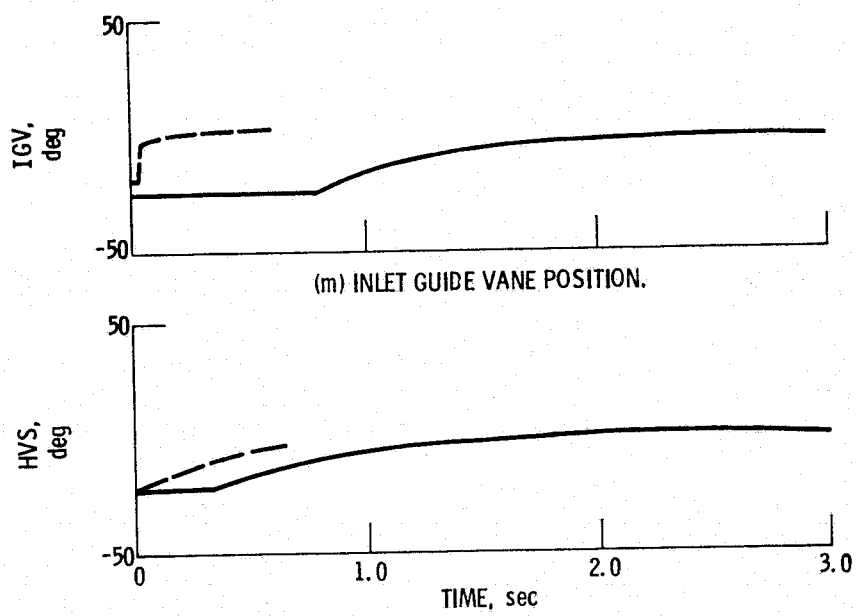

(m) INLET GUIDE VANE POSITION.

(n) COMPRESSOR VARIABLE VANE POSITION.

Figure 6.12. - Concluded.

H. Suboptimal Control

It has been shown that a substantial decrease in engine acceleration time can be achieved by using a minimum-time control strategy. However, the control strategy which has been developed is based on open-loop control. It is desirable that a closed-loop control strategy be developed which is capable of closely approximating the open-loop time-optimal results. The purpose of this section is to devise such a strategy.

The following strategy is based on the piecewise-linear model. Although further refinement of this model appears necessary, the general form will likely remain intact, and the following will still apply.

It has been previously noted that the turbine inlet temperature limit is an active constraint for the duration of each of the minimum time trajectories presented. This fact forms the basis for a closed-loop transition control law for fuel flow. Since turbine inlet temperature is modeled as an output, it can be expressed as a linear combination of state and control variables, i.e.,

$$TIT = c^T x + d^T u \tag{6.16}$$

For $TIT = T_{max}$, equation (6.16) may be solved for fuel flow (or any other control variable for which the coefficient d is nonzero) to yield:

$$w_f = \frac{1}{d_1}\left(T_{max} - C^T x - d_2 A_{noz} - d_3 IGV - d_4 HVS\right) \tag{6.17}$$

It still remains to find closed-loop control laws for A_{noz}, IGV, and HVS. We will consider the case for which IGV and HVS are limited to scheduled values ±7 degrees. Examination of a number of optimal tra-

jectories including those shown in figures 6.3 and 6.4 reveals the following facts:

(1) A_{noz} always starts at the higher value of 3.2 feet squared, then switches to the lower value of 2.8 feet squared. Furthermore, the switch occurs at fairly constant values of N_{comp}, averaging about 11 000 rpm.

(2) IGV always starts at the lower value (scheduled -7 degrees), then switches to scheduled +7 degrees. This switch also occurs at fairly constant values of N_{comp}, averaging about 12 000 rpm.

(3) HVS always has the scheduled -7 degrees value, never switching to the larger value.

Based on these observations, the following suboptimal closed-loop strategy is suggested.

$$A_{noz} = \begin{cases} 3.2 \text{ ft}^2, & N_{comp} \leq 11\ 000 \text{ rpm} \\ 2.8 \text{ ft}^2, & N_{comp} \geq 11\ 000 \text{ rpm} \end{cases}$$

$$\text{IGV} = \begin{cases} \text{Scheduled } -7 \text{ deg}, & N_{comp} \leq 12\ 000 \text{ rpm} \\ \text{Scheduled } +7 \text{ deg}, & N_{comp} \geq 12\ 000 \text{ rpm} \end{cases} \tag{6.18}$$

$$\text{HVS} = \text{Scheduled } -7 \text{ deg}$$

$$w_f = \frac{1}{d_1}\left(T_{max} - C^T x - d_2 A_{noz} - d_3 \text{IGV} - d_4 \text{HVS}\right)$$

The closed-loop control strategy shown in equation (6.18) was applied to the piecewise-linear model, and accelerations were obtained for various initial values of PLA to intermediate thrust. Results are presented in figure 6.13 for an initial PLA of 24 degrees. Terminal

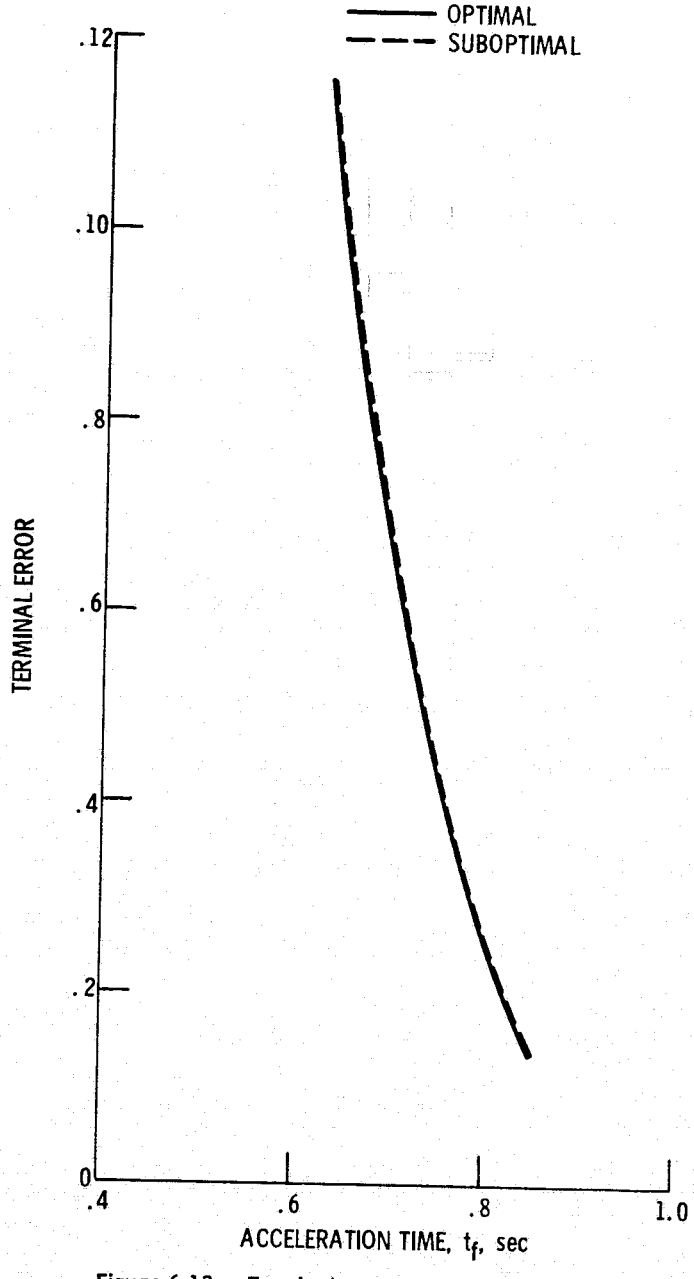

Figure 6.13. - Terminal error versus acceleration time. Part-power (PLA = 24 deg) to intermediate thrust acceleration. IGV and HVS, scheduled ± 7 deg.

error is presented as a function of acceleration time. Similar results for optimal open loop accelerations are repeated from figure 6.5 for comparison. It can be seen that the optimal and suboptimal results are virtually indistinguishable.

It is also of interest to determine the acceleration time required to reduce the terminal error to a fixed value, say 0.05. From figure 6.13, it can be seen that the required acceleration time for a terminal error of 0.05 is 0.80 second for an initial PLA of 24 degrees, for both the optimal and suboptimal results. Similar results were obtained for other initial values of PLA, and the results are shown in figure 6.14. As in figure 6.13, optimal and suboptimal results are virtually indistinguishable.

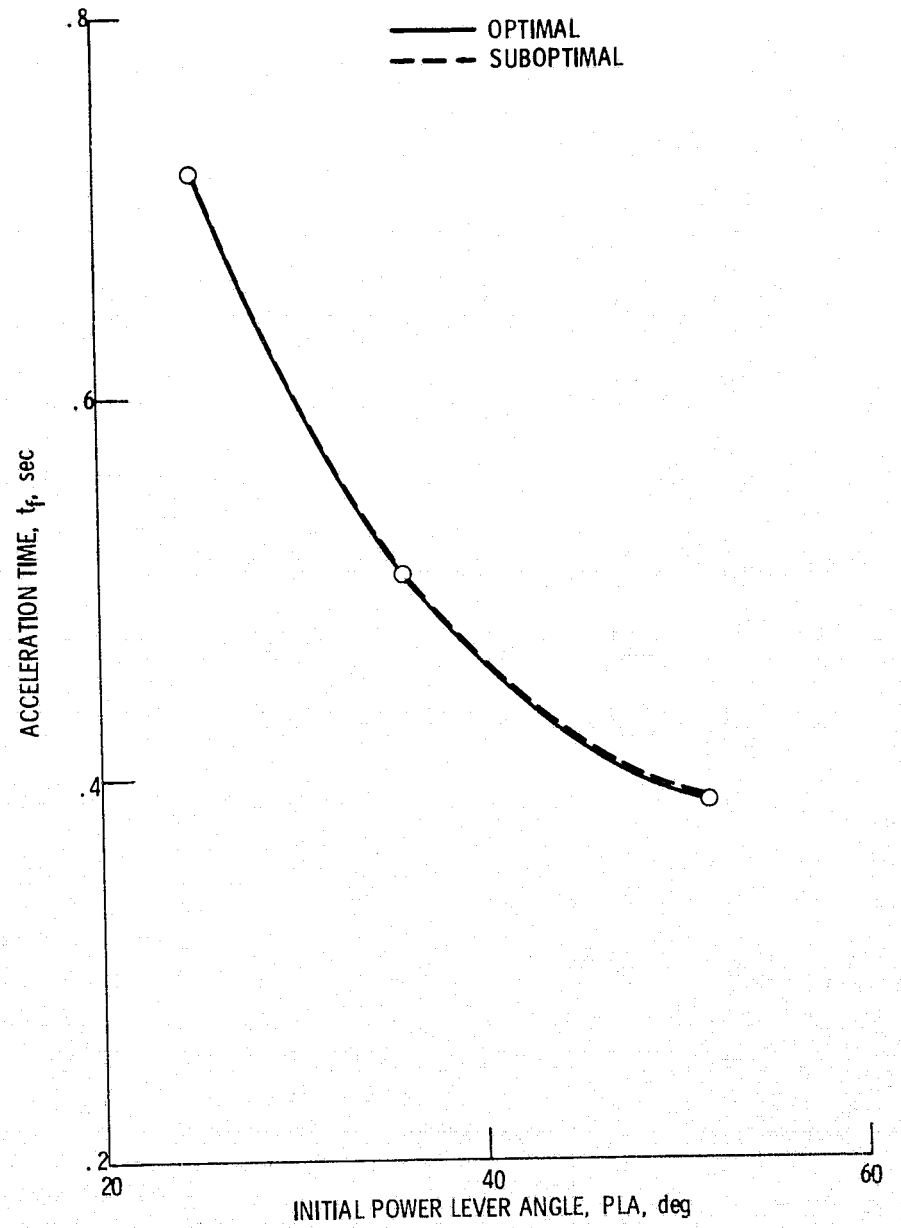

Figure 6.14. - Time required to accelerate to intermediate thrust with a fixed terminal error of 0.05. IGV and HVS, scheduled ±7 deg.

CHAPTER VII. CONCLUSIONS

Minimum time accelerations of aircraft turbofan engines are presented. The calculation of these accelerations is made by using a piecewise-linear engine model, and a new algorithm based on nonlinear programming. Use of this model and algorithm allows such trajectories to be readily calculated on a digital computer with a minimum expenditure of computer time.

The new algorithm may be used for solution of optimal control problems which are nonlinear in the state variables, and linear in the control variables. It is shown that the optimal control for such problems is bang-bang, except for possible singular arcs, which are not considered. The algorithm requires that a nominal bang-bang solution be found that satisfies the system equations and terminal constraints. The Euler-Lagrange equations are not utilized in the determination of this feasible solution; it is generally not a local minimum. Equations are derived for the determination of the Lagrange multipliers (sensitivity functions) which correspond to the initial feasible solution. These sensitivity functions are then utilized, along with nonlinear optimization (gradient search) techniques, to improve the feasible solution.

The new algorithm has several advantages over methods currently in use for solution of such problems. First, the system dynamic equations are uncoupled from the Euler-Lagrange equations: the Euler-Lagrange equations are not utilized in the determination of the initial

feasible solution. Second, use of the new algorithm minimizes the number of variables involved in the gradient search. With the new algorithm, the search variables are the constraint switching times - the times at which switches take place from one set of constraint functions to another. Other methods currently in use generally discretize the trajectory into a large number of intervals, and search for the optimal values of the controls for each interval.

The algorithm makes use of the fact that the optimal values of the control variables are determined by an equal number of active constraints. This situation always exists (except for possible singular arcs) when the performance criterion, system equations and constraint equations are all linear in the control variables. However, the control may also be fully determined by active constraints for some problems for which the equations are nonlinear in the control variables. It should be possible to extend the theory and algorithm presented herein to include such problems; this is an area worthy of further research.

The algorithm presented herein is used to find minimum-time acceleration histories for the F100 engine. A piecewise-linear engine model is used, having three state variables and four control variables. Minimum time solutions are obtained, and the resulting control histories are used as inputs to a nonlinear simulation of the F100 engine to verify the accuracy of the piecewise-linear solutions.

Comparison of the nonlinear and piecewise-linear solutions revealed significant differences in a few of the engine responses, the worst being a 35 percent error in the turbine inlet temperature, with

several of the variables matching to within 5 percent. To determine the source of these errors, the transient response to a small-perturbation fuel flow step was calculated using the nonlinear and three-and-sixteen-state linear models. It was discovered that there were significant differences in several of the engine responses for this case as well, notably fan speed and surge margins, for both the three- and sixteen-state variable linear models.

Based on these results, it appears that the calculation of linear models from a nonlinear simulation is a difficult task, and that there may be significant nonlinearities in the control effectiveness parameters. The linear models used herein were obtained by P&WA by using the offset-derivative method. There are at least three methods for identification of low-order linear models for aircraft engines which merit further study: (1) identification of high-order linear model via offset derivative method, followed by modal reduction to low order model; (2) least-squares identification of high-order model, followed by modal reduction to low order model; (3) least-squares identification of low order model.

Once accurate linear models are obtained, it is also of interest to determine the effect of state and control variable nonlinearities on the accuracy of the piecewise-linear results. Further research into the identification of simple nonlinear models may also be indicated.

Results presented herein indicate that improved steady-state and transient performance may be obtained by using optimal control strategy. Such strategy sometimes calls for operation of the controls in

a manner which has not been previously tested experimentally, even though the nonlinear simulation contains equations for predicting the effect of such control action. Further experimental testing is indicated in order to systematically explore the steady-state and transient effects of off-scheduled control action, and to determine if the predicted performance gains can be achieved.

In this report, it has been assumed that the control variables, i.e., fuel flow, nozzle area, inlet guide vane position, and compressor variable vane position, could jump instantaneously from one value to another. Actually, there are rate limits which apply to each of these control variables. It is possible to calculate optimal trajectories for which the control rate limits, in addition to the other constraints, are adhered to. This can be done by elevating the control variables to the role of state variables, and using the control variable rates as the new control variables. Furthermore, the algorithm presented herein can be used to solve this modified problem.

In addition to the open-loop optimal control strategy derived herein, a suboptimal closed-loop control logic is also derived which gives close approximation of the open loop performance. However, conclusive evidence on its general applicability would require extensive simulation and testing under many different flight conditions. Furthermore, implementation of the closed-loop control depends on being able to accurately and rapidly sense all engine states, and model all outputs. Further analytical research could help to identify types and accuracy of sensors needed to accomplish the control objectives.

APPENDIX A

OPTIMIZATION WITH STATE VARIABLE INEQUALITY CONSTRAINTS

In chapter II, the optimal control of a dynamic system which is nonlinear in the state variables and linear in the control variables is considered, and necessary conditions for optimality are derived. In chapter III, a new algorithm for solution of such problems is presented. In both chapters II and III, the path constraints are assumed to be either control or combined state/control inequality constraints, but not state variable inequality constraints. In this appendix, the results presented in chapters II and III are extended to apply to problems with state variable inequality constraints. To illustrate the use of the numerical technique, a state variable inequality constraint is added to one of the example problems from chapter V, and a local minimum solution is obtained.

A path constraint in which the control does not appear explicitly, i.e., $c_i(x,t) \leq 0$, is called a state variable inequality constraint. When a state variable inequality constraint is active for a finite time period (i.e., $c_i(x,t) \equiv 0$), the control may be determined from the requirement that all time derivatives of $c_i(x,t)$ must also be identically zero during this time period. If s time derivatives of $c_i(x,t)$ must be taken before the control appears explicitly, $c_i(x,t)$ is called a state variable inequality constraint of order s. The sth derivative of $c_i(x,t)$, i.e., $d^s c_i(x,t)/dt^s$, then serves as the path constraint from which a component of the control is determined. There

are s additional equality constraints,

$$c_i(x,t) = \frac{dc_i(x,t)}{dt} = \cdot \cdot \cdot = \frac{d^{s-1}c_i(x,t)}{dt^{s-1}} = 0$$

which must be satisfied at the initial point of the boundary segment on which the control is active. These are sometimes called "tangency" constraints.

1. Feasible Solution

In chapter III, a feasible solution having at least p segments is obtained for a problem in which there are p terminal constraints. If one of the active constraints for a given segment is a state variable inequality constraint of order s, then there are s additional point constraints which must be satisfied at the start of that segment. In this event, there must be s additional trajectory segments, whose durations provide the additional degrees of freedom necessary to satisfy the s constraints.

2. Calculation of Lagrange Multipliers

It is shown in chapter III that once a feasible solution is obtained, the Lagrange multipliers can be uniquely calculated. This is also the case if one of the active constraints is a state variable inequality constraint. Suppose, for example, there is a state variable inequality constraint of order s active in phase k. Then there are s additional point constraints which must be satisfied at $t = t_{k-1}$ as part of the determination of the feasible trajectory. There are also s additional trajectory segments for this case.

It can be shown (e.g., ref. 13) that at such a point constraint, there is a jump in λ which is proportional to the gradient of the

constraint. In this case, we have

$$\lambda^T(t_{k-1}^+) = \lambda^T(t_{k-1}^-) + \sum_{j=1}^{s} \varepsilon_j \frac{\partial}{\partial x}\left[\frac{d^j}{dt^j} c(t_{k-1})\right] \tag{A1}$$

For simplicity, we will consider the case in which a single first order state variable inequality constraint is active in segment k. The results which will be derived can be extended to the case of multiple, higher order state variable inequality constraints. For a first-order constraint, we have

$$\lambda^T(t_{k-1}^+) = \lambda^T(t_{k-1}^-) + \varepsilon \frac{\partial c}{\partial x}(t_{k-1}) \tag{A2}$$

Because of the point constraint which must be satisifed at $t = t_{k-1}$, there are $(p + 1)$ trajectory segments, and H must be continuous at the p interior points, $t = t_1, \ldots, t_p$. In addition, for final time free, equation (3.4) must also be satisfied.

Except at $t = t_{k-1}$, the requirement for continuity of H is achieved by satisfying (3.3). However, the requirement for continuity of H at $t = t_{k-1}$ must be given special consideration because of the jump in λ at $t = t_{k-1}$. The change in H at t_{k-1} is given by

$$\begin{aligned}
\Delta H &= \lambda^T(t_{k-1}^+)[f + gu(t_{k-1}^+)] - \lambda^T(t_{k-1}^-)[f + gu(t_{k-1}^-)] \\
&\qquad + b^T(t_{k-1})[u(t_{k-1}^+) - u(t_{k-1}^-)] \\
&= \left[\lambda^T(t_{k-1}^-) + \varepsilon \frac{\partial c}{\partial x}\right][f + gu(t_{k-1}^+)] - \lambda^T(t_{k-1}^-)[f + gu(t_{k-1}^-)] \\
&\qquad + b^T(t_{k-1})[u(t_{k-1}^+) - u(t_{k-1}^-)] \\
&= \left[b^T(t_{k-1}) + \lambda^T(t_{k-1}^-)g\right][u(t_{k-1}^+) - u(t_{k-1}^-)] \\
&\qquad + \varepsilon \frac{\partial c}{\partial x}[f + gu(t_{k-1}^+)]
\end{aligned}$$

But for $t = t_{k-1}^{+}$,

$$\frac{dc}{dt} = \frac{\partial c}{\partial x}\,[f + gu(t_{k-1}^{+})] = 0$$

Therefore, we have

$$\Delta H = [b^{+}(t_{k-1}) + \lambda^{T}(t_{k-1}^{-})g(t_{k-1})][u(t_{k-1}^{+}) - u(t_{k-1}^{-})] \qquad \text{at} \quad t = t_{k-1} \tag{A3}$$

In order to solve for ε and the p values of ν, we find $(p + 2)$ backward solutions of the $\mathring{\lambda}$ equation (2.13). The first $(p + 1)$ of these solutions are identical to (3.5); $\lambda^{(p+1)}(t)$ is obtained by integrating (2.13) backward, starting at t_{k-1}, with initial conditions $\lambda^{(p+1)}(t_{k-1}) = -\frac{\partial c}{\partial x}(t_{k-1})$. By superposition, $\lambda(t)$ is given by

$$\lambda(t) = \lambda^{(0)}(t) + \Lambda(t)\nu + \varepsilon\lambda^{(p+1)}(t) \tag{A4}$$

The $(p + 1)$ equations for the determination of ε and ν are given by

$$[u(t_i^{+}) - u(t_i^{-})]^{T}[b(t_i) + g^{T}(t_i)\lambda^{(0)}(t_i) + g^{T}(t_i)\Lambda(t_i)\nu + g^{T}(t_i)\lambda^{(p+1)}(t)\varepsilon] = 0$$

$$i = 1, \ldots, (k-2), k, \ldots, p \tag{A5}$$

$$[u(t_{k-1}^{+}) - u(t_{k-1}^{-})]^{T}[b(t_{k-1}) + g^{T}(t_{k-1})\lambda^{(0)}(t_{k-1}) + g^{+}(t_{k-1})\Lambda(t_{k-1})\nu - g^{T}(t_{k-1})\frac{\partial c}{\partial x}(t_{k-1})\varepsilon] = 0 \tag{A6}$$

$$a(t_f) - b^{T}(t_f)D^{-T}(t_f)C(t_f) + \frac{d\phi}{dt}(t_f) + \left[\frac{d\psi}{dt}(t_f)\right]^{T}\nu = 0 \tag{A7}$$

The calculation of ν and ε proceeds exactly as in (3.10) to (3.12), and will not be repeated here.

3. A Numerical Example

To illustrate the use of the equations which have been presented, a numerical example which includes an active state variable inequality constraint will be solved. Consider the problem of finding $u(t)$ which transfers the system

$$\begin{aligned} \dot{x} &= -x + u + 0.25 \\ \dot{y} &= -4y + u \end{aligned} \tag{A8}$$

from initial conditions $(x_0, y_0) = (1, 1)$ to terminal conditions $(x_f, y_f) = (0, 0)$ in minimum time. The system is subject to inequality constraints

$$\begin{aligned} |u| &\leq 2 \\ y + 0.2 &\geq 0 \end{aligned} \tag{A9}$$

This problem is identical to the one-piece linear approximation studied in chapter V, but with the addition of a state variable inequality constraint, $y + 0.2 \geq 0$.

When the state variable inequality constraint is active, i.e., $y + 0.2 = 0$, the control is determined from

$$\dot{y} = -4y + u = 0$$

and since $y = -0.2$, we have $u = -0.8$ as the equivalent path constraint.

Inspection of the optimal solution in figure 5.2 shows that the constraint $y + 0.2 \geq 0$ is violated. Therefore, we look for a feasible solution in which the constraint $y + 0.2 \geq 0$ is active on one of the segments. Specifically, we assume the optimal control history is given by

$$u = -2, \qquad 0 \le t \le t_1$$

$$u = -0.8, \qquad t_1 \le t \le t_2 \tag{A10}$$

$$u = 2, \qquad t_2 \le t \le t_f$$

and we seek values of t_1, t_2, and t_f such that the terminal constraints $x_f = y_f = 0$ and the intermediate constraint $y(t_1) = -0.2$ are satisfied. Solution of the multipoint boundary value problem results in $t_1 = 0.402$, $t_2 = 1.002$, $t_f = 1.086$.

The Lagrange multiplier time history which corresponds to this trajectory may be calculated once the three parameters ν_1, ν_2, and ε are known. These parameters are determined by requiring that equation (A5) (for $i = 2$), (A6) (for $k = 2$), and (A7) be satisfied. The resulting equations are given by

$$2.25\ \nu_1 + 2\nu_2 = -1$$

$$0.919\ \nu_1 + 0.715\ \nu_2 = 0$$

$$0.615\ \nu_1 + 0.143\ \nu_2 - \varepsilon = 0$$

Simultaneous solution of these three equations results in

$$\nu_1 = 3.12, \qquad \nu_2 = -4.01, \qquad \varepsilon = 1.35$$

The final conditions on λ are therefore given by

$$\lambda_x(t_f) = 3.12, \qquad \lambda_y(t_f) = -4.01$$

Also, λ_y is discontinuous at t_1:

$$\lambda_y(t_1^+) = \lambda_y(t_1^-) + 1.35$$

The switching function $(\lambda_x + \lambda_y)$ is presented as a function of time in figure A1. It confirms the fact that the initial feasible solution is a local minimum. The optimal trajectory is shown in figure A2.

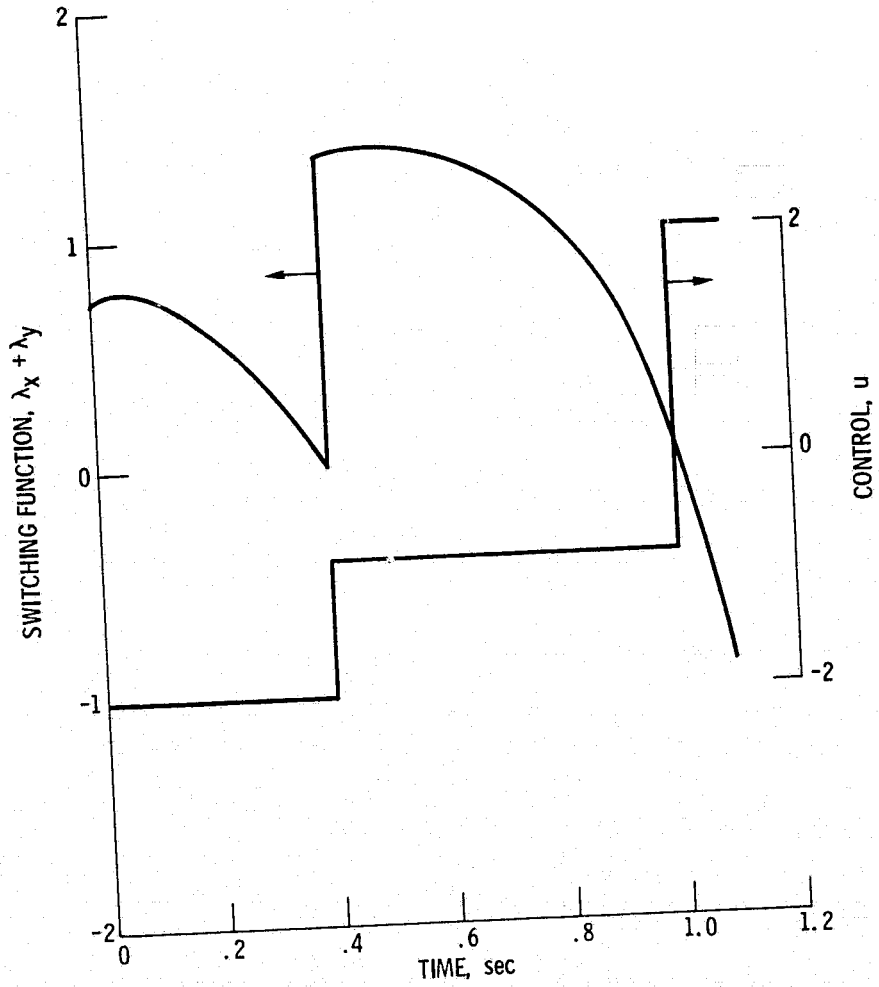

Figure A-1. - Switching function and control profile for optimization problem with state variable inequality constraint.

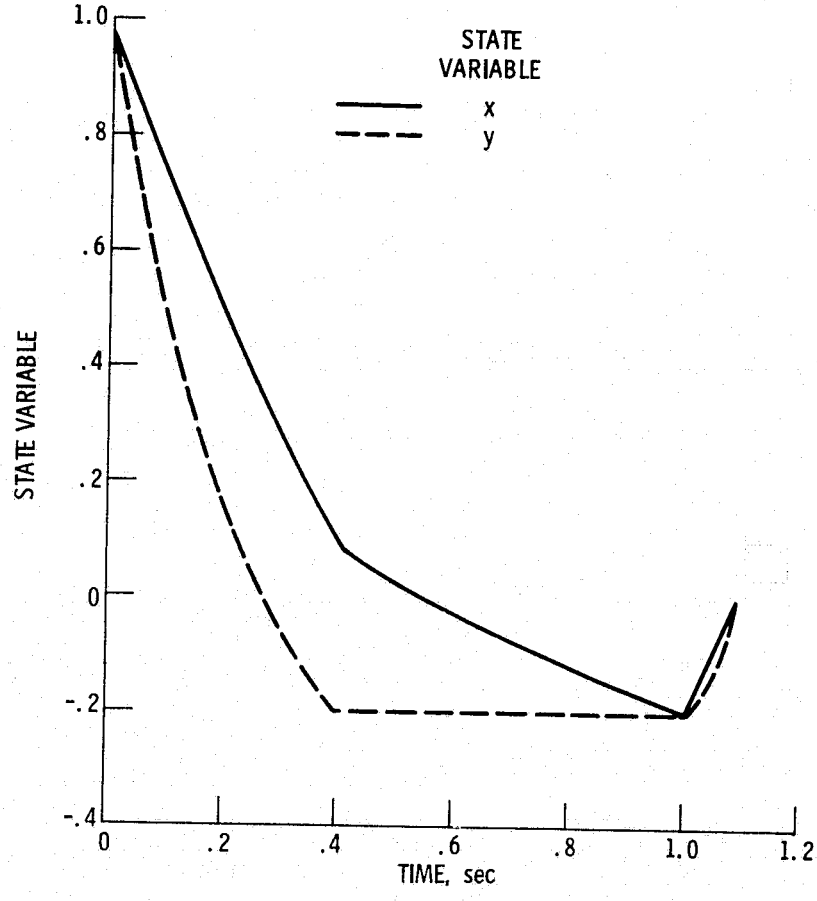

Figure A-2. - Optimal trajectory for problem with state variable inequality constraint.

APPENDIX B

DERIVATION OF LAGRANGE MULTIPLIER FUNCTIONS FOR FEASIBLE SOLUTION

Necessary conditions for the optimal control of a dynamic system which is nonlinear in the state and linear in the control are derived in chapter II. It is shown that except for singular arcs, the optimal control (r variables) is always determined by r active constraint boundaries. In chapter III, the nature of the optimal control strategy is used as the basis for a new algorithm for the solution of such optimization problems.

In chapter III, the first step is to obtain a feasible solution which satisfies all path and terminal constraints. This is accomplished by dividing the trajectory into at least p segments (for a problem with p terminal constraints) and requiring the control to be determined by a set of r active constraints for each segment; p of the junction times are varied in order to satisfy the terminal constraints. The Euler-Lagrange equations are not utilized in the determination of this feasible solution; it may or may not be a local minimum.

Once such a feasible solution is obtained, it is useful to calculate the Lagrange multiplier time histories, functions of which are switching functions which predict the change in the performance index obtainable from small changes in the control histories. In chapter III, it is shown that these Lagrange multipliers can be easily

and uniquely calculated. The calculation scheme makes use of the differential equations for the multipliers, and the continuity of the Hamiltonian at junction points. The Lagrange multiplier differential equations are derived in this appendix. Also, the requirement for continuity of the Hamiltonian at junction points is proved here.

If the initial feasible solution is not a local minimum, the procedure followed in chapter III is to introduce additional segments, having control determined by r different active constraints. The switching times associated with these segments are used in conjunction with a gradient search technique to systematically improve the performance index. The gradient search technique requires partial derivatives of the performance index with respect to the free switching times; these partial derivatives are derived in this appendix.

The problem statement which applies to the above problem is as follows. It is desired to find the values of the p junction times which result in minimizing the performance index

$$J = \phi(x_f, t_f) + \int_{t_0}^{t_f} (a + b^T u)dt \tag{B1}$$

subject to the system dynamical equations

$$\dot{x} = f + gu \tag{B2}$$

and terminal constraints

$$\psi_i(x_f, t_f) = 0, \qquad i = 1, 2, \ldots, p \tag{B3}$$

In addition, the control must satisfy

$$u = -D_i^{-T} C_i, \qquad t_{i-1} \leq t \leq t_i \qquad i = 1, 2, \ldots, w \geq p \tag{B4}$$

The system equations, terminal constraints, and control constraints may be adjoined to the performance index by using undetermined Lagrange multipliers. This results in

$$J^* = \phi(x_f,t_f) + \nu^T\psi(x_f,t_f) + \sum_{i=1}^{w} \int_{t_{i-1}}^{t_i} [a + b^T u$$

$$+ \lambda_i^T(f + gu - \dot{x}) + \rho_i^T(u + D_i^{-T}C_i)]dt \qquad \text{(B5)}$$

Necessary conditions for a local minimum are that we can find $\lambda_i(t)$, $\rho_i(t)$, and ν such that the first variation of J^* vanishes with respect to all allowable variations. The variation of J^* is given by

$$\delta J^* = \left(\frac{\partial\phi}{\partial x_f} + \nu^T \frac{d\psi}{\partial x_f}\right) dx_f + \left(\frac{\partial\phi}{\partial t_f} + \nu^T \frac{\partial\psi}{\partial t_f}\right) dt_f + \sum_{i=1}^{w} \int_{t_{i-1}}^{t_i} \left\{\left[\frac{\partial a}{\partial x} + \frac{\partial b^T}{\partial x} u\right.\right.$$

$$\left. + \lambda_i^T \left(\frac{\partial f}{\partial x} + \frac{\partial g}{\partial x} u\right) - \rho_i^T \left(\frac{\partial D_i^{-T}}{\partial x} C_i + D_i^{-T} \frac{\partial C_i}{\partial x}\right)\right]\delta x + \left(\lambda_i^T g + \rho_i^T + b^T\right)\delta u$$

$$\left. - \lambda_i^T \delta\dot{x}\right\} dt + \sum_{i=1}^{w} (a + b^T u)\, dt \Bigg|_{t_{i-1}}^{t_i} \qquad \text{(B6)}$$

Integration of (B6) by parts gives

$$\delta J^* = \left(\frac{\partial\phi}{\partial x} + \nu^T \frac{\partial\psi}{\partial x}\right)\delta x_f + \left(\frac{\partial\phi}{\partial t_f} + \nu^T \frac{\partial\psi}{\partial t_f}\right) dt_f + \sum_{i=1}^{w} \int_{t_{i-1}}^{t_i}$$

$$\left\{\left[\frac{\partial a}{\partial x} + \frac{\partial b^T}{\partial x} u + \lambda_i^T \left(\frac{\partial f}{\partial x} + \frac{\partial g}{\partial x} u\right) - \rho_i^T \left(\frac{\partial D_i^{-T}}{\partial x} C_i + D_i^{-T} \frac{\partial C_i}{\partial x}\right) + \dot{\lambda}_i^T\right]\delta x\right.$$

$$+ (\lambda_i^T + \rho_i^T + b^T)\delta u \, dt + \sum_{i=1}^{w} \left[(a + b^T u)dt - \lambda_i^T \, \delta x\right]_{t_{i-1}}^{t_i} \qquad \text{(B7)}$$

Since u is constrained by (B4), the δu are not free but are given by

$$\delta u = -\left(\frac{\partial D_i^{-T}}{\partial x} C_i + D_i^{-T} \frac{\partial C_i}{\partial x}\right)\delta x \qquad \text{(B8)}$$

If (B4) and (B8) are substituted into (B7), and we choose $\lambda_i(t)$ such that

$$\dot{\lambda}_i^T = -\frac{\partial a}{\partial x} + \frac{\partial b^T}{\partial x} D_i^{-T} C_i + b^T \frac{\partial D_i^{-T}}{\partial x} C_i + b^T D_i^{-T} \frac{\partial C_i}{\partial x}$$

$$- \lambda_i^T \left(\frac{\partial f}{\partial x} - \frac{\partial g}{\partial x} D_i^{-T} C_i - g \frac{\partial D_i^{-T}}{\partial x} C_i - g D_i^{-T} \frac{\partial C_i}{\partial x}\right) \qquad \text{(B9)}$$

then (B7) simplifies to

$$\delta J^* = \left(\frac{\partial\phi}{\partial x} + \nu^T \frac{\partial\psi}{\partial x}\right) dx_f + \left(\frac{\partial\phi}{\partial t_f} + \nu^T \frac{\partial\psi}{\partial t_f}\right) dt_f + \sum_{i=1}^{w}$$

$$[(a + b^T u)dt - \lambda_i^T \, \delta x]_{t_{i-1}}^{t_i} \qquad \text{(B10)}$$

Note that (B9) can be written

$$\dot{\lambda}_i^T = -\frac{\partial}{\partial x}(a - bD_i^{-T}C_i) - \lambda_i^T \frac{\partial}{\partial x}(f - gD_i^{-T}C_i) \tag{B11}$$

which is identical to (2.13).

The variations δx which appear in (B10) apply for fixed time t_i, and can be expressed in terms of the total variation dx and variation of time dt.

$$\delta x = dx - \dot{x}\, dt \tag{B12}$$

Now if we use (B12) in (B10), and choose

$$\lambda^T(t_f) = \frac{\partial \phi}{\partial x_f} + \nu^T \frac{\partial \psi}{\partial x_f} \tag{B13}$$

and if t_f is free,

$$H(t_f) \triangleq a + b^T u + \lambda^T(f + gu) = -\frac{\partial \phi}{\partial t_f} - \nu^T \frac{\partial \psi}{\partial t_f} \tag{B14}$$

then (B10) simplifies to

$$\delta J^* = \sum_{i=1}^{w-1} \left[(a + b^T u + \lambda_i^T \dot{x})dt - \lambda_i^T\, dx\right]_{t_{i-1}}^{t_i}$$

$$= \sum_{i=1}^{w-1} \left[\lambda_i^T(t_i) - \lambda_{i+1}^T(t_i)\right] dx(t_i) + \sum_{i=1}^{w-1} \left[b^T(t_i)u(t_i^-) + \lambda_i^T(t_i)\dot{x}(t_i^-)\right.$$

$$\left. - b^T(t_i)u(t_i^+) - \lambda_{i+1}^T(t_i)\dot{x}(t_i^+)\right] dt_i \tag{B15}$$

Note that (B13) and (B14) are identical to (2.7) and (2.8). We can also choose

$$\lambda_i(t_i) = \lambda_{i+1}(t_i)$$

so that the variation of J^* becomes

$$\delta J^* = \sum_{i=1}^{w-1} \left\{ b^T(t_i)[u(t_i^-) - u(t_i^+)] + \lambda_i^T(t_i)[\dot{x}(t_i^-) - \dot{x}(t_i^+)] \right\} dt_i$$

$$= \sum_{i=1}^{w-1} [H(t_i^-) - H(t_i^+)] dt_i \tag{B16}$$

If a particular t_i is one of the free junction times, the coefficient of dt_i must vanish for a local minimum solution.

$$H(t_i^-) = H(t_i^+) \tag{B17}$$

for free junction times t_i. On the other hand, if $t_i = t_{sw}$ is one of the fixed times, then we have

$$\frac{\partial J^*}{\partial t_{sw}} = \frac{\partial J}{\partial t_{sw}} = H(t_{sw}^-) - H(t_{sw}^+) \tag{B18}$$

APPENDIX C

MODEL ORDER REDUCTION

Suppose we have a linear system

$$\dot{x} = Fx + Gu$$

subject to linear inequality constraints

$$Cx + Du + E \leq 0$$

Also, suppose there are n states, and n_1 of the eigenvalues of F are much smaller than the remaining $n_2 = n - n_1$. Then the dynamics associated with the n_2 larger-eigenvalue modes are much faster than the dynamics of the n_1 lower eigenvalue modes. Therefore, the higher frequency modes will nearly always be in equilibrium (or oscillating at high frequency about equilibrium). In such a case, the calculation of optimal trajectories can be made significantly easier if the high frequency modes are assumed to be always in equilibrium. In carrying out that approximation, it is also desirable that the low frequency eigenvalues be retained exactly. Furthermore, it is desirable that n_1 of the original states be retained in the lower order approximate model.

Specifically, we seek a low frequency approximation of the system in which the first n_1 states of the original system are retained, and the eigenvalues of the reduced order system are exactly equal to the n_1 smaller eigenvalues of the original system. We proceed as follows.

We can find a transformation T which block-diagonalizes the system:

$$x = Tm; \qquad T^{-1}x = m \tag{C1}$$

where the m are modal coordinates. Differentiating the above gives

$$\dot{m} = T^{-1}\dot{x} = \Lambda m + \Sigma u \tag{C2}$$

where $\Sigma \triangleq T^{-1}G$ and $\Lambda = T^{-1}FT$ is block diagonal. If (C2) is partitioned into low frequency modes $m^{(1)}$ and high frequency modes $m^{(2)}$, the result is

$$\begin{aligned} \dot{m}^{(1)} &= \Lambda^{(1)}m^{(1)} + \Sigma^{(1)}u \\ \dot{m}^{(2)} &= \Lambda^{(2)}m^{(2)} + \Sigma^{(2)}u \end{aligned} \tag{C3}$$

The quasi-steady approximation is

$$\dot{m}^{(2)} \cong 0$$

which results in

$$m^{(2)} \cong -\Lambda^{(2)^{-1}}\Sigma^{(2)}u \tag{C4}$$

Now let $x^{(1)}$ have the same dimension as $m^{(1)}$ and denote the states of most interest in the low frequency approximation. We have

$$x^{(1)} = T_{11}m^{(1)} + T_{12}m^{(2)}$$

Differentiation results in

$$\begin{aligned} \dot{x}^{(1)} &= T_{11}\dot{m}^{(1)} + T_{12}\dot{m}^{(2)} \cong T_{11}\Lambda^{(1)}m^{(1)} + T_{11}\Sigma^{(1)}u \\ &= T_{11}\Lambda^{(1)}T_{11}^{-1}\left[x^{(1)} - T_{12}m^{(2)}\right] + T_{11}\Sigma^{(1)} \\ \dot{x}^{(1)} &= T_{11}\Lambda^{(1)}T_{11}^{-1}x^{(1)} + \left[T_{11}\Sigma^{(1)} + T_{11}\Lambda_1 T_{11}^{-1}T_{12}\Lambda^{(2)^{-1}}\Sigma^{(2)}\right]u \end{aligned} \tag{C5}$$

Also, we have

$$x^{(2)} = T_{21}m^{(1)} + T_{22}m^{(2)}$$

$$= T_{21}T_{11}^{-1}\left[x^{(1)} - T_{12}m^{(2)}\right] + T_{22}m^{(2)}$$

$$x^{(2)} \cong T_{21}T_{11}^{-1}x^{(1)} + (T_{21}T_{11}^{-1}T_{12} - T_{22})\Lambda^{(2)^{-1}}\Sigma^{(2)}u \qquad \text{(C6)}$$

The inequality constraints become

$$Cx + Du + E = C_1x^{(1)} + C_2x^{(2)} + Du + E$$

$$= C_1x^{(1)} + C_2\left[T_{21}T_{11}^{-1}x^{(1)} + (T_{21}T_{11}^{-1}T_{12} - T_{22})\Lambda^{(2)^{-1}}\Sigma^{(2)}u\right] + Du + E$$

$$= \left(C_1 + C_2T_{21}T_{11}^{-1}\right)x^{(1)} + \left[C_2\left(T_{21}T_{11}^{-1}T_{12} - T_{22}\right)\Lambda^{(2)^{-1}}\Sigma^{(2)} + D\right]u \leq 0 \qquad \text{(C7)}$$

APPENDIX D

THREE-STATE LINEAR MODELS. SEA-LEVEL-STATIC

(a) PLA = 20°

$$F = \begin{pmatrix} -2.09 & 2.09 & -0.537 \\ .0944 & -0.251 & -0.163 \\ 11.6 & -0.457 & -18.9 \end{pmatrix} \qquad x_e = \begin{pmatrix} 38.79 \\ 91.92 \\ 161 \end{pmatrix}$$

$$G = \begin{pmatrix} 7.27 & 0.054 & -0.478E-2 & -0.00398 \\ .756 & -0.0105 & .363E-3 & -0.00109 \\ 7.38 & -1.87 & .0584 & -0.00378 \end{pmatrix} \qquad u_e = \begin{pmatrix} 11.34 \\ 300 \\ -250 \\ -3050 \end{pmatrix}$$

$$C = \begin{pmatrix} 0.239 & -0.416E-2 & 0.336 \\ 1.77 & .0839 & -0.108 \\ .0521 & -0.587 & .0245 \\ -2.01 & 3.51 & -3.55 \\ -16.1 & 37.9 & -5.24 \\ .825E-2 & -1.60 & .384 \\ .0233 & 2.06 & .189E-2 \end{pmatrix} \qquad y_e = \begin{pmatrix} 11.26 \\ 73.3 \\ 54.1 \\ 102 \\ 83.8 \\ 120 \\ 73.2 \end{pmatrix}$$

$$D = \begin{pmatrix} 0.314 & -0.270E-2 & 0.150E-2 & -0.787E-4 \\ .445 & .515E-2 & .0114 & -0.131E-3 \\ .436 & -0.0130 & -0.508E-3 & .237E-2 \\ 12.3 & .150 & -0.376 & -0.476E-2 \\ 222 & 1.98 & -0.0285 & -0.491 \\ -0.621 & -0.0155 & -0.199E-2 & .686E-2 \\ 6.09 & .0382 & .108E-2 & -0.463E-2 \end{pmatrix}$$

(b) PLA = 36°

$$F = \begin{pmatrix} -2.23 & 0.988 & -0.462 \\ -0.316 & -0.232 & -0.106 \\ 24.5 & .435 & -7.91 \end{pmatrix} \qquad x_e = \begin{pmatrix} 77.2 \\ 109 \\ 226 \end{pmatrix}$$

$$G = \begin{pmatrix} 2.78 & 0.0138 & -0.0350 & -0.00211 \\ .743 & -0.0133 & -0.00478 & -0.00139 \\ 6.18 & -4.67 & .370 & .0135 \end{pmatrix} \qquad u_e = \begin{pmatrix} 34.9 \\ 300 \\ -250 \\ -914 \end{pmatrix}$$

$$C = \begin{pmatrix} 0.905 & -0.753E-3 & 0.243 \\ 3.10 & .0841 & -0.107 \\ -0.102 & -0.135 & -0.0137 \\ 4.39 & 1.73 & -1.89 \\ -5.63 & 28.0 & -0.594 \\ -0.177 & -0.398 & -0.00598 \\ 1.05 & 1.14 & .137 \end{pmatrix} \qquad y_e = \begin{pmatrix} 52.2 \\ 152 \\ 70.8 \\ 225 \\ 99.1 \\ 152 \\ 182 \end{pmatrix}$$

$$D = \begin{pmatrix} 0.285 & -0.0175 & 0.0130 & 0.117E-4 \\ .143 & .108E-2 & .0439 & -0.327E-3 \\ .703 & .291E-2 & -0.193E-2 & .102E-2 \\ 2.27 & .0589 & -0.199 & -0.541E-2 \\ 1.27 & -0.0720 & -0.0328 & -0.118 \\ 1.46 & .0123 & -0.383E-2 & .261E-2 \\ 2.05 & -0.862E-2 & .0136 & -0.370E-2 \end{pmatrix}$$

(c) PLA = 52°

$$F = \begin{pmatrix} -2.27 & 2.23 & -0.520 \\ -0.498 & -1.96 & -0.0639 \\ 22.8 & .936 & -6.11 \end{pmatrix} \qquad x_e = \begin{pmatrix} 87.6 \\ 116 \\ 276 \end{pmatrix}$$

$$G = \begin{pmatrix} 2.00 & -0.0366 & -0.0434 & -0.531E-3 \\ 1.30 & .00653 & -0.0103 & -0.445E-2 \\ 7.41 & -6.24 & .541 & -0.166E-2 \end{pmatrix} \qquad u_e = \begin{pmatrix} 50.8 \\ 300 \\ -250 \\ -259 \end{pmatrix}$$

$$C = \begin{pmatrix} 1.00 & 0.0466 & 0.224 \\ 2.70 & .0937 & -0.0741 \\ -0.101 & -0.136 & -0.0249 \\ 17.4 & 2.59 & -1.86 \\ -5.98 & 22.3 & -0.399 \\ -0.105 & -0.321 & -0.0596 \\ 1.30 & 2.21 & 1.97 \end{pmatrix} \qquad y_e = \begin{pmatrix} 78.7 \\ 180 \\ 78.9 \\ 221 \\ 150 \\ 170 \\ 237 \end{pmatrix}$$

$$D = \begin{pmatrix} 3.34 & -0.0147 & 0.0240 & 0.675E-4 \\ .256 & .0163 & .0665 & -0.550E-3 \\ .630 & .977E-4 & -0.528E-2 & .591E-3 \\ 2.82 & .0244 & -0.190E-2 & -0.634E-2 \\ 1.29 & -0.115 & -0.765E-2 & -0.0906 \\ 1.36 & -0.0107 & -0.0102 & .162E-2 \\ .962 & -0.268E-2 & .0307 & -0.138E-2 \end{pmatrix}$$

(d) PLA = 67°

$$F = \begin{pmatrix} -3.37 & 3.13 & -0.493 \\ -0.130 & -2.87 & -0.072 \\ -21.3 & 1.93 & -6.03 \end{pmatrix} \qquad x_e = \begin{pmatrix} 94.4 \\ 122 \\ 330 \end{pmatrix}$$

$$G = \begin{pmatrix} 1.59 & -0.0354 & -0.0848 & 0.155E-2 \\ 1.17 & .0165 & -0.795E-2 & -0.574E-2 \\ 5.74 & -7.34 & .804 & .0173 \end{pmatrix} \qquad u_e = \begin{pmatrix} 68.6 \\ 298 \\ -164 \\ 92.2 \end{pmatrix}$$

$$C = \begin{pmatrix} 0.945 & 0.0511 & 0.219 \\ 2.09 & .0249 & -0.0198 \\ .0769 & -0.187 & -0.0353 \\ 7.37 & 2.00 & -1.42 \\ -6.54 & 12.3 & -0.245 \\ .351 & -0.465 & -0.0817 \\ .454 & 3.16 & .282 \end{pmatrix} \qquad y_e = \begin{pmatrix} 105 \\ 203 \\ 86.4 \\ 254 \\ 179 \\ 187 \\ 290 \end{pmatrix}$$

$$D = \begin{pmatrix} 0.361 & -0.00523 & 0.0342 & 0.807E-4 \\ .210 & .0432 & .0799 & -0.561E-3 \\ .541 & -0.294E-2 & -0.191E-2 & 0.436E-3 \\ 1.59 & .135 & -0.671 & -0.444E-2 \\ 1.53 & .206 & -0.0967 & -0.110 \\ 1.16 & -0.025 & -0.437E-3 & 0.119E-2 \\ .838 & .0335 & .0215 & .819E-3 \end{pmatrix}$$

(e) PLA = 83°

$$F = \begin{pmatrix} -4.83 & 2.43 & -0.354 \\ .208 & -3.08 & -0.132 \\ 17.3 & 1.07 & -6.35 \end{pmatrix} \qquad x_e = \begin{pmatrix} 103 \\ 131 \\ 423 \end{pmatrix}$$

$$G = \begin{pmatrix} 1.65 & 0.753E-2 & -0.117 & 0.553E-3 \\ 1.08 & .0175 & .0208 & -0.814E-2 \\ 3.24 & -9.96 & .742 & -0.318E-2 \end{pmatrix} \qquad u_e = \begin{pmatrix} 106 \\ 284 \\ -174 \\ 400 \end{pmatrix}$$

$$C = \begin{pmatrix} 0.885 & 0.111 & 0.188 \\ 1.49 & .209E-3 & -0.129E-2 \\ .309 & .0845 & .0538 \\ 10.8 & .355 & -1.50 \\ -0.472 & 1.01 & .0930 \\ 1.01 & -0.265 & -0.130 \\ -1.06 & 2.89 & -0.457 \end{pmatrix} \qquad y_e = \begin{pmatrix} 150 \\ 230 \\ 100 \\ 192 \\ 192 \\ 217 \\ 383 \end{pmatrix}$$

$$D = \begin{pmatrix} 0.263 & -0.0267 & 0.0371 & 0.627E-3 \\ -0.0287 & -0.0106 & .0712 & .999E-4 \\ .396 & -0.492E-2 & .353E-2 & .792E-3 \\ -0.777 & -0.529 & -0.486 & .328E-2 \\ -0.485 & .0190 & -0.0108 & -0.0659 \\ .810 & -0.0548 & .0156 & .201E-2 \\ .846 & .0990 & -0.0137 & .374E-3 \end{pmatrix}$$

APPENDIX E

COMPUTER PROGRAM LISTINGS

```
      MAIN PROGRAM
      IMPLICIT REAL*8 (A - H,  O - Z)
      COMMON/CA/C(8,3,5),D(8,4,5),E(8),XI(3,5),UI(4,5),YI(8,5),XO(7),
     1XD(3)
      COMMON/CB/A(7,7,20),BX(7,20),T(20),VAL(80),JN(80),HIT(20),JHIT(20)
      COMMON/CO/ALFA(7,20),BETA(20),PARMS(3,4),TS(20),XSTO(7,20),
     1XLSTO(7,20),XLO(7),IT(3),JM(5),NPHASE
      COMMON/MTRANS/USLOPE(2),NN
      COMMON/NNOUT/NOUT
      COMMON/NS/NSTATE
      COMMON/OUTCNT/NOUTLM
      COMMON/TTRANS/PAR(20,20),PARIN(3,3),PARS(3,3),X(7),KFLAG,KMAX,
     1KOPT(20),KOUNT,NOPT(20),NOPTS
      DIMENSION Z(5),ZL(10),ZOPT(5)
      EXTERNAL FUNGRD
      LOGICAL CONV,UNITL,LOCAL
      NSTATE=7
      IF(NOPTS.EQ.0)GO TO 11
      DO 10 I=1,NOPTS
      J=NOPT(I)
   10 ZOPT(I)=TS(J)
   11 CONTINUE
      NOUTLM=-1
      IPRINT=-1
   12 CONTINUE
      NLDIM=NOPTS*(NOPTS-1)/2
      IF(NLDIM.EQ.0)NLDIM=1
      KOUNT=0
      NN=0
      NOUT=0
      N=NOPTS
      DO 1 I=1,20
    1 KOPT(I)=I
      CALL SETUP
      ZX=0.
      ZOL=1.D-5
      ZPSMCH=16.0**(-13)
      ZTA=0.5
      ZTEPMX=1.0
      UNITL=.TRUE.
      LOCAL=.FALSE.
      IF(NOPTS.EQ.0)GO TO 3
      CALL QNMDER(N,NLDIM,ZOPT,ZX,FUNGRD,ZL,Z,ZOL,ZPSMCH,ZTA,NFTOTL,
     1NGTOTL,NITER,ZTEPMX,UNITL,LOCAL,IPRINT,CONV)
      CALL OUTPT
      GO TO 2
    3 T(1)=TS(1)
      DO 4 I=2,NPHASE
    4 T(I)=TS(I)-TS(I-1)
      CALL TRAJ
      CALL LCALC
      CALL OUTPT
    2 CONTINUE
      STOP
      END
```

```
      SUBROUTINE FUNGRD(N,ZOPT,IFLAG,ZF,Z)
      IMPLICIT REAL*8 (A - H,  O - Z)
      REAL*8 IS
      COMMON/CA/C(8,3,5),D(8,4,5),E(8),XI(3,5),UI(4,5),YI(8,5),XO(7),
     1XD(3)
      COMMON/CB/A(7,7,20),BX(7,20),T(20),VAL(80),JN(80),HIT(20),JHIT(20)
      COMMON/CO/ALFA(7,20),BETA(20),PARMS(3,4),TS(20),XSTO(7,20),
     1XLSTO(7,20),XLO(7),IT(3),JM(5),NPHASE
      COMMON/LTRANS/ZLAM(7),IS(7,7,20)
      COMMON/NNOUT/NOUT
      COMMON/NS/NSTATE
      COMMON/TTRANS/PAR(20,20),PARIN(3,3),PARS(3,3),X(7),KFLAG,KMAX,
     1KOPT(20),KOUNT,NOPT(20),NOPTS
      DIMENSION XER(7),TEMP(7),Y(7),Z(N),ZOPT(N)
      DATA XER/7*0./
      DO 11 I=1,NOPTS
      J=NOPT(I)
   11 TS(J)=ZOPT(I)
    3 T(1)=TS(1)
      DO 1 I=2,NPHASE
    1 T(I)=TS(I)-TS(I-1)
      CALL TRAJ
      T(1)=TS(1)
      DO 5 I=2,NPHASE
    5 T(I)=TS(I)-TS(I-1)
      KRESET=0
    7 IF(KRESET.EQ.1)KRESET=2
      DO 14 I=1,NPHASE
      IF(T(I).GE.0.0)GO TO 14
      CALL RESET(I)
      KRESET=1
   14 CONTINUE
      IF(KRESET.EQ.1)GO TO 7
      IF(KRESET.EQ.2)CALL TRAJ
      IF(IFLAG.EQ.2)GO TO 12
      ZF=0.0
      DO 2 I=1,3
    2 ZF=ZF+((X(I)-XD(I))/XD(I))**2/2.0
      IF(IFLAG.EQ.1)RETURN
   12 CALL LCALC
      JJ=1
      KX=KOPT(1)
      LX=NOPT(KX)
      MX=KOPT(NOPTS)
      LOPT=NOPT(MX)
      DO 20 I=1,LOPT
      IF(I.NE.LX)GO TO 20
      DO 21 J=1,NSTATE
      Y(J)=BX(J,LX)-BX(J,LX+1)
      DO 21 K=1,NSTATE
   21 Y(J)=Y(J)-(A(J,K,LX+1)-A(J,K,LX))*XSTO(K,I)
      IX=I+1
      IF(IX.GT.NPHASE)GO TO 25
      DO 22 J=IX,NPHASE
```

```
      CALL UPDATE(Y,T(J),A(1,1,J),XER,NSTATE,1)
      IF(JHIT(J).EQ.0)GO TO 22
      DD=0.0
      DN=0.0
      DO 23 K=1,NSTATE
      DD=DD+ALFA(K,J)*BX(K,J)
      DN=DN+ALFA(K,J)*Y(K)
      DO 23 L=1,NSTATE
   23 DD=DD+ALFA(K,J)*A(K,L,J)*XSTO(L,J)
      PAR(J,I)=-DN/DD
      DO 24 K=1,NSTATE
      Y(K)=Y(K)-(BX(K,J+1)-BX(K,J))*PAR(J,I)
      DO 24 L=1,NSTATE
   24 Y(K)=Y(K)-(A(K,L,J+1)-A(K,L,J))*XSTO(L,J)*PAR(J,I)
   22 CONTINUE
   25 JJ=JJ+1
      KX=KOPT(JJ)
      LX=NOPT(KX)
   20 CONTINUE
      JJ=1
      KX=KOPT(1)
      LX=NOPT(KX)
      DO 4 I=1,LOPT
      IF(I.NE.LX)GO TO 4
      Z(KX)=0.0
      DO 8 K=1,NSTATE
      Z(KX)=Z(KX)-XLSTO(K,I)*(BX(K,LX+1)-BX(K,LX))
      DO 8 J=1,NSTATE
    8 Z(KX)=Z(KX)-XLSTO(K,I)*(A(K,J,LX+1)-A(K,J,LX))*XSTO(J,I)
      IX=I+1
      IRON=1
      IF(IRON.EQ.1)GO TO 26
      IF(IX.GT.NPHASE)GO TO 26
      DO 28 J=IX,NPHASE
      IF(JHIT(J).EQ.0)GO TO 28
      DO 27 K=1,NSTATE
      Z(KX)=Z(KX)-XLSTO(K,J)*(BX(K,J+1)-BX(K,J))*PAR(J,I)
      DO 27 L=1,NSTATE
      Z(KX)=Z(KX)-XLSTO(K,J)*(A(K,L,J+1)-A(K,L,J))*XSTO(L,J)*PAR(J,I)
   27 CONTINUE
   28 CONTINUE
   26 TE=DSQRT(2.*ZF)
      WRITE(6,10)ZOPT(KX),TE,Z(KX),LX
      JJ=JJ+1
      KX=KOPT(JJ)
      LX=NOPT(KX)
    4 CONTINUE
   10 FORMAT (1H ,3(G20.9),I2)
      IF(NOUT.EQ.0)CALL OUTPT
      NOUT=1
      RETURN
      END
```

```
      SUBROUTINE LCALC
      IMPLICIT REAL*8 (A - H,  O - Z)
      REAL*8 ID,IS,ISIN
      COMMON/CA/C(8,3,5),D(8,4,5),E(8),XI(3,5),UI(4,5),YI(8,5),X0(7),
     1XD(3)
      COMMON/CB/A(7,7,20),BX(7,20),T(20),VAL(80),JN(80),HIT(20),JHIT(20)
      COMMON/CO/ALFA(7,20),BETA(20),PARMS(3,4),TS(20),XSTO(7,20),
     1ZLSTO(7,20),ZLO(7),IT(3),JM(5),NPHASE
      COMMON/CX/F(3,3,5),G(3,4,5),DD(4,4,20),ID(7,7)
      COMMON/EPSS/EPS(20)
      COMMON/LTRANS/ZLAM(7),IS(7,7,20)
      COMMON/NS/NSTATE
      DIMENSION GSP(7),GSM(7),TEMP(7),ZER(7),ISIN(7,7)
      DATA ZER/7*0.0/
      DO 2 I=1,3
      ZLAM(I)=(XSTO(I,NPHASE)-XD(I))/XD(I)**2
    2 ZLSTO(I,NPHASE)=ZLAM(I)
      DO 11 I=4,NSTATE
      ZLAM(I)=0.0
   11 ZLSTO(I,NPHASE)=ZLAM(I)
      DO 3 I=1,NPHASE
      IA=NPHASE-I+1
      TX=-T(IA)
      CALL UPDATE(ZLAM,TX,A(1,1,IA),ZER,NSTATE,2)
      IF(IA.EQ.1)GO TO 3
      DO 4 J=1,NSTATE
    4 ZLSTO(J,IA-1)=ZLAM(J)
      IF(JHIT(IA-1).EQ.0)GO TO 3
      DO 5 J=1,NSTATE
      GSP(J)=BX(J,IA)
      GSM(J)=BX(J,IA-1)
      DO 5 K=1,NSTATE
      GSP(J)=GSP(J)+A(J,K,IA)*XSTO(K,IA-1)
    5 GSM(J)=GSM(J)+A(J,K,IA-1)*XSTO(K,IA-1)
      DOT=0.0
      DOTIN=0.0
      DO 6 J=1,NSTATE
      DOTIN=DOTIN+ALFA(J,IA-1)*GSM(J)
    6 DOT=DOT+ZLAM(J)*(GSM(J)-GSP(J))
      EPS(IA-1)=DOT/DOTIN
      DO 8 J=1,NSTATE
      ZLAM(J)=ZLAM(J)-EPS(IA-1)*ALFA(J,IA-1)
    8 ZLSTO(J,IA-1)=ZLAM(J)
    3 CONTINUE
      DO 10 I=1,NSTATE
   10 ZLO(I)=ZLAM(I)
      RETURN
      END
```

```
      SUBROUTINE OUTPT
      IMPLICIT REAL*8 (A - H,  O - Z)
      REAL*8 ID,IS,KAPPA
      COMMON/CA/C(8,3,5),D(8,4,5),E(8),XI(3,5),UI(4,5),YI(8,5),X0(7),
     1XD(3)
      COMMON/CB/A(7,7,20),BX(7,20),T(20),VAL(80),JN(80),HIT(20),JHIT(20)
      COMMON/CO/ALFA(7,20),BETA(20),PARMS(3,4),TS(20),XSTO(7,20),
     1ZLSTO(7,20),ZLO(7),IT(3),JM(5),NPHASE
      COMMON/CX/F(3,3,5),G(3,4,5),DD(4,4,20),ID(7,7)
      COMMON/EPSS/EPS(20)
      COMMON/LTRANS/ZLAM(7),IS(7,7,20)
      COMMON/MTRANS/USLOPE(2),NN
      COMMON/NS/NSTATE
      COMMON/OUTCNT/NOUTLM
      DIMENSION S(5),X(7),OUT(8),KAPPA(4),TEMP(7),ZER(7)
      DATA ZER/7*0./
      IF (NOUTLM.LT.0) RETURN
      M=1
      IM=JM(1)
      DO 50 I=1,4
      IF(IM.GT.0)GO TO 50
      M=M+1
      IM=JM(M)
   50 CONTINUE
      KK=1
      WRITE(6,7) TS(20)
      WRITE(6,13)
      WRITE(6,14)
      WRITE(6,20)
    7 FORMAT('1',4X,'TF= ',G11.4)
   13 FORMAT('1',4X,'TIME',7X,'THRUST',5X,'AIRFLOW',4X,'TIT',8X,'SMFAN',
     16X,'SMCOM',6X,'FTIT',7X,'PT3',8X,'NFAN',7X,'NCOMP',6X,'PT7M')
   14 FORMAT (5X,'WF',9X,'ANOZ',7X,'IGV',8X,'HVS',8X,'KAPPA1',5X,
     1'KAPPA2',5X,'KAPPA3',5X,'KAPPA4',5X,'H',10X,'D1',9X,'D2')
   20 FORMAT (5X,'D3',9X,'D4',9X,'D5',9X,'TERMERR')
      DT=0.1
      TIME=0.0
      N=1
      DO 41 I=1,NSTATE
      ZLAM(I)=ZLO(I)
   41 X(I)=X0(I)
      GO TO 16
    8 IF(TIME+DT.LE.TS(N).AND.KK.EQ.1)GO TO 1
      GO TO (10,11,18,12),KK
   10 TSTO=TIME+DT
      DTSTO=DT
   60 DT=TS(N)-TIME
      KK=2
      GO TO 1
   11 N=N+1
      IF(N.GT.NPHASE)RETURN
      IF(JHIT(N-1).EQ.0)GO TO 40
      IF(N.NE.IM+1)GO TO 51
      M=M+1
```

```
      IM=JM(M)
   51 DO 53 J=1,NSTATE
   53 ZLAM(J)=ZLAM(J)+EPS(N-1)*ALFA(J,N-1)
   40 DT=0.0
      KK=3
      GO TO 16
   18 DT=TSTO-TIME
      IF(TS(N).LT.TSTO)GO TO 60
      KK=4
      GO TO 1
   12 KK=1
      DT=DTSTO
      GO TO 8
    1 CALL UPDATE(X,DT,A(1,1,N),BX(1,N),NSTATE,1)
      TIME=TIME+DT
   16 NST=NSTATE-4
      DO 3 I=1,7
      OUT(I)=YI(I,M)
      DO 34 J=1,4
   34 OUT(I)=OUT(I)+D(I,J,M)*(X(J+NST)-UI(J,M))
      DO 3 J=1,NST
    3 OUT(I)=OUT(I)+C(I,J,M)*(X(J)-XI(J,M))
      TX=DT
      IF(DT.EQ.0.0.OR.TIME.EQ.0.0)GO TO 17
      CALL UPDATE(ZLAM,TX,A(1,1,N),ZER,NSTATE,2)
   17 DO 9 I=1,4
      KAPPA(I)=0.0
      DO 9 J=1,4
      JX=J+NST
    9 KAPPA(I)=KAPPA(I)-DD(J,I,N)*ZLAM(JX)
      H=0.
      DO 15 I=1,NSTATE
      H=H+ZLAM(I)*BX(I,N)
      DO 15 J=1,NSTATE
   15 H=H+ZLAM(I)*A(I,J,N)*X(J)
      DO 37 I=1,5
      S(I)=0.0
      DO 37 J=1,NST
   37 S(I)=S(I)+(X(J)-XI(J,I))**2/(XI(J,1)-XI(J,2))**2
      DO 52 I=1,5
   52 S(I)=DSQRT(S(I)/3.0)
      ZF=0.0
      DO 2 I=1,NST
    2 ZF=ZF+((X(I)-XD(I))/XD(I))**2/2.0
      TE=DSQRT(2.*ZF)
      WRITE(6,19)TIME,(OUT(I),I=1,7),(X(I),I=1,3)
      WRITE(6,4)(X(I+3),I=1,4),(KAPPA(I),I=1,4),H,(S(I),I=1,2)
      WRITE(6,6)(S(I),I=3,5),TE
    4 FORMAT(3X,11(G11.4))
    6 FORMAT(3X,3(G11.4),G11.5)
   19 FORMAT (3H0   ,G11.5,10(G11.4))
      GO TO 8
      END
```

```
      SUBROUTINE RESET(N)
      IMPLICIT REAL*8 (A - H,  O - Z)
      COMMON/CB/A(7,7,20),BX(7,20),T(20),VAL(80),JN(80),HIT(20),JHIT(20)
      COMMON/CO/ALFA(7,20),BETA(20),PARMS(3,4),TS(20),XSTO(7,20),
     1XLSTO(7,20),XLO(7),IT(3),JM(5),NPHASE
      COMMON/TTRANS/PAR(20,20),PARIN(3,3),PARS(3,3),X(7),KFLAG,KMAX,
     1KOPT(20),KOUNT,NOPT(20),NOPTS
      DO 12 J=1,4
      M=4*(N-1)+J
      IF(JN(M).NE.JN(M-4))GO TO 10
      JNT=JN(M+4)
      VALT=VAL(M+4)
   10 IF(JN(M).NE.JN(M+4))GO TO 11
      JNT=JN(M-4)
      VALT=VAL(M-4)
   11 JN(M)=JNT
   12 VAL(M)=VALT
      DO 7 I=1,7
      ALFT=ALFA(I,N)
      ALFA(I,N)=ALFA(I,N-1)
    7 ALFA(I,N-1)=ALFT
      BET=BETA(N)
      BETA(N)=BETA(N-1)
      BETA(N-1)=BET
      HITT=HIT(N)
      HIT(N)=HIT(N-1)
      HIT(N-1)=HITT
      JHITT=JHIT(N)
      JHIT(N)=JHIT(N-1)
      JHIT(N-1)=JHITT
      TT=TS(N)
      TS(N)=TS(N-1)
      TS(N-1)=TT
      T(N)=TS(N)-TS(N-1)
      T(N+1)=TS(N+1)-TS(N)
      IF(N.GT.2)T(N-1)=TS(N-1)-TS(N-2)
      IF(N.EQ.2)T(1)=TS(1)
      DO 2 I=1,5
      K=JM(I)
      IF(K.EQ.N)JM(I)=K-1
      IF(K.EQ.N-1)JM(I)=K+1
    2 CONTINUE
      DO 3 I=1,20
      K=NOPT(I)
      IF(K.EQ.N)NOPT(I)=K-1
      IF(K.EQ.N-1)NOPT(I)=K+1
    3 CONTINUE
      DO 4 I=1,19
      KX=KOPT(I)
      KY=KOPT(I+1)
      IF(NOPT(KY).GE.NOPT(KX))GO TO 4
      KT=KOPT(I+1)
      KOPT(I+1)=KOPT(I)
      KOPT(I)=KT
```

```
4 CONTINUE
  CALL SETUP
  WRITE(6,5)N,(JM(I),I=1,5)
5 FORMAT(1H ,7(I3))
  RETURN
  END
```

```
      SUBROUTINE SETUP
      IMPLICIT REAL*8 (A - H,  O - Z)
      REAL*8 ID,LX,MX
      COMMON/CA/C(8,4,5),D(8,4,5),E(8),XI(3,5),UI(4,5),YI(8,5),XO(7),
     1XD(3)
      COMMON/CB/A(7,7,20),BX(7,20),T(20),VAL(80),JN(80),HIT(20),JHIT(20)
      COMMON/CO/ALFA(7,20),BETA(20),PARMS(3,4),TS(20),XSTO(7,20),
     1ZLSTO(7,20),ZLO(7),IT(3),JM(5),NPHASE
      COMMON/CX/F(3,3,5),G(3,4,5),DD(4,4,20),ID(7,7)
      COMMON/MTRANS/USLOPE(2),NN
      COMMON/NS/NSTATE
      DIMENSION C1(4,4),C2(4,4),CS(2,3),WI(3,5),EI(4),EE(4),LX(4),MX(4)
      DO 100 I=1,7
      DO 100 J=1,20
  100 ALFA(I,J)=0.0
      DO 27 I=1,2
      DO 27 J=1,3
   27 CS(I,J)=0.0
      CS(1,1)=23./6400.
      CS(2,2)=34./4100.
      DO 41 K=1,20
      DO 41 I=1,4
      DO 41 J=1,4
   41 DD(I,J,K)=0.0
      NST=NSTATE-4
      DO 40 I=1,NST
      WI(I,1)=1.5*XI(I,1)-0.5*XI(I,2)
      DO 40 J=2,5
   40 WI(I,J)=XI(I,J)
      M=1
      IM=JM(1)
      DO 50 I=1,4
      IF(IM.GT.0)GO TO 50
      M=M+1
      IM=JM(M)
   50 CONTINUE
      DO 1 K=1,NPHASE
      IF(K.LE.IM)GO TO 2
      M=M+1
      IM=JM(M)
    2 DO 3 I=1,4
      EE(I)=0.0
      DO 3 J=1,4
      C1(I,J)=0.0
      C2(I,J)=0.0
    3 DD(I,J,K)=0.0
      DO 4 I=1,4
      LL=4*(K-1)+I
      N=JN(LL)
      NT=0
      IF(N.GT.8)GO TO 5
   19 DO 6 J=1,4
      DD(I,J,K)=D(N,J,M)
      DO 6 L=1,NST
```

```
 6 C2(I,J)=C2(I,J)+C(N,L,M)*G(L,J,M)
   DO 7 J=1,NST
   DO 7 L=1,NST
 7 C1(I,J)=C1(I,J)+C(N,L,M)*F(L,J,M)
   DO 8 J=1,NST
 8 EE(I)=EE(I)-C1(I,J)*XI(J,M)
   DO 9 J=1,4
 9 EE(I)=EE(I)-C2(I,J)*UI(J,M)
   GO TO 10
 5 IF(N.GT.12)GO TO 11
   DD(I,N-8,K)=1.0
   GO TO 10
11 IF(N.GT.16)GO TO 12
   DD(I,N-12,K)=1.0
   EE(I)=-VAL(LL)
   GO TO 10
12 IF(N.GT.20)GO TO 13
   DD(I,N-16,K)=1.0
   EE(I)=VAL(LL)
   GO TO 10
13 IF(N.GT.22)GO TO 14
   DD(I,N-18,K)=-1.0
   DO 15 J=1,4
   DO 15 L=1,NST
15 C2(I,J)=C2(I,J)+CS(N-20,L)*G(L,J,M)
   DO 16 J=1,NST
   DO 16 L=1,NST
16 C1(I,J)=C1(I,J)+CS(N-20,L)*F(L,J,M)
   DO 17 J=1,NST
17 EE(I)=EE(I)-C1(I,J)*XI(J,M)
   DO 18 J=1,4
18 EE(I)=EE(I)-C2(I,J)*UI(J,M)
   GO TO 10
14 N=3
   NT=1
   GO TO 19
10 IF(NT.EQ.1) EE(I)=EE(I)-VAL(LL)
 4 CONTINUE
   CALL DMINV(DD(1,1,K),4,DET,LX,MX)
   DO 20 I=1,NST
   DO 21 J=1,NST
21 A(I,J,K)=F(I,J,M)
   DO 20 J=1,4
   JX=J+NST
20 A(I,JX,K)=G(I,J,M)
   DO 22 I=1,4
   IX=I+NST
   BX(IX,K)=0.0
   DO 22 J=1,4
22 BX(IX,K)=BX(IX,K)-DD(I,J,K)*EE(J)
   DO 23 I=1,NST
   BX(I,K)=0.0
   DO 24 J=1,NST
24 BX(I,K)=BX(I,K)-F(I,J,M)*XI(J,M)
```

```
      DO 23 J=1,4
   23 BX(I,K)=BX(I,K)-G(I,J,M)*UI(J,M)
      DO 25 I=1,4
      DO 25 J=1,NST
      IX=I+NST
      A(IX,J,K)=0.0
      DO 25 L=1,4
   25 A(IX,J,K)=A(IX,J,K)-DD(I,L,K)*C1(L,J)
      DO 26 I=1,4
      DO 26 J=1,4
      IX=I+NST
      JX=J+NST
      A(IX,JX,K)=0.0
      DO 26 L=1,4
   26 A(IX,JX,K)=A(IX,JX,K)-DD(I,L,K)*C2(L,J)
    1 CONTINUE
      M=1
      IM=JM(1)
      DO 28 I=1,4
      IF(IM.GT.0)GO TO 28
      M=M+1
      IM=JM(M)
   28 CONTINUE
      DO 29 I=1,NPHASE
      IF(I.LE.IM)GO TO 31
      M=M+1
      IM=JM(M)
   31 JH=JHIT(I)
      IF(JH.EQ.0)GO TO 29
      IF(JH.GT.8)GO TO 30
      BETA(I)=HIT(I)-YI(JH,M)
      DO 32 J=1,NST
      ALFA(J,I)=C(JH,J,M)
   32 BETA(I)=BETA(I)+C(JH,J,M)*XI(J,M)
      DO 33 J=1,4
      JX=NST+J
      ALFA(JX,I)=D(JH,J,M)
   33 BETA(I)=BETA(I)+D(JH,J,M)*UI(J,M)
      GO TO 29
   30 IF(JH.GT.12)GO TO 34
      ALFA(JH-5,I)=1.0
      BETA(I)=HIT(I)
   34 IF(JH.LT.21)GO TO 29
      IF(JH.GT.22)GO TO 35
      BETA (I)=HIT(I)
      IF(JH.EQ.22)GO TO 101
      BETA(I)=25.+23.*4000./6400.-HIT(I)
      GO TO 102
  101 BETA(I)=30.+34.*9000./4100.-HIT(I)
  102 CONTINUE
      DO 36 J=1,NST
   36 ALFA(J,I)=CS(JH-20,J)
      ALFA(JH-15,I)=-1.0
      GO TO 29
```

```
35 IF(JH.EQ.23)GO TO 29
   BETA(I)=0.0
   DO 37 J=1,NST
   ALFA(J,I)=0.0
   DO 37 L=1,NST
   BETA(I)=BETA(I)+ID(J,L)*(WI(J,M+1)*WI(L,M+1)-WI(J,M)
  1*WI(L,M))/(WI(J,M+1)-WI(J,M))**2
37 ALFA(J,I)=ALFA(J,I)+2.0*(WI(L,M+1)-WI(L,M))*ID(J,L)/
  1(WI(J,M)-WI(J,M+1))**2
29 CONTINUE
   RETURN
   END
```

```
      SUBROUTINE TRAJ
      IMPLICIT REAL*8 (A - H,  O - Z)
      REAL*8 ID
      COMMON/CA/C(8,3,5),D(8,4,5),E(8),XI(3,5),UI(4,5),YI(8,5),X0(7),
     1XD(3)
      COMMON/CB/A(7,7,20),BX(7,20),T(20),VAL(80),JN(80),HIT(20),JHIT(20)
      COMMON/CO/ALFA(7,20),BETA(20),PARMS(3,4),TS(20),XSTO(7,20),
     1XLSTO(7,20),XLO(7),IT(3),JM(5),NPHASE
      COMMON/CX/F(3,3,5),G(3,4,5),DD(4,4,20),ID(7,7)
      COMMON/NS/NSTATE
      COMMON/TTRANS/PAR(20,20),PARIN(3,3),PARS(3,3),X(7),KFLAG,KMAX,
     1KOPT(20),KOUNT,NOPT(20),NOPTS
      DIMENSION Y(7),W(7)
      KFLAG=0
    1 DO 2 I=1,NSTATE
    2 X(I)=X0(I)
      KOUNT=KOUNT+1
      KT=0
      DO 4 M=1,NPHASE
   84 CALL UPDATE(X,T(M),A(1,1,M),BX(1,M),NSTATE,1)
      DO 104 I=1,NSTATE
  104 XSTO(I,M)=X(I)
   88 IF(JHIT(M).EQ.0)GO TO 80
      S=BETA(M)
      DO 81 I=1,NSTATE
   81 S=S-ALFA(I,M)*X(I)
      IF(DABS(S/BETA(M)).LE..0001)GO TO 83
      CALL VMULT(A(1,1,M),X,Y,NSTATE)
      SD=0.0
      DO 82 I=1,NSTATE
   82 SD=SD-ALFA(I,M)*(Y(I)+BX(I,M))
      T(M)=T(M)-S/SD
      KT=KT+1
      IF(KT.LE.10)GO TO 90
      KFLAG=1
      RETURN
   90 DTM=-S/SD
      CALL UPDATE(X,DTM,A(1,1,M),BX(1,M),NSTATE,1)
      DO 105 I=1,NSTATE
  105 XSTO(I,M)=X(I)
      GO TO 88
   83 IF(M.GT.1)TS(M)=T(M)+TS(M-1)
      IF(M.EQ.1)TS(1)=T(1)
      T(M+1)=TS(M+1)-TS(M)
   80 CONTINUE
      IF(IT(1).EQ.0)GO TO 4
      IF(K.EQ.0)GO TO 50
      DO 51 J=1,K
      CALL VMULT(PHI,PAR(1,J),W,NSTATE)
      DO 51 I=1,3
   51 PAR(I,J)=W(I)
   50 DO 100 I=1,3
  100 PAR(I,M)=Y(I)+BX(I,M)
      DO 102 K=1,4
```

```
      IN=JM(K)
      IF(M.NE.IN)GO TO 102
      DO 85 I=1,3
      L=IT(I)
      IF(L.GT.IN)GO TO 85
      SDS=0.0
      KX=K-1
      DO 86 J=1,3
      SDS=SDS-ALFA(J,K)*(PAR(J,L)-PAR(J,L+1))
      IF(KX.EQ.0)GO TO 86
      DO 103 JJ=1,KX
      JK=JM(JJ)
      IF(JK.LT.L.OR.JK.GE.10)GO TO 103
      SDS=SDS-ALFA(J,K)*PARMS(I,JJ)*(PAR(J,JK)-PAR(J,JK+1))
  103 CONTINUE
   86 CONTINUE
      PARMS(I,K)=-SDS/SD
   85 CONTINUE
  102 CONTINUE
    4 CONTINUE
      IF(IT(1).EQ.0)GO TO 106
   87 DO 61 J=1,3
      K=IT(J)
      DO 61 I=1,3
      PARS(I,J)=PAR(I,K)-PAR(I,K+1)
      DO 61 M=1,4
      IM=JM(M)
      IF(IM.LT.K.OR.IM.GE.10)GO TO 61
      PARS(I,J)=PARS(I,J)+PARMS(J,M)*(PAR(I,IM)-PAR(I,IM+1))
   61 CONTINUE
  106 CONTINUE
      RETURN
      END
```

```
      SUBROUTINE UPDATE(X,T,A,BX,NSTATE,L)
      IMPLICIT REAL*8 (A - H,  O - Z)
      DIMENSION X(NSTATE),BX(NSTATE),A(NSTATE,NSTATE),BS(10),BT(10),
     1XS(10),XT(10)
      N=12
      IF(L.EQ.2)GO TO 7
      DO 6 I=1,NSTATE
      BS(I)=BX(I)
    6 XS(I)=X(I)
      DO 2 K=1,N
      DO 3 I=1,NSTATE
      XT(I)=0.0
      BT(I)=0.0
      DO 3 J=1,NSTATE
      BT(I)=BT(I)+A(I,J)*T/DFLOAT(N-K+2)*BS(J)
    3 XT(I)=XT(I)+A(I,J)*T/DFLOAT(N-K+1)*XS(J)
      DO 4 I=1,NSTATE
      BS(I)=BT(I)+BX(I)
    4 XS(I)=XT(I)+X(I)
    2 CONTINUE
      DO 5 I=1,NSTATE
    5 X(I)=XS(I)+BS(I)*T
      RETURN
    7 DO 1 I=1,NSTATE
    1 XS(I)=X(I)
      DO 8 K=1,N
      DO 9 I=1,NSTATE
      XT(I)=0.0
      DO 9 J=1,NSTATE
    9 XT(I)=XT(I)-A(J,I)*T/DFLOAT(N-K+1)*XS(J)
      DO 10 I=1,NSTATE
   10 XS(I)=XT(I)+X(I)
    8 CONTINUE
      DO 11 I=1,NSTATE
   11 X(I)=XS(I)
      RETURN
      END
```

```
      SUBROUTINE VMULT(A,B,C,NSTATE)
      IMPLICIT REAL*8 (A - H,  O - Z)
      DIMENSION A(NSTATE,NSTATE),B(NSTATE),C(NSTATE)
      DO 1 I=1,NSTATE
      C(I)=0.
      DO 1 J=1,NSTATE
    1 C(I)=C(I)+A(I,J)*B(J)
      RETURN
      END
```

REFERENCES

1. Bryson, A. E., Jr.: "Control Theory for Random Systems." Proceeddings of the Thirteenth International Congress of Theoretical and Applied Mechanics, Moscow; August 1972.
2. Bryson, A. E.; and Hall, W. E.: "Optimal Control and Filter Synthesis by Eigenvector Decomposition," SUDAAR No. 436, Stanford University; December 1971.
3. Geyser, L. C. and Lehtinen, B.: "Digital Program for Solving the Linear Stochastic Optimal Control and Estimation Problem," NASA TN D-7820; March 1975.
4. Michael, G. J.; and Farrar, F. A.: "Development of Optimal Control Modes for Advanced Technology Propulsion Systems," United Aircraft Research Laboratories Report N911620-2, March 1974.
5. Michael, G. J.; and Farrar, F. A.: "An Analytical Method for the Synthesis of Nonlinear Multivariable Feedback Control," United Aircraft Research Laboratories Report M941338-2 (DDE Accession Number AD 762797); June 1973.
6. Weinberg, M. S.: "A Multi-Variable Control for the F100 Engine Operating at Sea Level Static," ASD-TR-75-28; Nov. 1975.
7. Sevich, G. T.; and Beattie, E. C.: "Integrated Flight Propulsion Control Design Techniques Starting with the Engine," 1974 SAE National Air Transportation Meeting, April 30-May 2, 1974; Dallas, Texas. SAE Paper #740481.

8. DeHoff, R. L. and Hall, W. E.: "Multivariable Design Procedures for the F100 Turbofan Engine," Final Report Contract No. F33615-75-C-2053, Systems Control, Inc. (Vt), Palo Alto, Calif., January 1, 1977.

9. Athans, M. and Falb, P. L.: "Optimal Control: An Introduction to the Theory and Its Applications," McGraw-Hill Book Company; 1966.

10. Wolske, G. D. and Flugge-Lotz, I.: "Minimum Fuel Attitude Control of a Nonlinear Satellite System with Bounded Control by a Method Based on Linear Programming," SUDAAR No. 374, Department of Aeronautics and Astronautics, Stanford University, Stanford, Calif.; May 1969.

11. Gill, Murray and Pitfield: "The Implementation of Two Revised Quasi-Newton Algorithms for Unconstrained Optimization," National Physical Laboratory, Division of Numerical Analysis and Computing, Report No. DNAC 11, 1972.

12. Luenberger, David G.: "Introduction to Linear and Nonlinear Programming," Addison-Wesley Publishing Company, 1973.

13. Miller, R. J. and Hackney, R. P.: "Research on F100 Multivariable Control," Pratt & Whitney Aircraft Group Report No. FR-7809; August 1976.

14. Anon.: "F100-PW-100(3) Transient Engine Simulation Deck," Pratt & Whitney Aircraft, Government Products Division, FR-6014, Oct. 15, 1973.

15. Bryson, A. E., Jr.; and Yu-Chi Ho: "Applied Optimal Control: Optimization, Estimation and Control," Blaisdell Publishing Company, 1969.

16. Dantzig, G.: "Linear Programming and Extensions," Princeton, University Press, 1963.

17. Polak, Elijah: "Computational Methods in Optimization," A Unified Approach, New York, Academic Press, 1971.

18. Szuch, J. R.; and Seldner, K.: "Real Time Simulation of F100-PW-100 Turbofan Engine Using the Hybrid Computer," NASA TM X-3261; August 1975.